Dalton Transactions

ROYAL SOCIETY OF CHEMISTRY

PERSPECTIVE

View Article Online
View Journal | View Issue

Cite this: *Dalton Trans.*, 2024, **53**, 9612

Metal-based carbon monoxide releasing molecules with promising cytotoxic properties

Ahmed M. Mansour, *†[a] Rabaa M. Khaled, †[b] Giarita Ferraro,[c] Ola R. Shehab [b] and Antonello Merlino *[c]

Carbon monoxide, the "silent killer" gas, is increasingly recognised as an important signalling molecule in human physiology, which has beneficial biological properties. A particular way of achieving controlled CO administration is based on the use of biocompatible molecules that only release CO when triggered by internal or external factors. These approaches include the development of pharmacologically effective prodrugs known as CO releasing molecules (CORMs), which can supply biological systems with CO in well-regulated doses. An overview of transition metal-based CORMs with cytotoxic properties is here reported. The mechanisms at the basis of the biological activities of these molecules and their potential therapeutical applications with respect to their stability and CO releasing properties have been discussed. The activation of metal-based CORMs is determined by the type of metal and by the nature and features of the auxiliary ligands, which affect the metal core electronic density and therefore the prodrug resistance towards oxidation and CO release ability. A major role in regulating the cytotoxic properties of these CORMs is played by CO and/or CO-depleted species. However, several mysteries concerning the cytotoxicity of CORMs remain as intriguing questions for scientists.

Received 11th January 2024,
Accepted 9th May 2024

DOI: 10.1039/d4dt00087k

rsc.li/dalton

1. Introduction

Carbon monoxide is a colourless and odourless gas that is often formed as a result of partial oxidation of carbon-based molecules. High concentrations of CO are hazardous to humans as it has affinity to haemoglobin (HbA) 210–250 times > than O_2. As a consequence, the resulting carboxyhaemoglobin (COHb) impairs O_2 storage and delivery in the body.[1,2] CO starts with unselective binding and unequal distribution in the case of the inhalation route causing coma, convulsions, respiratory depression, and even more fatal consequences. In 1949, Sjöstrand discovered that haemoglobin breakdown *in vivo* generated CO.[3] Elevated haem levels, following erythrocyte destruction, enhances endogenous CO generation, as evidenced by an increase in COHb levels.[4] Tenhunen and coworkers identified haem degradation *via* the haem oxygenase (HO) as the main mechanism for endogenous CO generation.[5] Enzymatic haem metabolism produces the vast bulk of CO in the human body. HOs (HO-1 and HO-2) catalyse this metabolism, which takes place in the liver and spleen reticuloendothelial system.[6] HO-1 produces approximately 16 mL h^{-1} of CO in the human body. However, the cellular CO amount is in the nanomolar range. Iron-dependent lipid peroxidation[7] and cytochrome P-450 self-inactivation[8] produce a limited amount of this distinct metabolite.

CO is not always harmful to humans. CO works as a signalling molecule in the neural system, and it has been shown to have vasorelaxant,[9] and heart protective properties.[10] Numerous papers have also demonstrated the significance of the CO activities in the immunological,[11] reproductive,[12] respiratory,[13] gastrointestinal,[14] liver,[15] and kidney[16] systems. The CO deficiency, on the other hand, has been linked to diabetes, sepsis, colitis, and vascular complications.[17,18] The development of prodrugs that can deliver CO steadily and measurably may offer a new way to directly administrate this therapeutic gas and tackle the drawback of unselective binding and distribution. It has been, and still is, difficult for pharmaceutical chemists to come up with safe, workable methods for administering therapeutic doses of CO. Among the methods used to supply potentially effective doses of carbon monoxide to specific organs and tissues, the creation of pharmacologically effective prodrugs known as CO releasing molecules (CORMs) is particularly interesting. Several CORMs have been synthetized and studied in the last years.[19] These molecules can distribute CO into biological systems in a secure and controlled manner. CORMs can be generally classified in five groups: bor-

[a]*Department of Chemistry, United Arab Emirates University, Al-Ain, United Arab Emirates. E-mail: Mansour_am@uaeu.ac.ae, inorganic_am@yahoo.com*
[b]*Department of Chemistry, Faculty of Science, Cairo University, Gamma Street, 12613, Egypt. E-mail: Olashehab@sci.cu.edu.eg*
[c]*Department of Chemical Sciences, University of Naples Federico II, Napoli, Italy. E-mail: antonello.merlino@unina.it*
† The authors contributed equally to this review article.

oncarboxylates,[19] oxalates,[20] α,α-dialkyl-aldehydes, silacarboxylates,[21] and metal carbonyl complexes (MCCs). Metal-free CO donors could offer advantages when compared to MCCs,[22,23] but their application is in part limited by the conditions needed for CO release or by the low kinetics of gas release.[24,25] The structures, CO releasing activity and some biological properties of CORMs have been critically discussed in previous reviews.[26–28] MCCs possess antimicrobial properties,[20,21,29] and bactericidal activity against different species including *Neisseria gonorrhoeae*,[30] *Pseudomonas aeruginosa*,[31] *Helicobacter pylori*,[32] and *Salmonella enterica serova typhimurium*.[33] Their role as modulators of inflammation in multiple pathological conditions is well documented. In addition, they contribute to the balance of the redox equilibrium acting as antioxidant molecules. Being reservoirs of CO, a known neurotransmitter, MCCs are involved in neuroprotection and neuronal differentiation processes.[34] These properties have been also summarized, together with CORM carrier conjugate systems.[35] However, a comprehensive examination of the cytotoxic properties of MCCs is missing. In this respect, it should be underlined that not all the MCCs reported in the literature were examined for cytotoxic properties. Here, we focused our attention on MCCs. In particular, an overview of the anticancer features of metal-based CORMs is reported,[35] with the intention of defining the mechanism of action of these potential drugs and discussing their potential therapeutical applications in relation to their biocompatibility and CO releasing properties. The review begins with a brief overview of early-generation CORMs, mechanisms of CO release, CO detection techniques, and it continues with the discussion of the anticancer properties of transition metal-based CORMs, including photo-induced CORMs. The discussion focusses on many cancer hallmarks, including proliferation, apoptosis, angiogenesis, inflammation, *etc*.

2. Metal-based CORMs

MCCs are able to directly release CO upon internal or external activation. To act as a CORM, a MCC needs to be readily soluble in water and ideally sufficiently stable when held at room temperature (r.t.). Furthermore, it should survive in the blood, remaining active up to the desired targets and should produce only non-toxic fragments after the CO release.[24] The properties of the auxiliary ligands in MCCs influence the metal core electron density (e.d.) and hence its stability toward oxidation. Also, the strength of the metal–ligand bonds could stabilize the metal ligand field, slowing down the possible ligand exchange reactions or, oppositely, speeding up CO substitution. As a result, the structure of the first coordination sphere is critical for tuning the chemistry and stability of a certain MCC to withstand the plasma proteins, react to a precise trigger, and develop a certain CO release profile.[25,36] The first transition MCCs were examined by Motterlini's group.[37] They showed that when $Fe(CO)_5$ and $Mn_2(CO)_{10}$ (denominated CORM-1) (Fig. 1) are exposed to a cold light, a

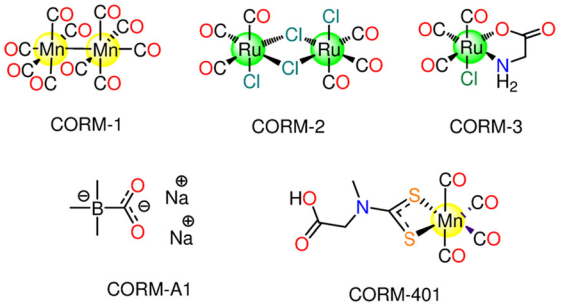

Fig. 1 First-generation CORMs: CORM-1, CORM-2, CORM-3 and CORM-401. The structure of the non-metallic CORM-A1 is also reported.

CO release is promoted and that these simple metal carbonyls can deliver controlled quantities of CO causing potent vasorelaxant effects in rat aortic rings pre-contracted with phenylephrine, similarly to endogenous CO.[37] Afterward, the first-generation CORMs were quickly replaced by Ru(II) carbonyl complexes due to their low bioavailability as well as the necessity for the photoactivation to produce substantial CO release. The first Ru(II) based complex to be investigated as CORM is CORM-2 ($[RuCl_2(CO)_3]_2$, Fig. 1). All the previously mentioned CORMs have poor solubility in water. Then, the scientists sought out MCCs with glycinate as an auxiliary ligand, such as $[Ru(CO)_3Cl(glycinate)]$, namely CORM-3 (Fig. 1). The CO release from this molecule is prompted by solvent-assisted ligand exchange. When administered into the body, CORMs are exposed to high concentrations of biomolecules, which promote ligand exchange reactions that result in the spontaneous release of CO. The half-life, $t_{1/2}$, value of CORM-3, for example, is 98 h at ambient temperature in water; yet, this value decreases to 3.6 min in human plasma, when it encounters glutathione and other biomolecules. Since the distribution of such CORMs in tissues largely depends on both $t_{1/2}$ value in a specific medium and the required time to reach their desired target, this could have an adverse effect on the ability to control site-specific delivery.[38] Several triggers were utilized to promote the CO release including changes in pH,[39] oxidation state,[40] and temperature.[41] In addition, the use of enzymes that cleave bonds at the ligand periphery in enzyme-triggered CORMs has been also explored.[42] Furthermore, it is now simple to control the time, location, and dose of CO release using light. The essential characteristics of the well-known classes of CORMs are outlined in the next sections.

3. CO release mechanisms

3.1. Thermally activated CORMs

The ligand exchange reaction with the medium is one of the mechanisms that promote the CO release from CORMs. For example, CORM-2 and CORM-3 are able to thermally release CO *via* the ligand exchange mechanism.[37,43] Several research groups presented a series of iron(0) CORMs featuring norbor-

nadiene ligands that thermally released CO *via* the loss of norbornadiene and/or substitution with solvent molecules.[44] Motterlini and co-workers proposed the water-soluble non-metallic CORM-A1 (Fig. 1). CORM-A1 is one of the most utilised CORMs in CO biology research because of its commercial availability, high water solubility, and fast CO release kinetics ($t_{1/2}$ = 2–21 min in phosphate buffered saline, PBS, solutions at pH 5.5 and 7.4 at 37 °C). The CO release mechanism of CORM-A1 is based on a protonation-induced decomposition, which leads to a spontaneous CO liberation consequent to the generation of an unstable borane carbonyl intermediate (Scheme 1).[45,46] The release mechanism was firstly proposed by Motterlini in 2005; he measured the CO released by the means of the myoglobin (Mb) assay.

In 2016 Klein and coworkers used gas phase FTIR to confirm that the rate of CO release was dependent on the rate of formation of the intermediate, which released CO at a constant rate with a half-life of 33 min, and that the pH of buffered solutions increased the intermediate rate formation.[47] This peculiar mechanism, different from the one of other CORMs, allows CO release from CORM-A1 with tunable rate through adjustments of pH and temperature, by changing the rate of protonation and decomposition, respectively. The CO release from this non-metallic compound is strongly influenced by the presence of other molecules. Bauer and coworkers identified NAD^+ and $NADP^+$ as accelerators of CO release, while H_2O_2 seemed to diminish and, when present in high excess, abolish its liberation.[19] CORM-A1 induces a gradual, significant dose-dependent vasorelaxation over time in isolated aortic rings. Besides, the *in vivo* treatment with this compound caused a moderate drop in arterial pressure. The CO-depleted form of CORM-A1 is inactive and does not exhibit the same impact, suggesting that CO is the mediator of the reported effects.[45]

3.2. Enzyme-triggered CORMs

At first, Schmalz and coworkers developed a novel idea known as "enzyme-triggered CO-releasing molecules (ET-CORMs)".[48] Dienol-$Fe(CO)_3$ compounds, featuring acycloxybutadiene ligands, easily decompose under mildly oxidative environments, which are triggered through enzymatic cleavage of the ester moiety by the intracellular esterases.[48,49] The ancillary ligands (cyclohexenone or cyclohexanedione) and the ester group that they include have a significant impact on the CO release activity and, consequently, on their biological activity. On the contrary, the equivalent enones in cyclohexanedione ET-CORM have no effect on the biological behaviour. The mechanism at the basis of the CO release from ET-CORMs typically involves two steps: first, hydrolysis of the ester, then oxidation of the resultant dienol-$Fe(CO)_3$ moiety to release CO, Fe-ions and the associated ligand (Scheme 2).[50] The variable biological activity was thought to be a reflection of how easily dienol-$Fe(CO)_3$ intermediates are oxidised.[42]

3.3. Redox

It has been reported that some Mo(0) and Fe(0) carbonyls can release carbon monoxide when exposed to ambient oxygen, changing the oxidation state of M^{n+}. Na[$Mo(CO)_3$(histidinate)], ALF186, can easily release all its three CO molecules *in vitro* and *in vivo* under biological conditions. Decarbonylation of ALF186 occurs after metal oxidation by O_2, the event that causes CO delivery and quick diffusion into the blood stream after injection *in vivo*. In the dark at 37 °C, ALF186 easily releases 75% of its total CO content (2.26 equivalents) in 2 h and one equivalent after about 30 min. Additionally, no CO is emitted under the comparable anaerobic conditions. The complex is not haemolytic and has minimal cytotoxicity.[51] Also, CORM-401 (Fig. 1) was found to interact with reactive oxygen species (ROS), which are widely acknowledged as essential mediators in CO signalling actions.[52]

3.4. Photoinduced CORMs

If CORM-2 spontaneously releases CO when injected into living tissues, other MCCs have been studied as photochemical CO-releasing agents since they do not release CO spontaneously but only when irradiated. In this respect, it should be underlined that the use of light as an external stimulus is advantageous, since light beam is non-invasive and can be easily changed in terms of energy, frequency, and spatial location. As a result of the fact that some MCCs release CO when lighted, these molecules also can regulate CO delivery. From a biological standpoint, a photoinduced CORM, photoCORM as it was called by Ford *et al.*,[53] and its photo-

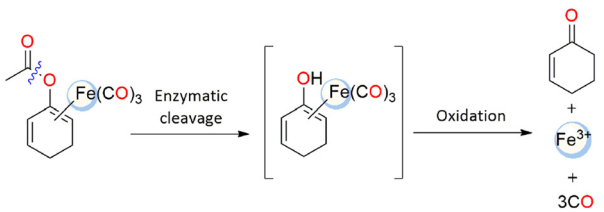

Scheme 2 Possible enzyme-triggered CO release mechanism from an ET-CORM.

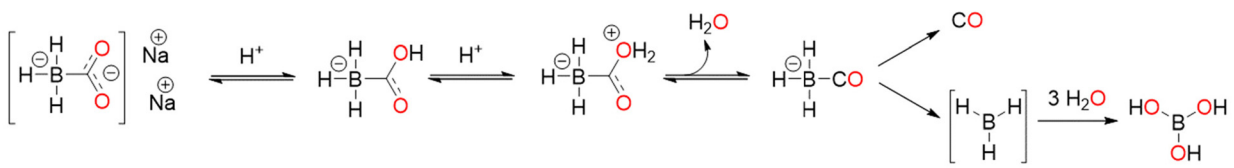

Scheme 1 Possible CO release mechanism of CORM-A1.

products, or iCORM, should be safe. Given that CO-depleted species have to be non-toxic, they should be identified and characterized and their reaction/interaction with the medium, oxygen or biomolecules should be studied. Besides, photoCORMs ought to be stable and soluble in aqueous solution at r.t. or, at the very least, soluble in mixed solvents like aqueous/dimethyl sulfoxide (DMSO) solutions, which are often used for testing the biological activity of metallodrugs. PhotoCORMs must release CO only after stimulation with a proper wavelength. Different excitation wavelengths can be used, depending on the MCC features, *i.e.*, the stability and the strength of the carbonyl-metal bond. It should be desirable the use of red light so that it can be irradiated through skin. The ability of the photoCORM to absorb visible light is vital for photo delivery to biological targets and stability.[54] An important limit of photoCORMs is their difficult localization after administration due to the rapid diffusion; the conjugation or functionalization with peptides, polymeric matrices or other supramolecular structures is a common strategy to get over toxicity to untargeted healthy tissues.[55]

Kinetic investigations have been conducted to unveil details of CO release mechanism and possible formation of intermediates during the illumination of photoCORMs, in particular using Mn(I) tricarbonyl complexes.[56–59] Quantum chemical calculations, in solution IR and EPR spectroscopy demonstrated the formation of $Mn(CO)_2$ species, upon illumination, which were easily oxidized in subsequent dark processes.[56,57] From Mn(I) tricarbonyl complexes, only one CO molecule is released photolytically; the remaining CO molecules require a second dark process. One CO molecule was photochemically released on very short timescales, according to femtosecond transient absorption UV pump/mid-IR probe spectroscopic studies; however, a portion of the excited molecules were shown to undergo geminate recombination.[59] It was confirmed by Lynam and Fairlamb[60] that illumination of tricarbonyl Mn (I) complex at 400 nm, in acetonitrile, resulted in loss of one CO and in the formation of a triplet dicarbonyl Mn(I) analogue, where the vacant coordination position is occupied by a solvent molecule. The lifetime of the dicarbonyl species was 20 ps. This species does not change during the experiment (800 μs), so any additional CO thermal loss must occur more slowly than 800 μs.

4. First-generation CORMs

Several studies have been done on the first-generation CORMs (CORM-1, CORM-2, and CORM-3), CORM-A1 and CORM-401. Therefore, it is essential to get an insight into the main features of these compounds and their biological impact.

4.1. CORM-1

In 2002, Motterlini and co-workers revealed that CORM-1 could release CO upon activation by cold light source. CORM-1 releases CO *via* dissociation and not by Mn–Mn cleavage.[61] Mimicking endogenously generated CO, CORM-1 triggers vasodilation on rat aortic rings contracted with phenylephrine, decreases coronary vasoconstriction *ex vivo* and acute hypertension in animal models. It was also noted that CORM-1 does not exhibit cytotoxic effects.[37]

In 2004, the effects of 50–600 μM CORM-1, genuine CO and non-adrenergic noncholinergic nerve stimulation on the internal anal sphincter (IAS) were compared. CORM-1 causes relaxation to the rat IAS, in a dose-dependent fashion, and its influence is not affected by neurohumoral antagonists as propranolol, hexamethonium, guanethidine, indomethacin and atropine. Also, the HO inhibitor Tin-protoporphyrin IX (SnPP-IX) used to show non-adrenergic noncholinergic relaxation suppression does not influence the effects of CORM-1. Conversely, the guanylate cyclase inhibitor ODQ decreases the relaxation of IAS caused by CORM-1.[62] Following the light stimulation, CORM-1 was found to have concentration-dependent vasodilatation in isolated porcine cerebral arterioles.[63,64] The CO released by CORM-1 elevates Ca^{2+}-activated potassium channels (KCa) activity by 4.9 and 3.5 times, respectively, in new born pig cerebral arteriole smooth muscle cells. In such cells, the KCa channels have poor Ca^{2+} sensitivity, and CO stimulates KCa channels *via* increasing Ca^{2+} sensitivity.[65] In Sprague-Dawley rats, intrarenal administration of CORM-1 increases renal blood flow, COHb levels, glomerular filtration rate, and subsequent urinary cGMP excretion. The renal protective role of HO is suppressed by the HO-inhibitor Co(III) Protoporphyrin (CoPP). Co-treatment with CORM-1 and CoPP reverses the inhibition effect on HO activity that could cause renal failure. In addition, CORM-1 elevates renal NO levels and nitrates/nitrites excretion, implying that alterations in NO release could contribute to the HO–CO system's renal effects.[66] To enhance the water solubility and bioavailability, Schiller and co-workers embedded for example CORM-1 into poly(L-lactide-*co*-D/L-lactide) fibres to produce nonporous non-woven. The CO release rate depends on frequency since the complex released CO four times faster after irradiation at 365 nm than at 480 nm. The non-woven released 3.4 μmol of CO per mg. The hybrid complex has no cytotoxic activity in the dark against 3T3 mouse fibroblasts but exhibits strong photo-cytotoxicity when irradiated at 365 nm.[67] The hydrophobicity of CORM-1 also encouraged the design and synthesis of a drug delivery system able to transport hydrophobic substances, including polymeric micelles and microbubbles (MB). In this frame, CORM-1-containing polymeric microbubbles (CO-MBs) have been developed. This has allowed for the ultrasound and magnetic resonance imaging-driven light-activated CO release. CO-MBs release one CO mole per mole of loaded CORM-1 upon irradiation. The results show that CO-MBs are promising theragnostic agents for reducing hypoxia-related and ROS-mediated damage to cells and tissues in cardiovascular disease.[68]

4.2. CORM-2

Motterlini and co-workers showed how CORM-2 instantly releases CO into organisms with a reported yield of 0.7 mol of CO per mole of CORM in DMSO/PBS solutions (pH 6.8). This

process is favoured by CORM-2 ligands exchange with solvent molecules like DMSO, as reported in Scheme 3. In fact, CORM-2 spontaneously liberates CO in contrast to CORM-1, which needed cold light as a trigger.[37] According to ^{13}C NMR spectroscopy, the freshly dissolved CORM-2 does not appear as a dimer in DMSO, since two distinct peaks corresponding to di-carbonyl and tri-carbonyl monomers were observed. It is probable that during the dissolution stage, DMSO behaves as a metal coordinating ligand encouraging the formation of monomers (Scheme 3). The appearance of di-carbonyl monomers may be taken as evidence that CO has been released.[37] In DMSO, the CO release from CORM-2 is slow with several reaction routes, that are involved in the formation of mono-, di- and tricarbonyl Ru(II) species.[69]

At r.t., the dimeric CORM-2 easily releases CO in murine serum, whereas the monomeric Ru(II) species do not. This indicates that a significant portion of CORM-2 in the presence of DMSO is inactive. Photochemical stimulation causes CO release from the inactive molecules. For this reason, the combination of thermal and photochemical techniques can significantly enhance CO delivery yield.[70] CORM-2 interferes with coagulation factors and enhances thrombus formation. In fibrinogen-deficient plasma, the modification of fibrinogen concentration with CORM-2 dramatically increases clot formation velocity (30–50%).[71] 20 μM of CORM-2 persuaded hydrogen peroxide induces cell damage as determined by lactate dehydrogenase (LDH) release from rat cardiomyocytes. On the other hand, the LDH activity is directly suppressed by 400 μM CORM-2. CORM-2 and its CO depleted form (iCORM-2) as well as the CO gas reduce the cisplatin-stimulated caspase-3 activity in Madin–Darby canine kidney MDCK and HeK cells, implying an anti-apoptotic action. Alternatively, CORM-2 and iCORM-2 cause considerable cell damage, including reduced viability, aberrant cytology, elevated apoptosis and necrosis, cell cycle arrest, and decrease mitochondrial enzyme activity. Low doses of CO, released from CORM-2, display cytoprotective properties. These findings indicate that iCORM-2 is cytotoxic, and that its build up would severely restrict its potential clinical use.[72] CORM-2 (10–100 μM), and not iCORM-2, inhibits the lipopolysaccharide-induced inflammation in murine RAW264.7 macrophages in a dose-dependent fashion.[73,74] CORM-2 reduces liver inflammation in septic mice,[75] LPS (lipopolysaccharide)- or CLP (cecal ligation and puncture)-induced endotoxemia and sepsis,[76] and has anti-inflammatory actions on the progression of intestinal ischemia–reperfusion injury (IRI) in rats suffering haemorrhagic shock.[77] Also, CORM-2 possesses CO-mediated reduction in leukocyte infiltration in harmed mice intestines *via* the interference with activation of nuclear factor κB (NF-κB), which is important for cellular proteins expression *via* a CO-regulated signalling pathway,[78] and intercellular adhesion molecule 1 protein expression, hence decreasing endothelial cells' pro-adhesive character.[79] CORM-2 can regulate a variety of genes with roles in intestinal inflammation and tumour development.[80]

CORM-2 has also other potential medicinal applications, including cardioprotective,[81] antimicrobial,[82–86] analgesic, and anti-nociceptive actions,[87] anti-apoptotic,[88] and angiogenic capabilities.[89] Also, it possesses CO-mediated protective effect to the kidney against ischemic injury.[90] After being dissolved in 10% (v/v) DMSO, CORM-2 was included in a basic cosmetic oil-in-water emulsion to produce a topical lotion. Topical CORM-2 treatment diminishes the chronic acute inflammatory erythema and epidermal hyperplasia following tumour effects

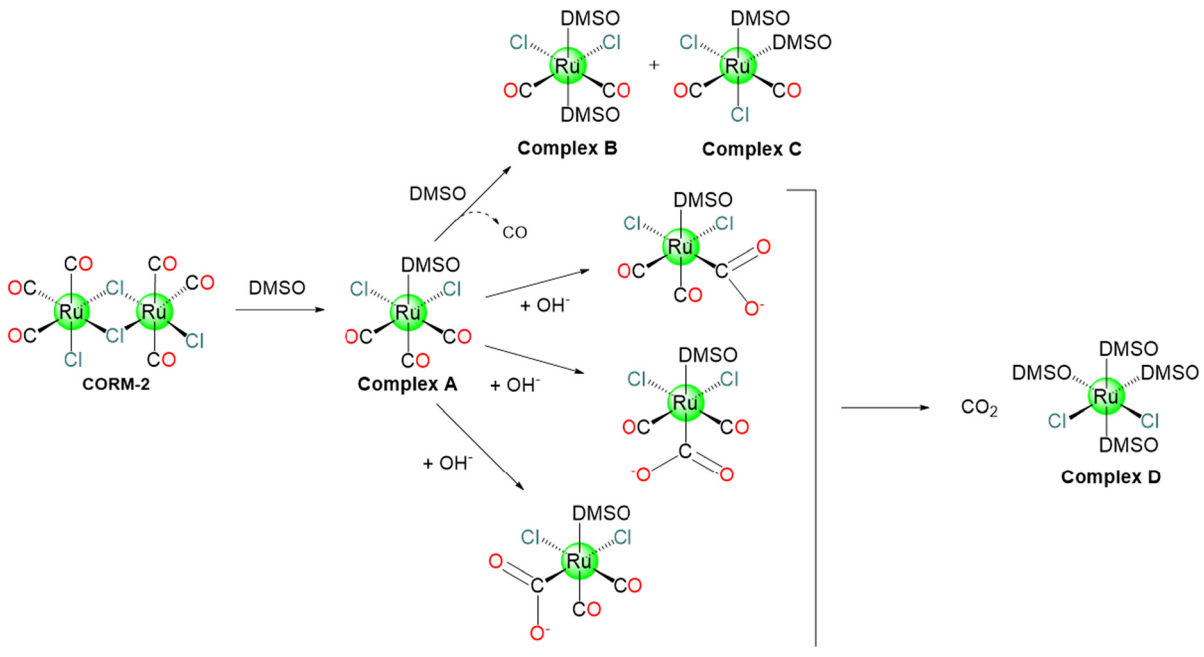

Scheme 3 Possible CO release mechanism of CORM-2.

in albino Skh-1 hairless mice with UVB-induced photo-carcinogenesis. CORM-2 provides a significant dose-dependent medium suppression of early tumour appearance.[91] Additionally, CORM-2 inhibits the abnormal growth of pulmonary artery smooth muscle cells in humans, accompanied with pulmonary hypertension.[92]

The therapeutic potential and inflammatory action of CORM-2 on a murine orthotopic lung cancer model was assessed *in vivo*. 80 mice were divided into two sets, control set and orthotopic lung cancer set. The tumour set was either left untreated or treated with DMSO or CORM-2. The body weight of the control group increased over time, whereas it greatly decreased in the tumour group. Administration of CORM-2 significantly reversed this negative effect and increased body weight significantly. It also increased the thymus and spleen indices. Treated mice showed no evident cancer emboli formation. CORM-2 inhibited local inflammation reaction as well as the central intracellular protein synthesis signalling, which in turn restricted abnormal cell proliferation and cancer.[93] 100 μM of CORM-2 and iCORM-2 reduce the viability of human primate peripheral blood mononuclear cells (PBMCs) and human leukaemia HL-60 cells. Also, CORM-2 and iCORM-2, in the concentration range of 0.01–100 μM, cause DNA damage. CORM-2 significantly decreases H_2O_2-induced oxidative stress in normal and cancer cells, while iCORM-2 increases the free radical levels of HL-60 cells in the presence of H_2O_2. Both CORM-2 and iCORM-2 exhibit geno- and cytotoxicity, antioxidant actions and the potential to induce the HO-1 gene. These effects could be caused by both the released CO and iCORM-2.[94]

Nanocomposites of ferritin (Fr) with CORM-2 have been prepared and tested for their ability to release CO *in vitro* and *in vivo*.[95] The X-ray structure of this molecule reveals the existence of 72 Ru binding sites at level of Glu, His and Cys residues. The CO release ability of the nanocomposites can be regulated by changing the metal ligands, using single point Fr mutants. It has been shown that the protein cage improves the performance of the CORM, significantly increasing its uptake and $t_{1/2}$ value for CO release that is 18-fold higher than CORM-3. Besides, the uptake of the nanocomposite is approximately four times higher than that of CORM-3 itself. Indeed, Fr enters the cell *via* receptor-mediated endocytosis. The nanocomposites also increase nuclear factor kappa B (NF-κB) activation 10-times more than CORM-3.[96] Using CORM-2, Ueno and co-workers also prepared Ru^{II} carbonyl-incorporated cross-linked hen egg white lysozyme (HEWL) crystals that release CO and significantly increased NF-κB activity.[97]

Overall, these data strengthen the potential of CORM-2 to act as a cytotoxic molecule able to trigger and interfere with different biological pathways. However, despite this evidence, many studies have highlighted the issues related to the lack of CO release from CORM-2 assessing that it does not reliably and efficiently deliver CO and questioning its role as donor for studying CO biology. Bauer and coworkers summarized most of the relevant data regarding this point.[19] These studies finger-point the most used method to follow CO release, the Mb assay, as responsible of an oversight that has hampered the recognition of the effects of $Na_2S_2O_4$ (sodium dithionite, used in the Mb assays) in facilitating CO release from CORM-2. The first insight was given by McLean in 2012, who stated that CO released from CORM-2 strictly depends on the sulphite species. Interestingly, it was found that in potassium phosphate buffer, CORM-2 did not release CO in the presence of reduced myoglobin alone, but only when a 0.1% Na-dithionite is added to the reaction mixture. In the same way, other sulphite compounds were also found to promote the release of CO.

4.3. CORM-A1

CORM-A1, $Na_2[H_3BCO_2]$, was proposed in 2005 by Motterlini and co-workers as a water-soluble borane-based CO donor. It releases CO, *via* the protonation process, slower than CORM-3. Dehydration caused by protonation was suggested to produce an unstable intermediate, a borane-carbonyl complex, which releases CO spontaneously. Based on Mb assay, the $t_{1/2}$ values of 60 μM CORM-A1 in 0.04 M PBS solutions at r.t. were found to be 2.5 min and 21 min at pH = 5.5 and 7.4, respectively.[45] Over the time, in isolated aortic rings, CORM-A1 induced a dose-dependent vasorelaxation that was inhibited by guanylate cyclase inhibitor ODQ and greatly increased by guanylate cyclase stimulator YC-1. Like this, pretreatment with YC-1 significantly enhanced the modest drop in mean arterial pressure that resulted after the *in vivo* injection of CORM-A1 (30 μmol kg^{-1} i.v.). iCORM-1 did not increase hypotension or vasorelaxation.[19,45] According to Chlopicki and co-workers, CORM-A1 modulated platelet bioenergetics to prevent platelet aggregation. The loss of cytosolic NAD^+ was found to be the cause of the antiplatelet action of CORM−A1, which in turn prevented glycolysis and mitochondrial respiration.[98] In mice, the release of CO from CORM-A1 results in a decrease in renal vascular resistance and an increase in renal blood flow (RBF).[99] CORM-A1 possesses strong antioxidant and antiapoptotic effects[100] and could be a promising therapy for non-infectious posterior uveitis.[101]

4.4 CORM-3

CORM-3 was proposed in 2003 by Motterlini's group and introduced as a "quick releaser" to generate one mole equivalent of CO (measured as COMb) ($t_{1/2}$: 4 to 18 min) at pH 7.4 in PBS and biological fluids (cell culture media, human blood plasma).[37] The molecule originates from CORM-2 and glycine.[43] CORM-3 is stable in water for more than 24 h at 37 °C and at acidic pH. However, because of the lability of the chloride and glycinate ligands, in biological fluids and physiological solutions, it releases CO[43] upon replacement of these ligands with higher metal affinity ligands, *e.g.*, glutathione. Such liability also allows CORM-3 to bind blood proteins. As it happens for CORM-2, CORM-3 mostly produces CO_2, not CO, under near-physiological conditions in the absence of a strong nucleophile or a reducing agent (Scheme 4).[19]

CORM-3 exhibits a $t_{1/2}$ value of 98 h at 37 °C in distilled water, while only 3.6 min in human plasma.[102] In solution,

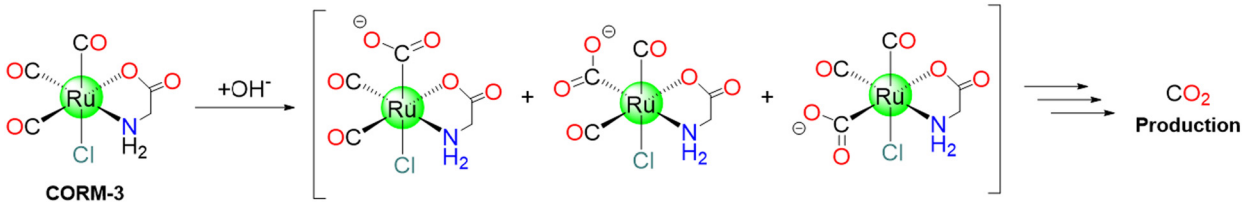

Scheme 4 Possible CO_2 release mechanism of CORM-3.

CORM-3 exhibits a pH-dependent equilibria. At pH = 3, it is readily produces the $[Ru(CO)_2(CO_2H)Cl(glycinate)]^-$ species. At physiological pH, $[Ru(CO)_2(CO_2H)OH(glycinate)]^-$ and $[Ru(CO)_2(CO_2)Cl(glycinate)]^{2-}$ coexist in solution.[102] In 2011, Santos and coworkers, using gas chromatography (GC) equipped with a thermal conductivity detector (GC-TCD), revealed that when CORM-3 is dissolved in aqueous solutions and closed in a flask, only CO_2 can be detected. This can be explained considering this mechanism: one CO is attacked by a water molecule, leading to the formation of CO_2. The results imply that plasma proteins, lacking haem, accelerate CORM-3 decomposition by allowing the formation and release of CO_2, that is accelerated by covalently binding of *cis*-$Ru^{II}(CO)_2$ moieties to protein residue side chains. The reaction with haem-containing proteins, like Mb, on the other hand, proceeds in a distinct manner because one of the three CO ligands is swiftly delivered to the haem. Also in this case, the remaining *cis*-$Ru^{II}(CO)_2$ moiety binds the protein.[103]

To probe at molecular level what happens when CORM-3 interacts with proteins, different techniques have been used. Inductively Coupled Plasma-Atomic Emission Spectroscopy (ICP-AES), Fourier-transform infrared spectroscopy (FTIR), Liquid-Chromatography Mass Spectrometry (LC-MS)[103] and crystallographic studies demonstrated that this molecule is able to bind different human proteins (for example serum albumin (HSA), transferrin and haemoglobin) but also small model proteins, like horse heart Mb and HEWL.[104] In this respect, useful information on the structure of the final adduct (s) formed between CORM-3 and proteins have been gained by solving the molecular structure of its HEWL adduct.[103] The X-ray structure, refined at 1.67 Å, shows that a Ru $(CO)_2$fragment binds the protein at level of one His (His15) and two Asp (Asp18 and Asp52) side chains (Fig. 2). Thus, the two ancillary ligands and one CO are released upon the protein binding. Water molecules complete the metal coordination sphere.

These findings indicate that in the CORM-3 protein adducts one CO ligand is lost. In preclinical research, CORM-3 was found to exhibit intriguing biological properties,[105–107] such as cardioprotective,[61,108] vasodilatory,[43,109] anti-oxidant,[110] anti-inflammatory,[111–113] antibacterial,[31,114–116] anti-ischemic,[106,117,118] and anti-apoptotic[119–121] activities. A few noteworthy instances of the therapeutic efficacy provided by CORM-3 include the prevention of myocardial infarction and heart failure,[107,122,123] kidney protection from cisplatin

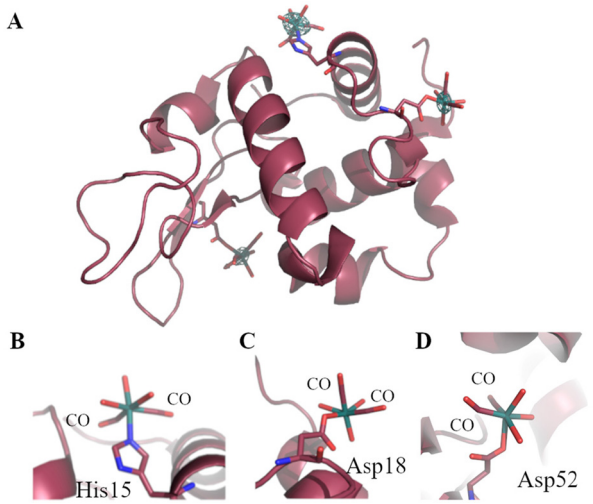

Fig. 2 Ribbon model of the adduct formed when CORM-3 reacts with HEWL (A). The $Ru(CO)_2$ fragments bound to His15 (B), Asp18 (C) and Asp52 (D) are highlighted. In panel A, anomalous difference electron density map close to the Ru centres is reported in green at 3.0σ.

toxicity[124] and the improvement in tissues preservation for transplantation.[108] Also, CORM-3 exhibits neuroprotective effect in rats,[125] as well as suppression of growth, invasion, and metastasis in tongue squamous cell carcinoma (TSCC) cells.[126] CORM-3 (10–100 μM), but not iCORM-3, suppresses LPS-induced inflammation in murine RAW264.7 cells. When CORM-3 is added 3 or 6 h after LPS exposure, it reduces nitrite levels. CORM-3 also significantly lowers the levels of tumour necrosis factor-α (TNF-α), another mediator of inflammatory functions.[73] In ischemia-induced acute renal failure (ARF), CORM-3 exhibits CO-mediated protective effect against renal damage.[90] The toxicity of CORM-3 is low as cynomolgus monkeys displayed no negative impacts after having a dose of 4 mg kg^{-1} for one month.[127] CORM-3 suppresses both the generation of $O_2^{\bullet-}$ (IC_{50} = 1.66 μM) and CD11b expression (IC_{50} = 1.20 μM) in human polymorphonuclear neutrophils (PMNs) and reduces CD54 and CD203 expression as well as histamine release in perivascular mast cells (MCs) with IC_{50} values of 6.78, 1.18, and 1.15 μM, respectively. CORM-3 has a potent anti-inflammatory effect by suppressing the oxidative burst in PMNs, overexpression of adhesion molecules in PMNs and vascular endothelial cells, histamine release, and MCs overexpression of an activation marker.[128] The pharmacologic

activities of CORM-3 on porcine aortic endothelial cells (PAEC) and PBMC were evaluated *in vitro*. High PAEC proliferation was noticed at doses of 300 and 500 μm of CORM-3, but at higher concentration (≥50 μm) it reduced ConA-activated primate lymphocyte proliferation as well as the primate xenogeneic reaction towards pig PBMC. These effects have been shown to be CO dependent.

TNF-α production is considerably suppressed *in vivo* when several doses of CORM-3 are administered. These findings indicate that CORM-3 possesses anti-inflammatory and immunomodulatory characteristics in primates, which may have clinical implications for allografted and xenografted organs.[129] In the concentration range of 1–20 μM, CORM-3, but not iCORM-3, dramatically elevates the mitochondrial oxygen consumption rate. Conversely, 100 μM of CORM-3 inhibit the *cytochrome c* oxidase and thus the ADP-dependent respiration. In the presence of Mb, the uncoupling action mediated by CORM-3 was blocked. CORM-3, but not iCORM-3, is a regulator of mitochondrial respiration, rising the levels of H_2O_2 that respiration generates.[110] CORM-3 has DNA as biological target, but the mode of action is quite different from cisplatin, since Ru(II) does not generate intramolecular DNA cross-links. It was verified that CORM-3 causes a significant increase in DNA strand breakage in poorly differentiated colon carcinoma RKO cells as evidenced by alkaline comet test.[130] A variety of challenges, including the instability of CORM-3 in water, short $t_{1/2}$ value (see paragraph 4.3) in human plasma, and limited cellular absorption, are impeding its clinical development.[36] Due to their instability, poor water solubility for CORM-2, lack of selectivity, and questionable reactivities to biomolecules, the clinical use of CORMs as therapeutic drugs is constrained.[24]

4.5. CORM-401

CORM-401, $[Mn(CO)_4\{S_2CNMe(CH_2CO_2H)\}]$ (Fig. 1), was introduced by Motterlini and co-workers in 2011.[131] CORM-401 releases 3.2 moles of CO molecules with $t_{1/2}$ = 0.8 min *via* dissociative reversible mechanism. It is soluble and stable in aqueous media, but CO is rapidly released in the presence of a CO receptor, such as Mb, that hampers the rebinding of CO.[131] When CORM-401 is pre-incubated in the presence of Na-dithionite, CO release is detected. The CO release is still detectable when CORM-401 is in buffer alone. As a result, while Na-dithionite is not necessary for CO release from CORM-401, but it does increase the CO release kinetics.[132] So, Hb-CO assay is performed as a suitable alternative to the Mb assay. The fact that CORM-401 releases three times more CO than CORM-3 (3.2 equiv. *vs.* one equivalent) makes it feasible to be administered in much less quantity.[131]

A CO release mechanism by CORM-401 was proposed on the basis of computational data.[133] The calculations suggest that CO release occurs *via* a three-step mechanism, involving: dissociation of an axial CO ligand from Mn; binding of a nucleophile to the vacant position and formation of an intermediate that then dissociates and releases CO (Scheme 5).

Since its discovery, CORM-401 showed a variety of therapeutic applications, including anti-inflammatory,[134–136] antibacterial,[136–139] angiogenic,[140] anti-carcinogenic,[141,142] anti-metastatic, anti-ischemic,[143] and cytoprotective properties under the oxidative stress caused by H_2O_2.[144,145] A photodynamic therapy (PDT)-driven, controlled CO release system, was constructed using CORM-401. Exposure to near-IR light triggered fast intracellular CO release from CORM-401 by limiting the H_2O_2 generated during PDT. *In vitro* and *in vivo*, the integration of PDT and CO therapy had strong synergistic anticancer benefits and enhanced therapeutic safety.[146,147] For treatment of diabetic wounds, a multifunctional hydrogel dressing containing CORM-401 was designed. The CORM-401 dressing demonstrated blood glucose control, CO dependent antioxidative stress, antibacterial and anti-inflammatory activities.[148] The cell viability of murine RAW264.7 macrophages was lowered by 25% when 100 μM of CORM-401 was administered, while nitrite generated in response to one μg ml^{-1} lipopolysaccharide (LPS) treatment decreased by 70%.[131] In addition, a two-part metabolic reaction takes place by CO delivered by CORM-401 which are inhibition of glycolysis,[148] and uncoupling of mitochondrial respiration.[148,149] It was reported that the oral administration of CORM-401 lowers body weight gain and enhances insulin resistance in an obese model.[149]

Even after considering all the prior successes of first-generation CORMs, there are still unresolved issues that present intriguing challenges for researchers. When it comes to the chemical and physical CORMs features, which molecule has the main role, the CORM or the iCORM? In addition, some reports concluded that, in the absence of a strong nucleophile or reducing agent, CORM-2 and CORM-3 primarily produce CO_2 rather than CO, under conditions close to the physiological ones. Furthermore, it is known that such CORMs are extremely reactive towards a variety of biologically relevant molecules and that reaction with an oxidant and/or a nucleophile influences or completely determines the amount of the released CO. The reactivity of such CORMs towards biomolecules has been rarely examined.

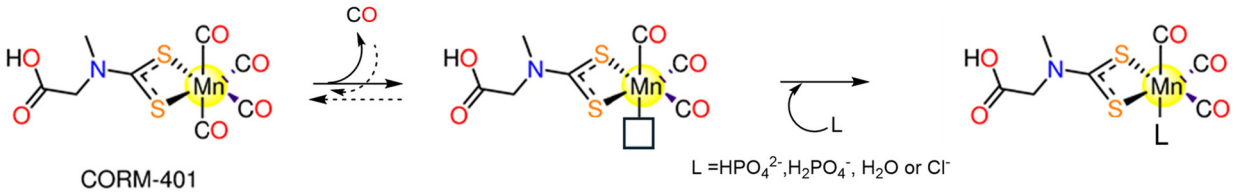

Scheme 5 Possible CO release mechanism of CORM-401.

5. Detection of carbon monoxide

The CO release rates in CORMs must be measured and quantified using reliable and precise methods. A variety of assays have been developed to measure the release of CO, including colorimetric CO sensing,[150] myoglobin assay,[132] laser infrared absorption,[151] and GC.[152] GC-TCD is used as gold standard in the quantification of CO from different sources, providing information also on the amount of other gas species.[53] However, this method is not efficient when a continuous monitoring of the reaction is needed.[153] In the Mb assay, the formation of CO is detected and quantified spectrophotometrically. The reduced deoxy-Mb interacts with the released CO producing carbonmonoxy-Mb (MbCO). The deoxy-Mb absorption band at 557 nm declines whereas the MbCO absorption bands at 540 and 577 nm rise. Despite myoglobin assay has been and still is widely utilized its efficacy was questioned due to long-term instability, interference with coloured CORMs, turbidity and CO loss from the CORM being reliant on the quantity of $Na_2S_2O_4$ used as a reducing agent.[132,155]

FTIR analysis was also used to quantify CO release from CORMs,[53] because of the distinctive band at 2142 cm^{-1} of CO gas. It should be noted that FTIR spectra are largely dependent on total gas pressure. For this reason, CO detection in different samples should be carried out at the same total pressure of 1 atm.[24] Rimmer and co-workers conjugated FTIR technique with GC equipped with a thermal conductivity detector (GC-TCD).[53] This approach can track the CORM breakdown's CO release in real time. This may be carried out immediately in the reaction chamber without gas extraction from the sample. In the case of CORMs that are light-activated, the irradiation can be directly coupled to the setup. Hence, it is possible to measure CO *in situ* during the irradiation. Moreover, IR absorption spectroscopy may also quantify and identify various gaseous byproducts.[153]

cis-$[Rh_2(C_6H_4PPh_2)_2(O_2CCH_3)_2](CH_3COOH)_2$ was used as a chromogenic technique for CO detection. The interchange of the axial acetic acid ligands with CO causes colour variation from violet to orange yellow. The probe has remarkable recognition properties, for instance a visible colour shift at concentrations of CO that begin to be harmful (50 ppm). However, the rhodium complex dissolves well only in organic solvents making its utilization for detection and quantification difficult.[154]

CO can be detected also using fluorescent probes. Some research groups employed a cyclopalladated probe (CO Probe 1, COP-1) to perform palladium-mediated carbonylation process. Through heavy-atom electronic effects, the Pd atom quenches the fluorescence of boron dipyrromethene (BODIPY). Binding of CO to the cyclopalladated probe leads to production of Pd(0) and strongly fluorescent BODIPY dye. The emission increases 10 times in the presence of CO, with a minimum detectable concentration of one μM of CO. The palladium probe is non-toxic and may be used in biological systems.[156]

Another research group used a haem protein in the fabrication of another fluorescent probe, named COSer. This sensor can bind CO specifically because it contains a circularly permuted yellow fluorescent protein that has been introduced into the regulatory domain of the CO-sensing protein from bacteria. In response to CO, the fluorescence intensity of the probe doubles after 10 min.[157] In contrast to COSer, the COP-1 probe amplifies the fluorescence signals more. The irreversible interaction between CO and COP-1 probe adds an advantage to COP-1 compared to the reversible one in the case of COSer. Both COSer and COP-1 serve distinct functions; COSer can be used for real-time detection of CO, while COP-1 is more efficient for detection of low CO concentrations because of its great sensitivity.[158] In general, the ability to detect low concentrations of CO quickly and selectively is crucial. So, more specific, sensitive, and quantitative CO detection techniques are required to avoid the drawbacks of the previously mentioned methods.

6. Next generation CORMs

For researchers interested in investigating the potential of using MCCs as CO delivery systems, the complexes by Motterlini and co-workers marked a turning point. They were inspired to continue their trials to develop CORMs based on other metals and co-ligands that could be used to deliver CO clinically. It was rapidly apparent that to develop stable, biocompatible CORMs that could be activated both internally and externally, it was necessary to find specific metal–CO patterns and unique ligand design principles. Metals like Cr, Mn, Co, Ni, W, and Mo interact with CO gas to generate volatile MCCs even when the metals are in their elemental solid state. Metal carbonyls of groups 3–5, 9 and 10, have not been examined as CORMs because of their lability. The most promising metal candidates for CORMs, except for the radioactive element Technetium, are those from Group 6 (Cr and Mo), Group 7 (Mn and Re) and Group 8 (Fe, and Ru), which satisfy the 18-electron rule. Due to their highly regulated substitution chemistry and oxidative stability, Mn(I) carbonyl derivatives can be employed with many auxiliary ligands, including biomolecules. Unfortunately, there is worrying evidence that Mn is toxic in the brain, hence it is highly advised against using drugs that contain Mn.[159] Contrarily, ruthenium has been tested on animals in a variety of potential antitumour drugs,[160] and NO-scavenging compounds, and has been found to be non-toxic.[161] In addition to Mn(I) (Table 1) and Ru(II) ions, metal carbonyls of other elements such as Co(0), Fe(0), and Re(I) have been investigated in the context of CORMs with an emphasis on their CO releasing kinetics and cytotoxic properties (Table 2). In the next section, the ability of these CORMs to release CO under various conditions and their cytotoxic characteristics were discussed.

6.1. Manganese(I) CORMs

In 2008, the research group of Schatzschneider examined the potential of **1** (Fig. 3) to release CO when irradiated with UV light (λ = 365 nm).[162,163] About 1.96 moles of CO were released

Table 1 Summarized results regarding Mn-based photoCORMs with cytotoxic activity against different cell lines

CORM	Activation wavelength	Solvent used	CO release kinetics	CO equivalents (Myoglobin assay)	Experimental cancer model	Anticancer activity	Ref.
Manganese(I) CORMs (section 6.1)							
1	365 nm	DMSO		1.96 moles	HT-29	When irradiated, **1** reduced the cell biomass by 30%.	162
2	≥520 nm	CH_2Cl_2, CH_3CN and 20% (v/v) CH_3CN/H_2O	k_{CO} (min^{-1}): 21.94 ± 0.01 (CH_2Cl_2) 11.216 ± 0.01 (φ_{550}: 0.48 ± 0.01) (CH_3CN) 4.987 ± 0.01 (CH_3CN/H_2O)		HeLa and MDA-MB-231	About 60% reduction in cell viability upon illumination.	165
3	≥520 nm	CH_2Cl_2	k_{CO}: 15.28 ± 0.01 min^{-1}				165
4	10–15 mW visible light	CH_2Cl_2, CH_3CN, 20% (v/v) DMSO/H_2O and 40% (v/v) CH_3CN/H_2O	k_{CO} (min^{-1}): 4.32 ± 0.01 (CH_2Cl_2) 1.05 ± 0.01 (CH_3CN) 0.23 ± 0.01 (CH_3CN/H_2O) 0.61 ± 0.01 (DMSO/H_2O)		MDA-MB-231	**4** decreased the cell viability by 50% upon illumination *via* CO-triggered apoptosis.	166
5	365 nm	CH_2Cl_2 DMSO		1.3 moles	A549, HeLa, HCT-15 and normal PBMCs	Suppression to colon (7.15 ± 0.24 μM), lung (12.5 ± 1.33 μM), and cervical (20.7 ± 0.94 μM) cells upon illumination. Nontoxic to PBMCs.	167
6a–6e	365 nm	DMSO	$t_{1/2}$ (min) = 5.7, 6.4, 4.8, 9.5 and 6.9 in that order.	**6a–6e**: 2.4, 1.0, 2.1, 1.4, and 2.0 equiv.	MCF-7	IC_{50}/UV (μM) = 3.1 ± 0.1, 21 ± 1, 10 ± 1, 2.91 ± 0.07 and 9.7 ± 0.6 in that order.[a]	168
7a–7e	366 nm	DMSO PBS	$t_{1/2}$ (min) = 9.5, 11.4, 13.9, 3.9 and 8.7 in that order.	**7a–7e**: 1.4, 1.4, 1.5, 1.7, and 2.2 equiv.	MCF-7	**7a–7e** are cytotoxic under dark and light conditions. IC_{50}/UV (μM) = 2.91, 12.25, 1.79, 1.43 and <1 in that order.[b]	169
8a–8b	Low-power visible light	PBS, and CH_3CN.	k_{CO} (min^{-1}): PBS: 1.54 ± 0.02 (**8a**), 0.44 ± 0.02 (**8b**) CH_3CN: 0.91 ± 0.02 (**8a**), 0.51 ± 0.02 (**8b**)		MDA-MB-231	The cell viability is decreased by 50% upon illumination.	170
9	365 nm	DMSO			HeLa, A549, and HCT-15	IC_{50} (μM): 15.7 ± 0.98 (A549) and 28.7 ± 0.16 (HCT-15).	171
10	365 nm	DMSO		1.8 equivalents	A549, MDA-MB-231, HeLa, HCT-15 and normal HEK-293 cells	IC_{50} (μM): 15.4 ± 0.67 (HeLa), 15.8 ± 1.75 (A549) and 14.5 ± 0.97 (HCT-15).[171] IC_{50} (μM): 24.12 ± 1.03 (HeLa), 21.37 ± 1.72 (A549), 13.69 ± 0.91 (HCT-15) and 21.89 ± 0.59 (MDA MB-231). **10** showed low toxicity against normal HEK-293 cells (>50 μM).[145]	171 and 172
11	Low power visible light	CH_3CN and 2% (v/v) CH_3CN/PBS	k_{CO} (min^{-1}) = 2% CH_3CN/PBS: 0.13 (φ = 0.39 ± 0.03) CH_3CN: 10.5 ± 0.02 (φ = 0.35 ± 0.03)		HT29 and normal HEK-293 cells	- The viability of HT-29 cells decreased by 47%. Negligible effect on HEK-293 cells.	173
12a–12d	400–700 nm and 350 nm	Aqueous DMF 10% (v/v) and CH_3CN	**12a–12d**: k_{CO} (s^{-1}) in CH_3CN = 1.92 × 10^{-3}, 2.76 × 10^{-3}, 3.30 × 10^{-3} and 4.46 × 10^{-3}.		HeLa	Reduced the viability of HeLa cells after 30 min of illumination, with IC_{50} = 7.29–36.05 μM.	174

Table 1 *(Contd.)*

CORM	Activation wavelength	Solvent used	CO release kinetics	CO equivalents (Myoglobin assay)	Experimental cancer model	Anticancer activity	Ref.
13a–13d	365, 405, 435 nm	CH_3CN	$t_{1/2}$ (s) = 365 nm: 11.03, 12.47, 12.69 and 44.54 **405 nm:** 8.46, 17.20, 46.28 and 59.59 **435 nm:** 92.31, 95.75, 56.81 and 65.90. k_{CO} (s^{-1}) = **365 nm:** 2.62×10^{-2}, 1.21×10^{-2}, 1.84×10^{-2} and 1.95×10^{-2}. **405 nm:** 1.39×10^{-2}, 1.38×10^{-2}, 1.45×10^{-2} and 5.70×10^{-2} **435 nm:** 6.66×10^{-3}, 1.81×10^{-2}, 4.88×10^{-3} and 6.40×10^{-3}	(equivalents) **365 nm:** 2.04, 2.43, 2.17, 2.05 **405 nm:** 1.64, 2.23, 2.01, 1.55 **435 nm:** 1.08, 1.24, 1.85, 1.32	- HEK-293T and A549.	- The photoCORMs and their iCORMs, exhibited dose-dependent cytotoxicity. Irradiation with blue or purple light showed no influence on the cytotoxicity.	175
14–15	15 mW visible light	2% (v/v) CH_3CN aqueous solution and CH_2Cl_2	k_{CO} min^{-1} in CH_2Cl_2 = 1.03 (φ_{380} = 0.35 ± 0.02) (**14**) and 0.66 (φ_{380} = 0.23 ± 0.02) (**15**).		HT-29	Dose-dependent viability suppression upon irradiation, IC_{50} = 40 and 70 μM for **14** and **15**.	176
16a–16e	365 nm	DMSO	$t_{1/2}$ (min) of **16a–16e** = 5 (φ: 0.36), 13 (φ: 0.10), 6 (φ: 0.28), 15 (φ: 0.12) and 10 (φ: 0.16), respectively. k_{CO} mol^{-1} min^{-1} = 10.8, 0.8, 8.0, 1.9 and 3.4		Normal HL-7702 and SK-Hep1	-**16b**: the lowest cytotoxicity due to its poor solubility. - **16c** has high cytotoxicity against SK-Hep1 cells.	177 and 178
17a–17d	365 nm				HCT-15, A549, HeLa and normal HEK-293 cells.	- **17b**: cytotoxic against A549 but had a little effect on HCT-15 (13.18 ± 2.57 μM) and HeLa (12.05 ± 3.12 μM) cells. It showed cytotoxicity against normal HEK-293 cells. - **17c**: cytotoxic against HCT-15 (33.12 ± 5.03 μM), A549 (929.83 ± 3.25 μM) and HeLa (11.41 ± 2.61 μM) cells. Not toxic against HEK-293. - **17d**: less toxic against all tested cell lines	179
18a–18g	365 nm			**18a**: 2.65 ± 0.13 **18c**: (spontaneous release): 3.61 ± 0.089 (equivalents)	HCT-15, A549, HeLa and normal HEK-293 cells	- **18c**: highly active even at small doses, IC_{50} = 6.74 ± 1.77 (A549), 2.54 ± 0.579 (HeLa), and 4.92 ± 0.89 (HCT-15) μM - **18c** showed no cytotoxicity against normal HEK-293 cells.	180
19	Low-power visible light	CH_3CN	In CH_3CN: k_{CO} = 0.13 min^{-1}		HT29 and normal HEK-293 cells	10%–48% decrease in viability upon illumination but no cytotoxicity against HEK-293 cells.	181
20a–20d	420 nm		$t_{1/2}$ (s) **20a**: 2.3 ± 0.1 **20b**: 3.31 ± 2.30 **20c**: 5.65 ± 1.0 **20d**: 3.46 ± 0.1 **B_{12}–20a**: 12.9 ± 0.6 **B_{12}–20b**: 13.7 ± 1.5 **B_{12}–20c**: 15.8 ± 1.9 **B_{12}–20d**: 13.3 ± 1.4	(equivalents) **20a**, **20b** and **20d**: 1.45 ± 0.03, 2.3 ± 0.02, 2.49 ± 0.02 **B_{12}–20a**: 2.26 ± 0.06 **B_{12}–20b**: 2.74 ± 0.13 **B_{12}–20c**: 2.20 ± 0.05 **B_{12}–20d**: 2.39 ± 0.09	MCF-7, A549-LD, A549-HD, HT29-LD, HT29-HD and 16HBE14o- cells.	- The B_{12}-conjugated photoCORMs were less toxic against MCF-7 cells than their free analogues. - **B_{12}–20b** and **B_{12}–20c** showed moderate cytotoxicity (IC_{50} = 40 and 17 μM). iCORMs of **20b** and **B_{12}–20b** showed more toxicity in a dose-dependent manner than their **20b** and **B_{12}–20b** analogues. - The iCORM of **20b** showed maximum effect at 12.5 μM.	183

Table 1 *(Contd.)*

CORM	Activation wavelength	Solvent used	CO release kinetics	CO equivalents (Myoglobin assay)	Experimental cancer model	Anticancer activity	Ref.
21a–21d	525 and 468 nm	DMSO, CH_2Cl_2	At 468 nm in DMSO: **21b**: $t_{1/2}$ = 1.91 ± 0.16 min (k_{CO} = (0.60 ± 0.05) × 10^{-2} s^{-1})	**21b**: 525 nm: one 468 nm: 3 (equivalents)	HepG2	- At 525 nm, the complexes showed significant cytotoxicity. - **21b** (IC_{50} = 7.1 μM) was the most photo-toxic complex.	184
22a–22d	525 and 468 nm	DMSO, CH_2Cl_2	At 468 nm in DMSO: **22b**: $t_{1/2}$ = 2.27 ± 0.27 min (k_{CO} = (0.50 ± 0.05) × 10^{-2} s^{-1})	**22b**: 525 nm: one equivalents, 468 nm: 3 equivalents	HepG2	At 525 nm, the complexes showed significant cytotoxicity.	184
23	400–700 nm	10% (v/v) DMF/H_2O, DMSO/H_2O, and CH_3CN	k_{CO} of **23-AuNPs** = 33.7 × 10^{-3} s^{-1}		A549	- **23**: IC_{50} = 39.2 μM in red light, and 89 μM under dark conditions. - **23-AuNPs** caused apoptosis that is dependent upon caspase 3/7 in A549 cells with IC_{50} = 232 μg mL^{-1} upon illumination.	185
24a–24f	365 nm	DMSO, CH_2Cl_2			HepG2	- In the dark: IC_{50} = 18.1 (**24a**) and 11.8 (**24c**) μM, while **24b** and **24d** were inactive. - Upon irradiation: IC_{50} = 7.9 (**24a**), 6.6 (**24c**), 5.7 (**24b**) and 6.7 (**24d**) μM.	186
24g	625 nm	PBS	k_{CO} and $t_{1/2}$ = (1.8 ± 0.5) × 10^{-2} s^{-1} and 39 ± 10 s (φ_{625}) = (4.30 ± 0.03) × 10^{-2}		U87, MCF-7 and HeLa	The targeted/localized CO release improved cytotoxicity through apoptosis towards MCF-7, HeLa and U87 cells.	187
25a–25b	468 nm	DMSO and H_2O	k_{CO} and $t_{1/2}$ = In H_2O: 2.1 × 10^{-3} s^{-1} and 5.4 min (**25a**) and = 2.2 × 10^{-3} s^{-1} and 5.2 min (**25b**) In DMSO: 1.1 × 10^{-3} s^{-1} and 10.26 min (**25**) and = 1.3 × 10^{-3} s^{-1} and 8.93 min (**25b**)	In H_2O: 0.66 (**25a**) and 1.31 (**25b**) equivalents	SW-620, MDA-MB-231 and normal HEK-283T cell.	Both complexes showed inactivity towards the tested cells under dark and illumination circumstances up to 50 μM.	188
26–27	468 nm	DMSO and 25% (v/v) DMSO/H_2O	k_{CO} and $t_{1/2}$ in DMSO = (26.0 ± 0.18) × 10^{-3} s^{-1} and 4.54 ± 0.17 min for **26** = (7.0 ± 0.10) × 10^{-4} s^{-1} and 17.28 ± 3.6 min for **27**.		MDA-MB-231 and HEK-293T cells	- **26**: no cytotoxicity in absence and presence of light. - **27**: concentration-dependent cytotoxic behaviour (IC_{50} = 19.62 μM in the dark and 11.43 μM) upon irradiation. The same cyto-toxic behaviour was against normal HEK 283T cells. - The viability of cells cotreated with 30 nM paclitaxel and 10 μM **27** was 27%, suggesting that **27** might increase the cytotoxicity of paclitaxel in the context of resistance.	189
28	468 nm	DMSO and 20% (v/v) DMSO/H_2O	k_{CO} and $t_{1/2}$ in DMSO = 5.05 × 10^{-4} s^{-1} and 21.21 min		THP-1 and BM cells	- Under dark conditions: **28** prevented THP-1 from multiplying whereas exhibiting no effect on BM cells. - Upon irradiation, **28** demonstrated THP-1-like potency to that observed in the dark and generated a severe effect on BM cells that could be the cause of the photo-released CO.	190

Table 1 *(Contd.)*

CORM	Activation wavelength	Solvent used	CO release kinetics	CO equivalents (Myoglobin assay)	Experimental cancer model	Anticancer activity	Ref.
MnCO-Ferritin	456 nm	PBS buffer pH 7.4	$t_{1/2}$ in PBS = 2.5 ± 0.2 min		HEK293 cells	- The quantity of discharged CO from **MnCO-Ferritin** is modulated by the degree of irradiation -The light-activated CO-releasing characteristics of **MnCO-Ferritin** lead to NF-κB activation	191

[a] In the dark: IC_{50} (μM) = 7.4 ± 0.2 (**6a**), >1 ± 0.1 (**6b**), 11.4 ± 0.9 (**6c**), 52 ± 2 (**6d**) and 9.9 ± 0.7 (**6e**). [b] In the dark: IC_{50} (μM) = 51.93 (**7a**), 22.89 (**7b**), 3.22 (**7c**), 17.32 (**7d**) and 6.49 (**7e**).

to the Mb solution. In the dark, **1** was inactive against HT29 cells up to 100 μM, however, the complex acquired activity when irradiated, as it reduced the cell biomass by 30%. The activation wavelength, the solvent used, the CO release kinetics and equivalents, based on the Mb solution, the experimental cancer model, and the cytotoxic properties of all the tested Mn(I) PhotoCORMs are presented in Table 1.

Next, Mascharak synthesized photoCORMs **2–4** (Fig. 3), which liberates CO upon illumination with 15 mW visible light.[165] These molecules display good stability in some organic solvents under dark conditions. The k_{CO} values of **2–4** in CH_2Cl_2 are 21.94 ± 0.01, 15.28 ± 0.01 and 4.32 ± 0.01 min^{-1}, respectively. In CH_3CN, the k_{CO} value of **4** is 1.05 ± 0.01 min^{-1}. However, a slower CO release was observed in 20% DMSO/H_2O and 40% CH_3CN/H_2O solutions of **4** with k_{CO} values of 0.61 ± 0.01 and 0.23 ± 0.01 min^{-1}, respectively. Complex **2** reduced the viability of HeLa and MDA-MB-231 cell lines by 60% upon illumination.[165] The highly fluorescent 2-(2-pyridyl) benzothiazole ligand provides an interesting method for tracking CO distribution within the cells.[164] When tested against MBA-MB-231 cells, **4** exhibited 50% decrease in the viability upon illumination *via* the CO-triggered apoptosis.[166]

The Mn-based metallo-crown ether **5** (Fig. 3) has good solubility in some organic solvents and releases CO by 365 nm light. Complex **5** was stable in the dark up to 6 h, while upon illumination it releases about 1.3 moles of CO. The complex showed selective suppression to colon, lung, and cervical cancer cells upon the illumination with IC_{50} values of 7.15 ± 0.24, 12.5 ± 1.33 and 20.7 ± 0.94 μM, respectively. On the other hand, **5** is nontoxic to the normal cells.[167]

Five 2,2′-bipyridine complexes **6a–6e** (Fig. 3), bearing imidazole derivative in the axial position, were examined as CO prodrugs when exposed to 365 nm UV light.[168] About 1.0–2.4 CO equivalents were photo-released from **6a–6e** with $t_{1/2}$ of 4.8–9.5 min according to Mb assay. Under the dark conditions, **6a**, with imidazole ring, showed the highest cytotoxicity (IC_{50} = 7.4 ± 0.2 μM) against breast cancer MCF-7 cell line, while the **6b** analogue, with methyl-substituted imidazole ring, displayed the lowest cytotoxicity (IC_{50} > 1 ± 0.1 μM). The presence of a methyl group on an imidazole moiety can result in steric hindrance and impair CO release, or it could change the imidazole nitrogen electronegativity, resulting in decreased reactivity. Complexes **6c–6e** showed significant cytotoxicity against MCF-7 cells with IC_{50} values of 11.4 ± 0.9, 52 ± 2 and 9.9 ± 0.7 μM, respectively. Upon the illumination, **6a**, **6c** and **6e** showed cytotoxicity, however illumination did not seem to induce a touchable enhancement in cytotoxicity. Alternatively, **6b** and **6d** did not exhibit cytotoxicity upon illumination.[168] Afterward, the same research group prepared another series of bipyridine-based Mn photoCORMs (**7a–7e**) which were also activated by 365 nm light.[169] **7a–7e** are stable in the dark for 4 h in DMSO. When dissolved in PBS, these molecules displayed good dark stability over 16 h in the presence of Mb and Na-dithionite. The number of equivalents of released CO increased on going from **7a** to **7e** (1.4, 1.4, 1.5, 1.7, and 2.2 equivalents, respectively) as the number of methyl groups on

Table 2 Summarized results regarding Mo, Co, Fe, Ru and Re photoCORMs with cytotoxic activity against different cell lines

Compound	Activation method	Solvent used	CO release kinetics	CO equivalent	Experimental cancer model	Anticancer activity	Ref.
- Molybdenum(0) CORMs (Section 6.2)							
29	Redox	PEG300/H_2O (1 : 4) Deoxygenated aqueous media		one equivalents after 0.5 h and 2.26 equivalents after 2 h, in the dark	LLC-PK1, RAW264.7 macrophages and HepG2 cells	- LLC-PK1 and RAW264.7 cells: no toxicity - HepG2 cells: the rate of survival reduced by 30% at 100 μM	51 and 192
30	Reaction with $FeCl_3$	Cell culture medium			- Normal HEK-293 or NIH3T3 cells	Neither the CORM nor the probable byproduct was toxic. OCORS produced and released CO into the stomach of the animals without causing systemic exposure	194 and 195
		Aqueous solution			- Pig models		
- Cobalt(0) CORMs (section 6.3)							
31a–31g	Direct release	DMSO/H_2O CH_3OH/H_2O	$t_{1/2}$ for **31a–31g** = 41.8, 58.8, 71.8, 62.7, 34.8, 71.6 and 47.1 min		- HeLa cells - Rat models[a]	- IC_{50} for **31a–31g** = 36.20, 73.39, 124.88, 36.89, 42.95, 79.29 and 51.56 μM. - With low LD_{50} values, these complexes showed minimal *in vivo* toxicity against rats.	196
32a–32e	Direct release	- DMSO	$t_{1/2}$ for **32a–32e** in buffered Mb = 55.1, 53.2, 40.1(54.7)[a], 41.8 (78.5)[a], 60.5, 33.5 and 71.6(143.4)[a]		- HeLa and HepG2. - Mice and rat models	- IC_{50} for **32a–32e** against HeLa: 83.24 ± 6.2, 110.21 ± 8.6, 40.61 ± 2.7, 36.20 ± 2.5, 85.85 ± 6.4, 78.45 ± 5.9 and 79.29 ± 4.1 μM. -IC_{50} for **32a–32e** against HepG2: 79.54 ± 6.7, 139.04 ± 9.1, 58.79 ± 3.2, 39.25 ± 1.9, 75.04 ± 4.7, 69.85 ± 3.4 and 68.57 ± 2.4.	197
		- Ethanol					
		- Buffered Mb solution			- Zebrafish larvae	- Animal tests showed that **32a** and **32f** had the smallest LD_{50} (300–500 mg kg^{-1}). The rest of the complexes were less toxic with **32d** and **32g** having the highest LD_{50} values of 2500–5000 mg kg^{-1} and >5000 mg kg^{-1} - **32d** induced developmental toxicity on zebrafish larvae. At 0.5 and 1.0 μM, it showed no toxicity, but at 5.0, 10, and 20.0 μM it was toxic	
33a–33k	Direct release	- H_2O	$t_{1/2}$ (min)		- HeLa, A549, HT-29, HepG2, and MCF-7.	- Low activity against tested cancer cells when compared to cisplatin. When compared to 5-FU, **34a** and **34b** showed superior activity and selectivity to the HT-29 (37.9 and 55.8 μM) and MCF-7 (33.6 and 49.3 μM) cells	198
34a–34e		- Culture medium	**33a–33k**: 32.8, 21.8, 30.5, 34.7, 38.9, 42.6, 26.4, 16.8, 30.9, 24.8 and 16.9		- Myocardial H9c2 cells	- Compared to **33d**, **34a** had a higher ability to down-regulate COX-2 expression.	
		- 0.5% Sodium carboxymethyl cellulose : DMSO (3 : 1 v/v)	**34a–34d**: 25.6, 26.8, 16.3 and 15.8		- SHR rats	- **33a**, **33j**, and **34a** acted as antioxidants to myocardial H9c2 cells exposed to H_2O_2. - A concentration-dependent antihypertensive impact on SHR rats	

Table 2 *(Contd.)*

Compound	Activation method	Solvent used	CO release kinetics	CO equivalent	Experimental cancer model	Anticancer activity	Ref.
35a–35e **36a–36e** **37a–37c**	Direct release	- DMSO - 0.1 M PBS at pH = 7.4			HepG2, MDA-MB-231 and HeLa cells	- IC_{50} = 4.7–548.6 μM. - **35a**, but not its iCORM, exhibited notable selectivity towards HepG2 cells (IC_{50} = 4.7 ± 0.76 μM). At 50 μM, **35a** had a cytotoxic effect against HepG2, MDA-MB-231 and HeLa cells with cell viability of 21.21%, 12.14% and 23.99%	199
- Iron(II) and Iron(0) CORMs (Section 6.4)							
38 (CORM–F3)	Metal oxidation	DMSO, ethanol	$t_{1/2} \approx 55$ min	0.25 M mol^{-1}		Causes vasorelaxation and prevent inflammation *in vitro*	200
38 (CORM–F3) 39 (CORM–F7) 40 (CORM–F8) 41 (CORM–F11)	Metal oxidation	DMSO	k_{CO} (nmol min^{-1}) = **38:** 0.19, **39:** 0.007, **40:** 0.041, **41:** 0.041		- Thoracic aortic rings of male adult Sprague-Dawley rats - Murine RAW264.7 macrophages	- 100 μM of **38** induced vascular relaxation in isolated aortic segments and suppressed endotoxin-stimulated inflammation reaction of RAW264.7 macrophages in a concentration-dependent manner - **38** and **40** showed less toxicity against RAW246.7 macrophages	201
42a–42k	Metal oxidation	H_2O Ethanol	$t_{1/2}$ (min) **42a:** one **42i:** >3000		Murine RAW264.7 macrophages	Only **42b** exhibited no cytotoxicity even at 100 μM	203
43 (CORM–S1)	> 400 nm	Aqueous solution		470 nm: two equivalents	Ca^{2+}-and voltage-activated K^+ (BK, Slo1) channels	When exposed to light, a higher outward current was generated with similar variation in membrane potential, giving a measurement for released CO	204
44–48	Enzyme-triggered				Murine RAW264.7 macrophages	- **45** and **48** showed no toxicity against murine RAW267.4 macrophages up to 100 μM - **44**, **46** and **47** had IC_{20} values in the ranges 11–28 μM and 14–38 μM - **47** showed the highest inhibition of NO generation. At 15 and 5 μM, **47** suppressed LPS-induced NO production by up to 68 ± 6% and 33 ± 6% - 5 μM of **46** led to 30 ± 7% suppression of NO production, while **44** (25 μM) reduced NO generation by only 16 ± 10% - For up to 50 μM, **45** and **48** did not inhibit NO production	48, 205 and 206
44–56	Enzyme-triggered	PBS (0.1 M, pH = 7.4) and DMSO mixture (≈ 17% DMSO)	$t_{1/2}$ (min) **44:** 43[b] (128),[c] **45:** __,[b] **46:** 21,[b] **47:** 5,[b] **56:** 28,[b] **49:** __,[b] **50:** 133,[b] **51:** 25,[b] **52a:** 478,[b] **52b:** 51,[b] **53:** 10,[b] **54:** 6119,[c] **55:** 108[b]	**44:** 2.2[b] (2.4),[c] **45:** 0.3,[b] **46:** 2.4,[b] **47:** 3.0,[b] **56:** 2.6,[b] **49:** 0.1,[b] **50:** 1.0,[b] **51:** 3.1,[b] **52a:** 1.7,[b] **52b:** 2.3,[b] **53:** 2.1,[b] **54:** 0.6,[c] **55:** 1.3[b]	Murine RAW264.7 macrophages	**47** and **51** showed promising suppression of NO-production. The NO-inhibition was shown to be highly influenced by the enone by-products of monoester-bearing complexes but not in the case of diester-containing ones	49

Table 2 *(Contd.)*

Compound	Activation method	Solvent used	CO release kinetics	CO equivalent	Experimental cancer model	Anticancer activity	Ref.
44, **46** and **57**	Enzyme-triggered	- DMSO - Used as RAMB (randomly methylated-beta-cyclodextrin) complexes			HUVEC	- EC_{50} = 8.2 ± 1.5 and 7.22 ± 1.12 μM for **46** and **RAMB@46** *vs.* EC_{50} = 448.9 ± 50.23 and 457.3 ± 8.23 μM for **44** and **RAMB@44** - The **44**-derived suppression of VCAM-1 expression decreased over time, and the **57**-derived inhibition seemed to rise. Both **44** and **57** prevented NFκB irrespective of IκBα degeneration. Both ET-CORMs stimulated Nrf-2, which in turn caused HO-1 to be expressed	42
44, **46** and **52b**	Enzyme-triggered	DMSO			Pre-contracted small rat mesenteric arteries.	- **44** and **46** caused significant dilation, while **52b** did not cause any effect - **46** did not cause vasodilation in the case of KCl- pre-treated mesenteric arteries	206
58	Direct release	**58–60:**	$t_{1/2}$ (min) **61:** 18	One mole of CO/mole of each complex	- Pre-contracted rat aortic smooth muscle cells (A7r5)	- **58–60** caused more significant cytotoxic effects on vascular and inflammatory cells and isolated vessels compared to **61**	207
59		DMSO			- Murine RAW264.7 macrophages	- Against macrophages, the IC_{50} values of **58–60** and **61** were 9.1, 11.9, 23.6 and 797 μM	
60		**61:** H_2O				- **58** and its iCORM caused vasorelaxation in isolated aortic rings and reached maximum after 60 min. **59** and **60** led to the same results, however their iCORMs had less vasorelaxation effect	
61						- **58–60** caused a total loss in the cell viability of murine smooth muscle cells - **61** caused fast dose-dependent vasorelaxation that reached maximum after 10 min - In contrast to **58**, the iCORM of **61** showed minimum vasorelaxation. **61** and not its iCORM greatly reduced LPS-induced NO production without any obvious toxicity up to 100 μM	
44–48	Enzyme-triggered	**44**, **45**, **46** and **54:** mixture of 0.2 mL DMSO to 1.0 mL PBS			- HUVEC	- **46** and **53** showed cytotoxicity at low concentrations. **46** was toxic only against HUVEC cells, while **53** showed cytotoxicity against HUVEC and PTEC cell lines. **52b** and **56** had decreased toxicity	208
52b					- PTEC	- The cell damage caused by cold preservation was decreased in a concentration-dependent manner by **44**. Only ET-CORMs containing 2-cyclohexenone reduced the damage caused by cold preservation.	
53–56						- The cell protection was dramatically diminished when acetate in **44** was replaced with pivalate in **45** - VCAM-1 expression was significantly suppressed by **44**, **52b** and **56** and to some degree by **45**	

Table 2 *(Contd.)*

Compound	Activation method	Solvent used	CO release kinetics	CO equivalent	Experimental cancer model	Anticancer activity	Ref.
62a–62d	Enzyme-triggered	DMSO	$t_{1/2}$ = 5 h		HUVEC	Only when the CORM and PGA were administered together in an *in vitro* test, the CO-induced suppression of the inflammation reaction and an elevation of the expression of HO-1 become apparent	209
63–66	Enzyme-triggered and direct release for **63** and **66**	DMSO			Murine bone marrow-derived DCs	- FumET-CORMs caused substantial suppression of LPS-stimulated pro-inflammatory signaling routes and blockage of downstream (IL)-12 or -23 production. **63–66** can change dendritic cells into anti-inflammatory phenotypes. - **64** and **65** were nontoxic below 25 μM	210
44, **46**, **62c**, **62d**, **67** and **68**	Enzyme-triggered	PBS (0.1 M; pH 7.4)/ DMSO (5 : 1) mixture		(Equivalents) **46:** 2.5 **67–68:** >1.5 within 50 h	HUVEC	The utilization of certain membrane associated enzymatic activity could allow tissue-targeted CO administration based on the finding that extra- and intracellular CO release generate anti-inflammatory characteristics	211
69–70	Enzyme-triggered				HUVEC	**69** and **70** were toxic in a dose-dependent manner, with **69** being more toxic. While both CORMs induced HO-1, they could not decrease TNF-α-mediated expression of VCAM-1	213
71a–71i	Enzyme-triggered and Direct release	PBS (0.1 M; pH 7.4)/ DMSO (5 : 1) mixture		(equivalents) - Spontaneous release: **71a:** 1.8 after 2.5 days **71b** and **71c:** 2 after 2 days. **71d:** 3 after 10 h. - PLE-triggered: **71b** and **71c:** 0.6 after 5 days **71d:** 3 after 10 h. **71e** and **71f:** 3 **71g** :1.5	HUVEC	- **71e** and **71f** showed no toxicity up to 500 μM. **71h** and **71i** were toxic > 50 μM. - The anti-inflammatory effect of **71h** and **71i** was stronger than **71e** and **71f.** This was noticeable for the suppression of the expression of VCAM-1, but there was not a significant variance in HO-1 inhibition among the two Mito-CORM classes. While **71h** and **71i** suppressed mitochondrial respiration in both basal and stressful settings, glycolysis increased. **71e** and **71f** elevated both mitochondrial respiration and glycolysis	214

- Ruthenium(II) CORMs (Section 6.5)

Table 2 *(Contd.)*

Compound	Activation method	Solvent used	CO release kinetics	CO equivalent	Experimental cancer model	Anticancer activity	Ref.
72a–72i	Ligand exchange	DMSO	$t_{1/2}$ (min) **72a**: 4.9 **72b**: 3.2		- L929 murine fibroblast cells.	- Very weak antiproliferative activity against murine L929 fibroblasts (IC_{50} = 62.69–255.48 mg l^{-1})	215
73a–73d		Methanol	**72c**: 1.1 **72d**: 2.1		- Mice and rat models.	- Against mice: LD_{50} values of 800–1000 mg kg^{-1} (**72a** and **72h**), 1100–1500 mg kg^{-1} (**72g** and **74b**) and 150–200 mg kg^{-1} (**73a**)	
74a–74b			**72e**: 1.6 **72f**: 1.0			- On rats *in vivo*: a little impact on liver function but did cause physiological harm to liver cells. Detrimental effect on the kidney in both functional and physiological approaches	
			72g: 10.6 **72h**: 2.6 **72i**: 13.2 **73a**: 10.6 **73b**: 2.5 **73c**: 2.4 **73d**: 4.3 **74a**: 15.8 **74b**: 14.2			- No accumulation in major tissues or organs and are unable to pass through the blood–brain barrier	
75a–75n		Aqueous solutions (PBS pH 7.4 or H_2O)	**75d**: 50 min		Murine RAW264.7 macrophages	- Up to 100 μM, no toxicity. - Reduction in NO generation in a concentration-dependent mechanism. **75k** was the most efficient at reducing NO generation	216
76	Decomposition	PBS pH = 7.4			RAW264.7 cells	- Decrease ROS production during the release of CO and had no bactericidal activity	217
					HeLa cells	- No toxicity against RAW264.7 cells - Anti-inflammatory properties - HeLa cells have been incubated with 50 μM of **76** before being subjected to COP-1, and considerable rise in intracellular fluorescence was observed - No increase in the amount of COHb in sheep blood when incubated at 37 °C	
77–79		- DMSO/PBS			- Balb/c mice	- At 2.5 mg, **78** significantly slowed tumour growth of CT-26 cancer cells in Balb/c mice *in vivo*. **77** had no effect on the tumor	218
		- PBS - Animal experiments: 20% propylene glycol - Cytotoxicity: DMSO or DMF (maximum 0.5% v/v)			- Murine CT-26 cells, CH1/PA-1, A549 and SW480	- **77** and **78**, *in vitro*, showed toxicity against CH1/PA-1 (**77**: 56 ± 3, **78**: 55 ± 1 μM), A549 (**77**: 212 ± 24, **78**: 16 ± 5 μM) and SW480 (**77**: 48 ± 4, **78**: 44 ± 7 μM) cell lines with IC_{50} values that were nearly the same	
80–81	350 nm	0.8% (v/v) DMSO/H_2O mixture			A431 and HEK-293 cells	- Increased cytotoxicity against A431 cells at 350 nm - **81** was promptly taken up by A431 and HEK-293 cells and distributed throughout the cytoplasm	221

Table 2 *(Contd.)*

Compound	Activation method	Solvent used	CO release kinetics	CO equivalent	Experimental cancer model	Anticancer activity	Ref.
82a–82e	365 nm	DMSO			MCF-7	Except for **82d** (IC_{50} = 45.08 ± 3.5 μM), the studied complexes showed no toxicity to MCF-7 cells under dark conditions. By light, the complexes developed cytotoxicity based on the type of the substituent (**82a** (14.32 ± 1.2 μM) > **82d** (23.0 ± 2.8 μM) > **82b** (23.2 ± 3.2 μM) > **82c** (24.3 ± 3.5 μM) > **82e** (26.9 ± 3.1 μM)).	222
83a–83l	365 nm	DMSO	$t_{1/2}$ (s) at 60 μM		- Murine RAW264.7 macrophages	Although it showed minimum toxicity against murine RAW264.7 macrophages,	223
		Ethanol	**83a**: 166 **83b**: 276 **83c**: 249 **83d**: 189 **83e**: 1209 **83f**: 632 **83g**: 962 **83h**: 1096 **83i**: 1450 **83j**: 966 **83k**: 2699 **83l**: 2472		- HT-29 cells	**83a** exhibited anticancer action under illumination. At 50 μM, **83a** and **83h** showed 12.5% and 6.65% loss in cells activity by illumination.	
- Rhenium(I) and Rhenium(II) CORMs (section 6.6)							
84–90	pH-dependent	CH_3OH	$t_{1/2}$ (min) **Precursor**: 1.0,[d] 2.5[e] and 5.7[f]	One mol mol^{-1} of complex	Neonatal rat ventricular cardiomyocytes (NRCs)	The precursor complex and **88a**, **89a** and **89b** protected NRCs from ischemia-reperfusion stress *in vitro*	39
		DMSO PBS	**84–86**: no CO release **87**: 8.4,[d] 12.3[e] and 14.0[f] **88a**: 29.8,[d] 41.3[e] and 42.3[f] **88b**: 19.9,[d] 27.0[e] and 40.7[f] **89a**: 9.7,[d] 10.2[e] and 17.2[f] **89b**: 15.2,[d] 20.3[e] and 23.6[f]				
91a–91b	pH-dependent	H_2O	20 min for **91a** and **91b**	One mol mol^{-1} within two h	Cardiomyocytes	Non-toxic, even after CO release, and showed cellular protection against ischemia-reperfusion injury.	225
		DMSO					
92	365 and 405 nm	CH_3CN	Φ at 365 nm = 0.21 ± 0.01	At 405 nm: one CO	PPC-1	- Nontoxic to PPC-1 cells	226 and
		Aqueous media	Φ at 405 nm = 0.11			- Built up in the cytoplasm yet did not pass through the nuclear membrane	227
93–94	360 nm	CH_3CN PBS	k_{CO} (min^{-1}) In PBS: 0.32 ± 0.02 (**93**) and 0.27 ± 0.02 (**94**) In CH_3CN: 0.30 ± 0.02 (**93**)	UV-A light: one CO molecule	MDA-MB-231	**93** was rapidly internalized by the cancerous cells	170
95	Low-power UV light	CH_3CN MTT assay: 2 : 3 v/v CH_3CN/PBS	k_{CO} = 0.31 min^{-1}		MDA-MB-231	A dose-dependent loss in the viability caused by CO-induced apoptosis upon exposure to light	228

Table 2 *(Contd.)*

Compound	Activation method	Solvent used	CO release kinetics	CO equivalent	Experimental cancer model	Anticancer activity	Ref.
96a–96e	Low-power UV light (5 mW cm^{-2})	CH_3CN	k_{CO} (min^{-1}) **96a**: 0.07 ± 0.02 **96c**: no CO release **96d**: 1.59 ± 0.02 **96e**: 0.07 ± 0.02	**96a**: three CO **96d** and **96e**: one CO	MDA-MB-231	The luminescent complexes, with auxiliary ligands of varying lipophilicity, exhibited significant cellular uptake and distributed largely throughout the cytoplasm. **96d** displayed moderate nuclear accumulation along with cytosolic distribution.	229
97–98	365 nm	DMSO			HepG2 and HeLa	**97** against HepG2: IC_{50} = 14.2 ± 4.8 μM **98** against HeLa: IC_{50} = 12.4 ± 2.9 μM	171

[a] In myoglobin and aqueous plasma solutions. [b] Using PLE enzyme. [c] Using LCR enzyme. [d] At pH 5.8. [e] At pH 6.3. [f] At pH 7.4.

the benzyl moiety increased. This could be due to enhanced electron donation *via* higher methyl groups number, which in turn raised the e.d. on the Mn ion and hence strengthened Mn–CO π-back bonding. However, there is no consistent variation in the $t_{1/2}$ values based on the number of methyl groups, 9.5 (**7a**), 11.4 (**7b**), 13.9 (**7c**), 3.9 (**7d**), and 8.7 (**7e**). When incubated with MCF-7 cells, **7a–7e** exhibited cytotoxic effects under both the dark and illumination conditions.

Mascharak and co-workers described the antiproliferative activity of two water-soluble Mn(I) complexes, **8a** and **8b** (Fig. 3).[170] Under dark conditions, for not less than 48 h, **8a** and **8b** showed good stability in CH_3CN, water, and PBS. *Via* the illumination with broad-band low-power visible light, **8a** showed CO release associated with the appearance of fluorescence at about 400 nm due to the de-ligation of 2-(2-pyridyl) benzothiazole ligand. According to Mb assay, the complexes showed k_{CO} values of 1.54 ± 0.02 (**8a**) and 0.44 ± 0.02 min^{-1} (**8b**) in PBS and 0.91 ± 0.02 (**8a**) and 0.51 ± 0.02 min^{-1} (**8b**) in CH_3CN. With a concentration of 100 μM, **8a** and **8b** caused 50% decrease in the cell viability of MDA-MB-231 cells upon illumination.[170]

Two novel binuclear semi-rigid ester Mn(I)-based carbonyl complexes, **9** and **10** (Fig. 3), were prepared and proved to release CO *via* illumination at 365 nm.[171] The reduced Mb solution of **10** remained stable for 12 h, however, by exposure to the light source, **10** released 1.8 equivalents of CO. Upon illumination, **9** showed cytotoxicity against lung (IC_{50} = 15.7 ± 0.98 μM) and colon (IC_{50} = 28.7 ± 0.16 μM) cancer cells only, while **10** showed cytotoxicity against cervical, lung, and colon cancer cell lines with IC_{50} values of 15.4 ± 0.67, 15.8 ± 1.75 and 14.5 ± 0.97 μM, respectively.

In DMSO, **10** (Fig. 3) showed no CO release in the dark in the presence of Mb and Na-dithionite up to 18 h.[172] However, it released CO when exposed to a 365 nm light, according to Mb assay and FTIR studies. Complex **10** showed cytotoxicity toward cervical (HeLa), lung (A549), colon (HCT-15) and breast (MDA MB-231) cancer cell lines with IC_{50} values of 24.12 ± 1.03, 21.37 ± 1.72, 13.69 ± 0.91 and 21.89 ± 0.59 μM, respectively. With IC_{50} > 50 μM, **10** showed low toxicity against normal HEK-293 cells. Both iCORM and CO may contribute to the cytotoxicity of **10**. The mechanism by which **10** triggered apoptosis was mediated by the production of ROS and consequently the loss of mitochondrial membrane potential.[172]

To track the photoCORM into the target cells, Mascharak and co-workers introduced the luminescent complex **11** (Fig. 3), which was activated to release CO *via* illumination with light > 400 nm.[173] An equivalent Re(I)-based tricarbonyl complex was prepared but it was activated with UV-light (λ < 315 nm). An equivalent Re(I)-based tricarbonyl complex was prepared but it was activated with UV-light (λ < 315 nm). Complex **11** showed good solubility in CH_3CN, CH_2Cl_2, and $CHCl_3$. In a 2% (v/v) CH_3CN/PBS solvent mixture, the k_{CO} value of **11** was 0.13 min^{-1} (φ = 0.39 ± 0.03), while in CH_3CN, a k_{CO} value of 10.5 ± 0.02 min^{-1} (φ = 0.35 ± 0.03) was observed. In the dark, when human colorectal adenocarcinoma HT-29 cells were co-incubated with **11**, no cell

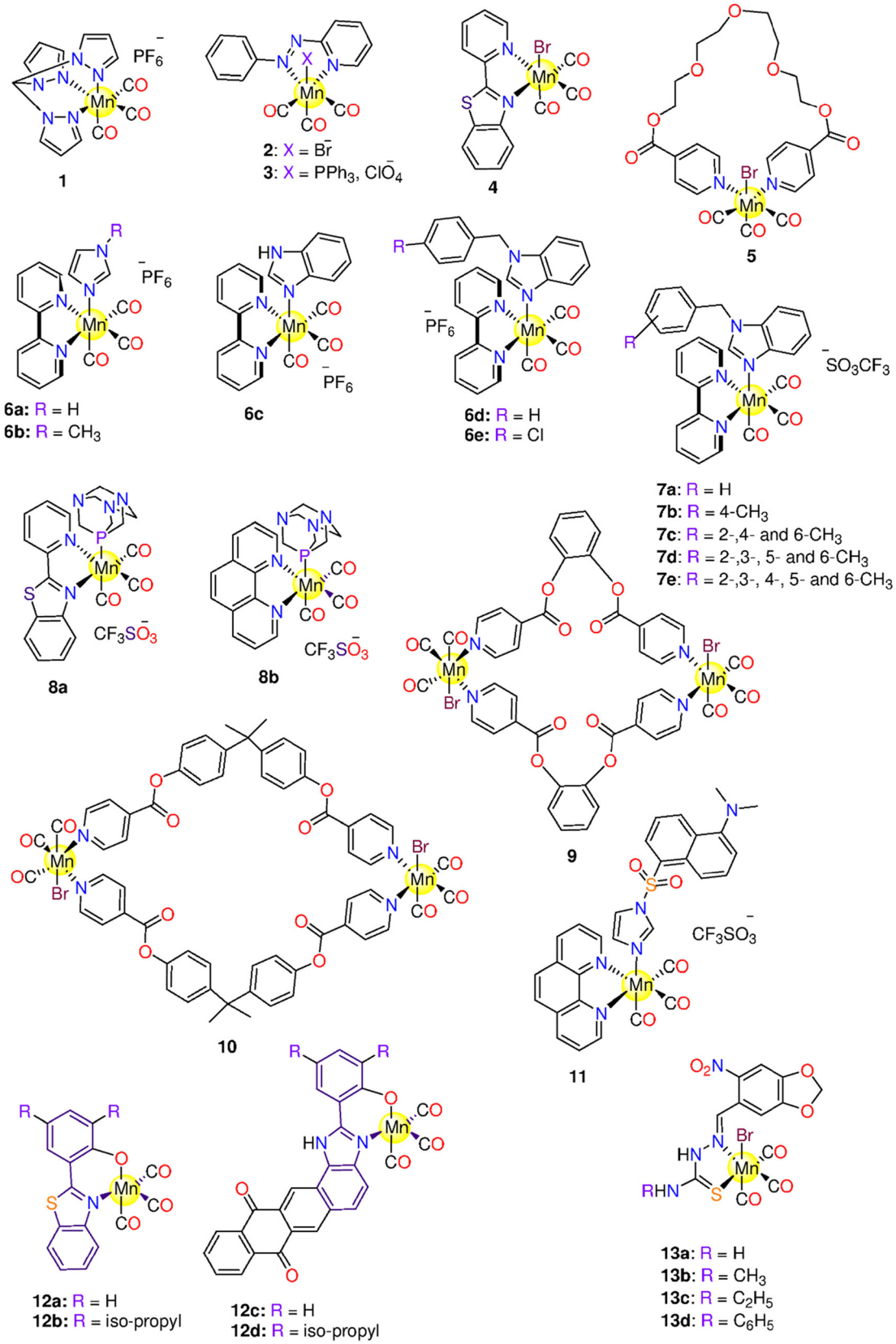

Fig. 3 Structures of the Mn(I) photoCORMs **1–13**.

damage was seen, even at 100 μM. When illuminated with low power vis light, cells viability decreased by 47%. Interestingly, **11** had a negligible effect on normal HEK-293 cells in the light or under dark conditions. Notably, the low cytotoxicity of the photolyzed solution indicates that CO release may exclusively induce cytotoxicity.[173]

Musib and co-workers prepared four Mn(I) complexes, **12a–12d** (Fig. 3), that liberate CO rapidly *via* activation with visible light (400–700 nm).[174] Photoactivation led to variations in the luminescence features of the complexes, which allowed tracking photo-released CO. **12a–12d** were soluble in DMSO, dimethyl formamide (DMF) and CH_3CN. In the dark, the solutions of **12a–12d** in 10% (DMF/H_2O) were stable for up to 72 h. When illuminated at 350 nm, the complexes had less luminescence than the corresponding free ligands. It was seen that the greater the π-accepting character, the greater the *trans* effect, which resulted in Mn–CO bond lability and so, more CO release. In the dark, the complexes were non-toxic with IC_{50} > 50 μM. Complexes **12a–12d** reduced the cell viability of HeLa after 30 min of the illumination, with IC_{50} values ranging from 7.29 to 36.05 μM.[174]

Four Mn(I) photoCORMs, **13a–13d** (Fig. 3), containing 6-nitro-piperonal thiosemicarbazone ligands, were found to have both antibacterial and cytotoxic characteristics.[175] The photoCORMs were categorized as fast CO releasers. When exposed to a UV/Vis light source (365 (UV), 405 (purple) and 435 (blue) nm), the CO release $t_{1/2}$ values were between 11 and 95 s. While the purple and blue lights caused the release of around 1.5 and 1.0 equivalents of CO, respectively, the UV-light produced two equivalents of CO. PhotoCORMs **13a–13d** and their iCORMs, exhibited dose-dependent cytotoxicity against A549 as well as normal HEK-293T cell lines. Irradiating the cultures with blue or purple light showed no influence on the cytotoxicity of these molecules. The results imply that some CORMs have cytotoxic effects on HEK-293T, but that CO release from these molecules is not the only toxic mechanism.[175]

As a continuation of their efforts on finding the appropriate Mn(I) photoCORMs with desirable properties for the clinical applications, Mascharak and co-workers synthesized two visible light-activated luminescent photoCORMs, **14** and **15** (Fig. 4), functionalized with diazabutadiene ligand.[176] For 24 h, **14** showed good stability in 2% (CH_3OH/H_2O) mixture as well as CH_2Cl_2 and $CHCl_3$. The CO release kinetics of **14** and **15**, in CH_2Cl_2, were fast with k_{CO} values of 1.03 and 0.66 min^{-1} and φ_{380} = 0.35 ± 0.02 and 0.23 ± 0.02, respectively. In comparison to the hydrophilic complex **14**, the lipophilic luminescent complex **15** demonstrated strong membrane permeability, allowing for fast accumulation in the cell and driving CO-triggered cell death more effectively. In HT-29 cells, **14** appeared to accumulate mostly in the cytoplasm due to its hydrophilicity, while **15** accumulated along the cell membrane because of its lipophilicity. The 3-(4,5-dimethylthiazol-2-yl)-2,5-diphenyltetrazolium bromide (MTT) assay showed a concentration-dependent inhibition of the viability of HT-29 cells upon the irradiation with IC_{50} = 40 and 70 μM for **14** and **15**, respectively. Interestingly, the ligands and the iCORMs did not show any cytotoxicity in the dark or upon illumination. The activation of Caspase-3/7 confirmed the CO-induced apoptotic cell death.[176]

Five Mn(I) photoCORMs, **16a–16e** (Fig. 4), with benzimidazole ligands, were found to release CO rapidly when illuminated at 365 nm.[177] The synthesis and photoactivatable properties of **16a** and **16e**, upon the exposure to 468 nm LED, were previously reported by our research groups.[178] **16a–16e** were soluble in organic solvents, such as tetrahydrofuran (THF), DMSO and CH_3CN, however they were insoluble in water. The complexes displayed good stability for 24 h in the dark. By comparing the $t_{1/2}$ values of the complexes (going from 5 min for **16a** to 15 min for **16d**), it was observed that extending the degree of conjugation and unsaturation in the ligand framework is helpful for increasing the time of CO release, and so the luminescence intensity of **16a–16e** could steadily be increased. The CORMs showed k_{CO} values in the range 1.9 to 10.8 mol^{-1} min^{-1} according to the CO sensor data. Since the emission bands of **16a–16e** extended to the visible light region, their features of luminescence could satisfy the needs of bioimaging studies. After the incubation of HL-7702 (human normal liver) and SK-Hep1 (hepatic adenocarcinoma) cells with **16a–16e**, bright green fluorescence was found. Complex **16c** displayed the highest cytotoxicity against SK-Hep1, owing to high lipo-solubility and biocompatibility of the benzimidazolyl moiety. Compound **16b**, on the other hand, showed the lowest cytotoxicity due to its restricted solubility.[177,178]

The binuclear selenolato-bridged Mn(I) metallacycles **17a–17d** (Fig. 4) were highly soluble in polar protic and aprotic organic solvents.[179] Complex **17c** showed instability in the dark and released relatively little amounts of CO as well as liberated its CO molecules upon the illumination at 365 nm. When tested against cancer cell lines, **17c** demonstrated toxicity against HCT-15, A549 and HeLa cell lines with IC_{50} = 33.12 ± 5.03, 29.83 ± 3.25 and 11.41 ± 2.61 μM, respectively. Interestingly, **17c** was safe to HEK-293 cells. Complex **17b** had a significant cytotoxicity against A549 cancer cells, but it only had little effect on HCT-15 and HeLa cancer cells. It also showed cytotoxicity against normal HEK-293 cells. On the other hand, **17d** was less toxic against both normal and cancerous cell lines.[179]

Similarly, a series of thiolato bridged Mn-based photoCORMs, **18a–18g** (Fig. 4), soluble in polar organic solvents, was found to release CO when irradiated at 365 nm.[180] When the deoxy-Mb solution of **18a** was kept in the dark, no spectral changes were observed. However, when exposed to a 365 nm wavelength a release of about 2.65 ± 0.13 equivalents of CO was found. Alternatively, **18c** showed very slow spontaneous CO release (about 3.61 ± 0.089 equivalents) in the dark under the Mb assay conditions. According to MTT assay, **18c** was more active even at lower concentrations with IC_{50} values of 6.74 ± 1.77, 2.54 0.58, and 4.92 ± 0.89 against A549, HeLa and HCT-15 cancer cells, in that order. Excitingly, the same complex was not toxic against HEK-293 cells. The spon-

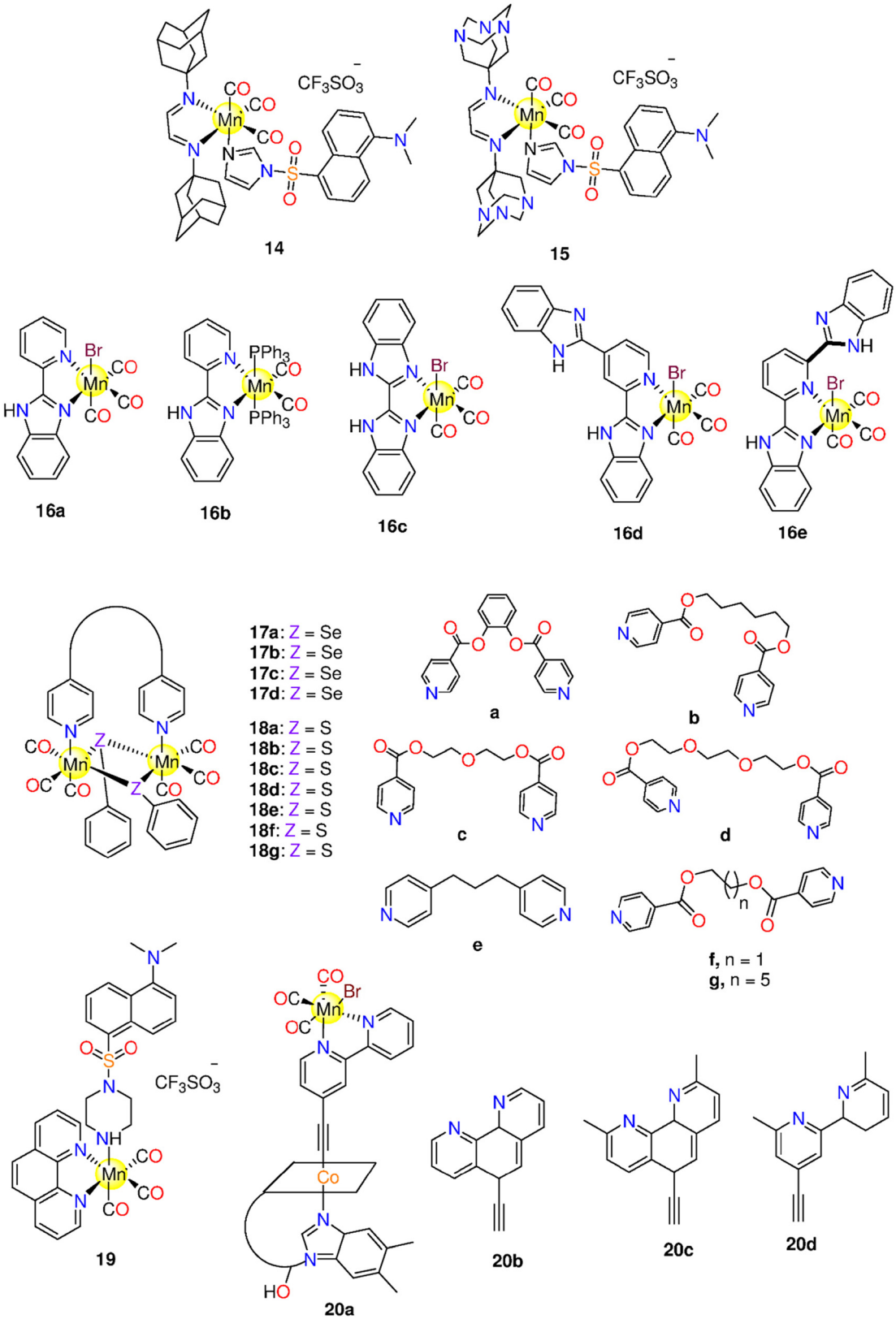

Fig. 4 Structures of the Mn(I) photoCORMs **14–20**.

taneous ability of **18c** to liberate CO in the dark could be the cause of its broad-spectrum cytotoxicity.[180]

The luminescent photoCORM **19** (Fig. 4) was synthesized to facilitate luminescent tracking in a cellular medium.[181] Complex **19** was dark-stable for 24 h in 2% (v/v) (CH_3CN/PBS). Myoglobin assay confirmed that, in acetonitrile, **19** released CO upon illumination with kCO value of 0.13 min^{-1}. IR spectroscopy indicated loss of all the CO molecules upon the exhaustive photolysis. Upon the complexation with Mn(I), the pipdansyl ligand emission was reduced. Following photolysis of **19** in solution, the ligand luminescence intensity was totally recovered. Replacing the imidazole linker in **11** with piperazine resulted in a greater luminescence intensity of **19** when compared to **11**.[173] The strong luminescence of **19** hampers to see the HT-29 cells when their concentration is lower than that of **11**.[173] The cytotoxicity of **19** against HT-29 cells revealed 10–48% decrease in viability upon illumination, but no significant changes in the absence of light were observed. Complex **19** did not show toxicity against HEK-293 cells even at 100 μM concentration.

In 2020, the CO releasing and cytotoxicity properties of **20a–20d** (Fig. 4), bearing ethynyl-α-diimine ligands coupled with vitamin B_{12}, were examined. These photoCORMs were tested on several cancer cells to see whether or not the effect of CO on vitality was cell-type dependent.[182] It was observed that the cytotoxicity of **20a–20d** was affected by the cell density. The higher the cell confluence, the lower the cytotoxic effect, and *vice versa*. When the complexes were subjected to 420 nm light source, they quickly released 2.3 equivalents of CO. The type of the α-diimine ligand has no impact on the CO release kinetics. Under dark conditions, the B_{12}-conjugated photoCORMs were less toxic against MCF-7 than their free analogues (<10 μM). Complexes **B_{12}–20b** and **B_{12}–20c** showed moderate cytotoxicity against MCF-7 cells with IC_{50} = 40 and 17 μM, respectively. When the cytotoxicity under illumination and dark conditions were compared, no specific patterns were seen. Complex **20b** and its **B_{12}** conjugate showed good stability under the physiological conditions. When the iCORMs of **20b** and **B_{12}–20b** were examined, it was surprisingly found that the iCORMs showed more toxicity, in a dose-dependent manner, than their **20b** and **B_{12}–20b** analogues. The iCORM of **20b** showed maximum effect at concentration of 12.5 μM. The results indicated that both CO and iCORM might be involved in these photoCORM cytotoxicity.[183]

In the same year, some of us synthesized two series of visible-light induced photoCORMs, **21a–21d** and **22a–22d** (Fig. 5), using some *N*,*N*-bidentate ligands. In DMSO and CH_2Cl_2, the complexes were dark-stable. However, when illuminated at 525 nm, these photoCORMs released CO. Both **21b** and **22b** release one and three CO molecules at 525 and 468 nm, respectively. Upon irradiation at 468 nm, **21b** and **22b** exhibited $t_{1/2}$ values of 1.91 ± 0.16 min (k_{CO} = (0.60 ± 0.05) × 10^{-2} s^{-1}) and 2.27 ± 0.27 min (k_{CO} = (0.50 ± 0.05) × 10^{-2} s−1), respectively. The compounds did not exhibit cytotoxicity against human hepatocarcinoma HepG2 cells in the dark, but after being exposed to illumination at 525 nm, they showed significant cytotoxicity. The cytotoxicity could be related to the released CO ligands or iCORM, which inhibited the proliferation of the cell line. Complexes **21b** and **22b** liberated CO upon illumination in the same fashion, but the cytotoxicity of

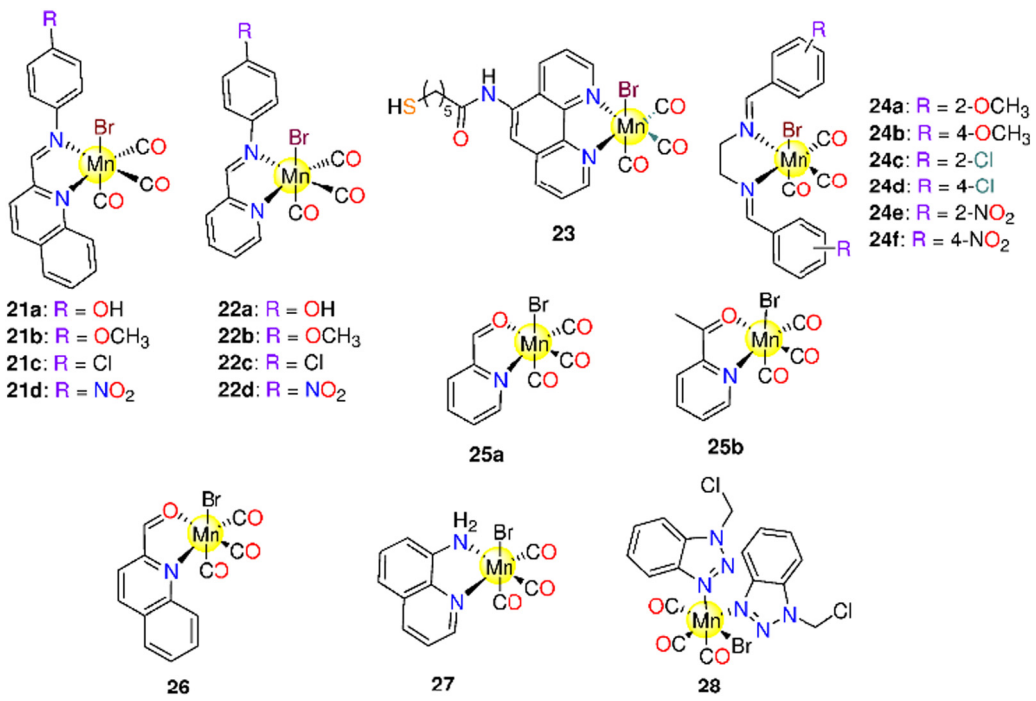

Fig. 5 Structures of the Mn(I) photoCORMs **21–28**.

21b (IC_{50} = 7.1 μM) was higher than that of **22b**. This finding suggested that the iCORM is the primary cause of the acquired cytotoxicity.[184]

Complex **23** (Fig. 5), incorporating 1,10-phenanthroline derivative, was found to be soluble in some organic solvents and in 10% (v/v) DMF/H_2O mixture. In the dark, **23** showed good stability for 5 days in 10% (v/v) DMSO/H_2O mixture at pH 7.2. Gold nanoparticles (AuNPs) were functionalized with **23** to yield water-soluble **23**-AuNPs, which demonstrated good stability at room temperature for 5 days under dark condition. The CO photo release from **23** and **23**-AuNPs was assessed using 400–700 nm light. In the dark, the loaded nanoparticles were nontoxic to A549 cells, whereas they caused apoptosis in the same cell line, with IC_{50} = 232 μg mL^{-1}, upon irradiation with red light. Complex **23** was cytotoxic to cells, with an IC_{50} of 39.2 μM when exposed to red light and 89 μM in the dark. The primary mechanism underlying the photo-cytotoxicity was dual photosensitization with red light, which resulted in fast, synergistic CO release and singlet oxygen ($^1O_2$) production. In A549 cells, photo-triggered CO release led to TURN-ON luminescence.[185]

In 2021, six Mn(I) photoCORMs, **24a–24f** (Fig. 5), containing *N*,*N*-bidentate Schiff-base ligands bearing different substituents at the *ortho*- and *para*-positions, were also proposed and investigated to study how the substituents affected the kinetics of CO release. The complexes maintained the dark stability in both coordinating and non-coordinating solvents. However, in coordinating solvents, upon the incubation, interchange between the bromo ligand and solvent molecules occurred. When **24a–24f** were exposed to a 365 nm light source, they released CO. Complexes **24a** and **24c**, with *o*-OCH_3 and *o*-Cl groups, had the highest cytotoxicity in the dark (IC_{50} = of 18.1 and 11.8 μM) and upon illumination (IC_{50} = of 7.9 and 6.6 μM) against HepG2. On the other hand, **24b** and **24d** were inactive in the dark, however, the illumination enhanced their cytotoxicity indicating that iCORM or synergism between CO and the iCORM were responsible for their biological activity.[186]

The *fac*-$Mn(CO)_3$ fragment of the peptide azopyridine bioconjugate **24g** was capable of being effectively internalized and the local CO release was obtained following red-light illumination without changing the nature of the peptides. The targeted/localized CO release improved cell cytotoxicity *via* apoptosis against U87 (human malignant glioblastoma), MCF-7, and HeLa cell lines. The k_{CO} and $t_{1/2}$ values of **24g** are (1.8 ± 0.5) × 10^{-2} s^{-1} and 39 ± 10 s, respectively.[188]

Recently, we synthetized two water-soluble Mn-based 468 nm-activated photoCORMs, **25a** and **25b** (Fig. 5).[188] Upon incubation in water for 16 h, both complexes showed a slightly decrease in absorbance, which is due to bromo-DMSO exchange. The fact that complex **25b**, which contains 2-acetyl pyridine, is able to liberate CO more quickly than **25a** suggests that the methyl group is involved in controlling the kinetics of CO release. The Mb assay indicated that the solvent plays a part in influencing the CO release kinetics by demonstrating that the route for CO release in water (k_{CO} and $t_{1/2}$ = 2.1 × 10^{-3} s^{-1} and 5.4 min (**25a**) and 2.2 × 10^{-3} s^{-1} and 5.2 min (**25b**)) is slower than in DMSO (k_{CO} and $t_{1/2}$ = 1.1 × 10^{-3} s^{-1} and 10.26 min (**25a**) and 1.3 × 10^{-3} s^{-1} and 8.93 min (**25b**)). In water, **25a** and **25b** released about 0.66 and 1.31 equivalents of CO, respectively. Both complexes are not cytotoxic for malignant and normal cells under dark and light conditions. The fact that the tested photoCORMs remained inactive even under illumination proved how crucial the kind of iCORM is for controlling the cytotoxicity of Mn(I) photoCORMs.

Following that, we looked at the dark stability of **26** and **27** (Fig. 5), their CO release kinetics when exposed to 468 nm, and their cytotoxicity against MDA-MB-231 in both dark and light settings.[189] Upon incubation for 16 h in 25% (v/v) DMSO/H_2O solution, **26** exhibited pronounced change in the metal–ligand charge transfer band. On the other hand, **27** appeared to be stable under the same conditions. The k_{CO} and $t_{1/2}$ values were found to be (26.0 ± 0.18) × 10^{-3} s^{-1} and 4.54 ± 0.17 min for **26** and (7.0 ± 0.10) × 10^{-4} s^{-1} and 17.28 ± 3.6 min for **27**, respectively. Neither in the presence of light nor without it, complex **26** exhibited any discernible cytotoxicity towards MDA-MB-231 cells. On the other hand, **27** owned a dose-dependent cytotoxic effect with IC_{50} = 19.62 μM in the dark and 11.43 μM upon illumination. A similar behaviour was seen when the complexes were tested against normal HEK-293T cells. Accordingly, iCORM or synergism between free CO and iCORM play an essential part in controlling the cytotoxicity of these photoCORMs. Complex **27** was combined with the chemo-therapeutic agent paclitaxel and tested against MDA-MB-231 cells. Viability of the cells cotreated with paclitaxel and **27** was 27%. This value is significantly lower than that obtained when the same cells are exposed to only paclitaxel as well as lower than that of the cells treated with **27**, suggesting that this compound might increase the cytotoxicity of paclitaxel in the context of resistance.[189]

Recently, we introduced **28** (Fig. 5), featuring 1-(chloromethyl)-1*H*-benzotriazole, which released CO at 468 nm.[190] The dark stability tests carried out in various solvents and/or in the presence of biomolecules show a significant likelihood of ligand exchange with the coordinating solvents and histidine. For histidine, HEWL, and calf thymus (CT-DNA), the CO release process plateau was reached after 75, 21, and 25 min, respectively. Complex **28** inhibited THP-1 (human acute monocytic leukaemia) proliferation in the dark, but it does not have negative effects on BM cells, contrarily to the free ligand, which was not cytotoxic to THP-1 and normal BM cells. Upon illumination, **28** generated an acute effect on the normal cells that could be the cause of the photo-generated CO. Because the uncoordinated benzotriazole ligand is inactive under identical experimental conditions, the iCORM may be a Mn(II) complex and be less potent than the parent complex.

Fujita and co-workers designed a photoactive ferritin based CO-releasing system,[191] able to release CO under light irradiation. In particular, the amount of CO released from the Fr cage can be altered by light exposure. The mutation R52C allowed to stabilize the binding sites of MnCO moieties within the nanocage. Through X-ray crystallography the authors identified 48 Mn binding sites with partial occupancies

(0.60–0.80), even if no electron density peaks could be assigned to CO ligands. The presence of CO coordinated to Mn was detected by ATR-IR spectroscopy, following the signal of CO-stretching frequencies. The CO release from the MnCO-loaded nanocages was studied as function of irradiation time: the nanoconstruct $t_{1/2}$ was 2.5 ± 0.2 min, while than that of CORM-1 was 11.4 ± 0.8 min under the same conditions. As a confirmation of the CO-releasing properties of the Fr construct, HEK-293 cells treated with MnCO-Fr, after 10 min of light exposure, showed a cooperative activation of NF-κB accomplished by CO with TNF-α. These results support the potential of protein cages as carriers for CORMs.

6.2 Molybdenum(0) CORMs

Complex **29** (Na[Mo(CO)$_3$(histidine)], Fig. 6) is a water-soluble oxygen-activated CORM that is stable in the deoxygenated aqueous solutions in inert atmosphere.[192] **29** could be activated by O_2 to release CO into the circulatory system and other tissues after oral, intraperitoneal, or intravenous administration. Under aerobic conditions, **29** releases one CO equivalent after 30 min and 2.26 equivalents after 2 h in the dark. However, this behaviour slightly varies with lowering pH, as it slows down by around 50% at pH of 2.5 (the stomach's pH). After 24 h of incubation, **29** is not harmful to LLC-PK1 or RAW264.7 cells, however when 100 M of **29** is given to HepG2 cells, their survival rate drops by about 30%. Mice given daily intraperitoneal injections of 20 mg kg^{-1} of **29**, dissolved in PEG300/water (1 : 4), for 40 days did not exhibit any evident behavioural abnormalities or issues with their internal or exterior organs. Acute toxicity appeared only at a dose of 500 mg kg^{-1} that is substantially higher dose than what is required for therapeutic activity in the majority of diseases.[51] **29** interacts with HSA and HEWL. Upon interaction with HEWL at solid state a polyoxomolybdate cluster $[PMo_{12}O_{40}]^{3-}$ is formed.[51]

The phospholipid phosphatidylcholine was mixed with Mo(CO)$_5$L and Mo(CO)$_4$L$_2$ (L = Ph$_2$P(CH$_2$)$_6$SO$_3$Na) to generate new distinct aggregates. Metallosomes are mixed vesicles with features comparable to liposomes that can be produced using both compounds. FTIR spectroscopy revealed that these mixed systems act as photoCORMs in the presence of UV/Vis light. Toxicity inquiries of various mixed aggregate systems against human dermal fibroblasts have showed that metallosomes have relatively low toxicity like liposomes that are free of metallo-surfactants. Micro-FTIR microscopy, coupled with synchrotron radiation, was utilised to examine the penetration of the studied complexes into cells, revealing metallo-surfactant penetration.[193]

Recently, researchers developed an oral CO releasing system, based on Na$_3$[Mo(CO)$_3$(N≡C–CH$_2$CO$_2$)$_3$], **30** (Fig. 6),[194] that allows for tuneable CO liberation into the gastrointestinal tract, while limiting the release of any other component contained in the device, which could pose a safety risk. The surrounding silicon membranes of the CO release system as well as the load of the Mo(0) complex and iron(III) chloride solution govern CO release rates. Therapeutic CO was generated and released by the reaction of **30** with FeCl$_3$. Neither the CORM nor the probable by-product isocyano-acetate were toxic to human embryonic kidney HEK-293 or mouse embryonic fibroblast NIH3T3 cells. It was demonstrated that the CO releasing system locally produced and released CO into the stomach of the animals without causing systemic exposure.[195]

6.3 Cobalt(0) CORMs

The binuclear Co-based CORMs, Co$_2$(CO)$_6$HCC–CH$_2$OCOR (**31a–31g**) (Fig. 7) showed slight solubility in water and good solubility in DMSO, DMF, CH$_2$Cl$_2$, and THF.[196] In the pH range of 2–10, the DMSO/H$_2$O or CH$_3$OH/H$_2$O mixtures of the complexes showed stability for 7–10 h. This series of the Co(0) complexes released CO *via* oxidation. As CO releasers, most of the complexes have $t_{1/2}$ value of about 60 min. The $t_{1/2}$ values were affected by the CORM structure. *In vivo*, these complexes release CO at a comparatively modest rate. Among the entire series, **31a** with the acetyl substituent had the maximum cytotoxicity against HeLa cells, with an IC$_{50}$ value of 36.20 μM. Compound **31b** showed less toxicity than **31a** revealing the role of the acetyl substituent in controlling the toxicity of this class of Co(0) CORMs. As examples, **31a** and **31f** were discovered to raise intracellular ROS levels, decrease cell division and proliferation, trigger apoptosis in HeLa cells, and stop the cell cycle in the G$_2$/M phase. Following the release of CO, Co(0) may undergo oxidation to produce the active species Co(II) and Co(III), which are attracted to endogenous substrates like DNA and RNA-containing proteins causing cell damage. The CO ligands in CORMs make it easier for these molecules the membrane penetration, which improves medication cellular absorption.[196]

Afterward, the same research group prepared another series of Co based CORMs, **32a–32e** (Fig. 7), which were categorized as slow CO releasers with $t_{1/2}$ values in the range 33.5–71.6 min in Mb solution. However, when measured in blood plasma *in vivo*, the $t_{1/2}$ values were longer. When tested against HeLa and HepG2 cell lines, the complexes **31a**, **31e** and **32a–32e** had IC$_{50}$ values in the ranges 36.2–110.21 μM and 39.25–171.34 μM, respectively. Complex **31a** showed the highest potency against both cell lines with IC$_{50}$ = 36.20 ± 2.5 and 39.25 ± 1.9 μM, respectively. Animal tests on rats demonstrated that **31a** and **32e** had the smallest LD$_{50}$ values

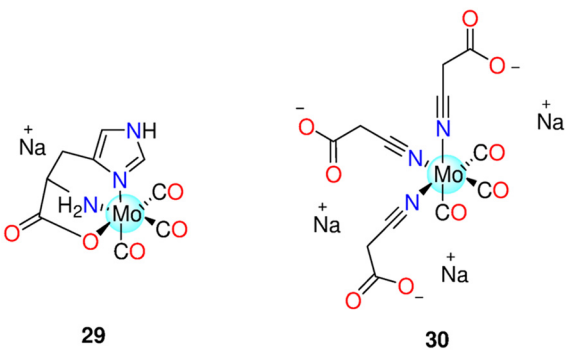

Fig. 6 Structures of the Mo(0) CORMs **29** and **30**.

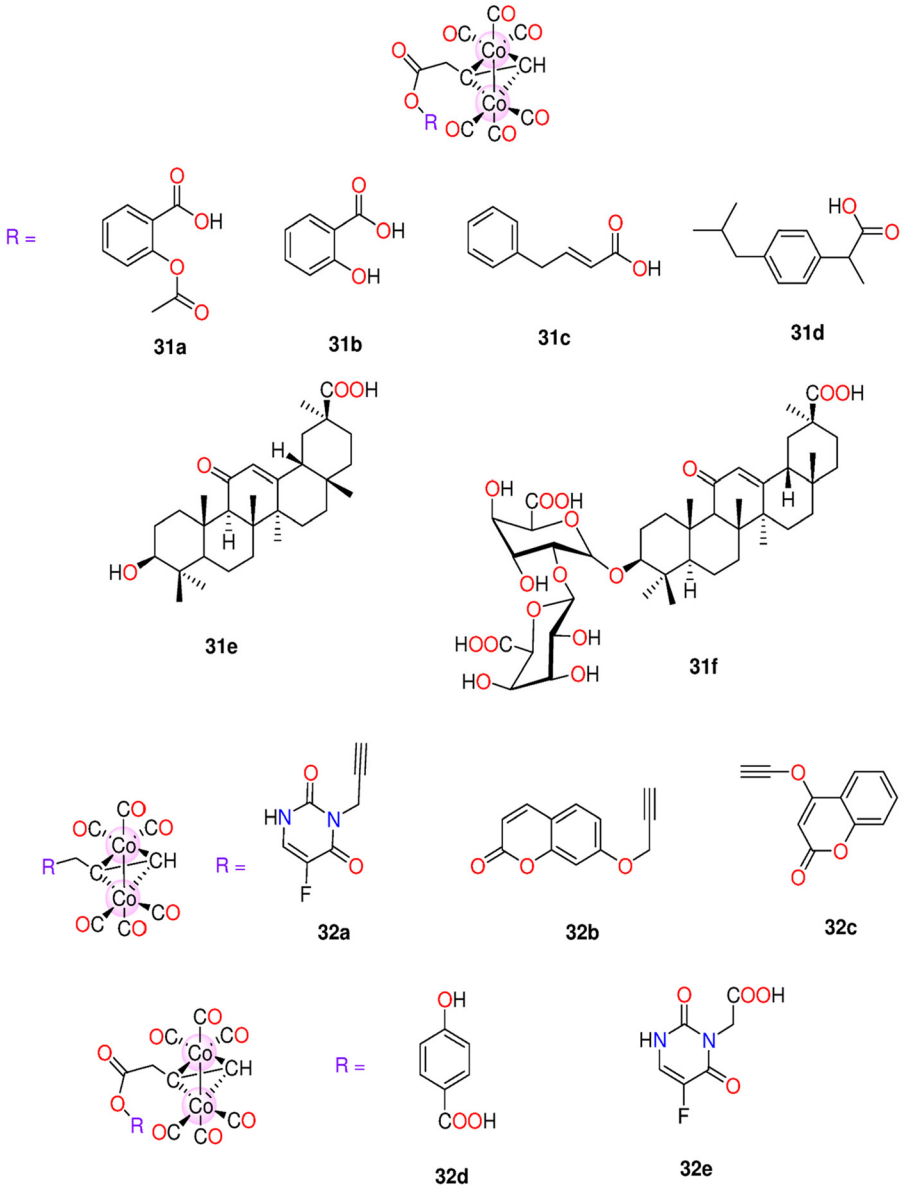

Fig. 7 Structures of the Co(0) CORMs **31a–31f** and **32a–32e**.

(300–500 mg kg^{-1}). The biodistribution of CORMs in the tissues and organs has been correlated to side chain substituents, which have a substantial impact on the kinetics of CO release, potency, and cell viability. After numerous successive dosages, the CORMs damaged the liver and kidneys both morphologically and functionally. Zebrafish larvae were significantly impacted by developmental toxicity caused by both **31a** and **32e**. At low concentrations (0.5 and 1.0 μM), they showed no cytotoxicity, but at higher concentrations (5.0–20.0 μM) they are toxic.[197]

Next, similar binuclear complexes, **33a–33k** and **34a–34e** (Fig. 8), were synthesized. The $t_{1/2}$ values were proven to be dependent on the structures of the non-CO ligands similar to **31a–31g** and **32a–32e**. Complex **33f**, with pyridine ring and chloride atom in the 3-position of the phenyl ring, had the longest $t_{1/2}$ value (42.6 min), while **34d** was the fastest CO releaser with $t_{1/2}$ = 15.8 min. All complexes showed lower activity against the proliferation of HeLa, A549, HT-29, HepG2, and MCF-7 cells when compared to cisplatin. However, when compared to 5-Fluorouracil, **34a** and **34b** showed superior activity and selectivity to the HT-29 (37.9 and 55.8 μM) and MCF-7 (33.6 and 49.3 μM) cell lines. With respect to **33d**, **34a** had a higher ability to down-regulate cyclooxygenase-2 (COX-2) expression. This might be due to celecoxib structural fragment, a COX-2 specific inhibitor, being present in **34a**. After being exposed to H_2O_2 for an hour, myocardial H9c2 cells were treated with **33a**, **33j**, and **34a**, which enhanced the survival rate of the cells. This suggested that the complexes have a protective effect against oxidative damage. The efficacy of **33a** to increase H9c2 cell viability was the highest, while **34a** signifi-

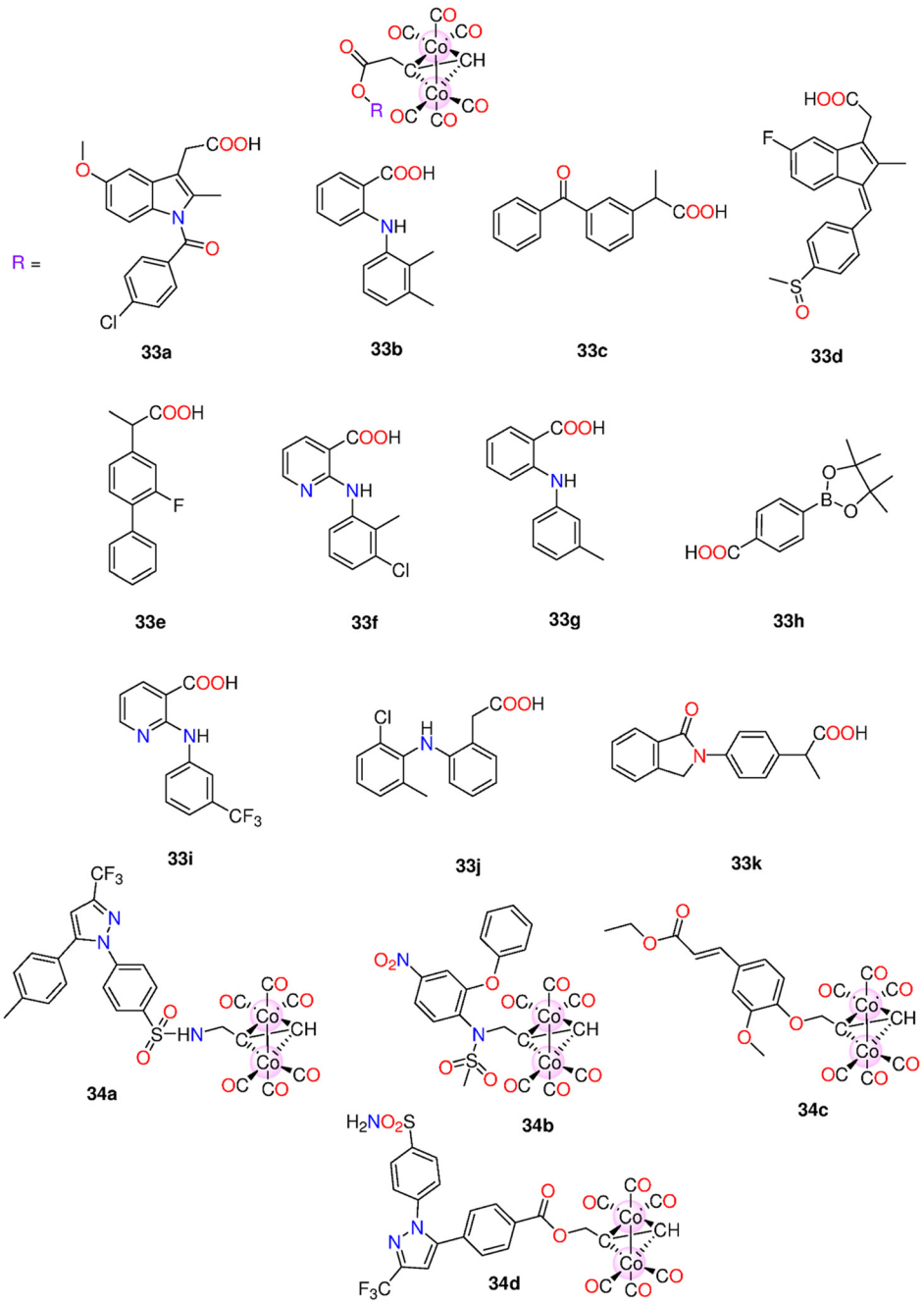

Fig. 8 Structures of the Co(0) CORMs **33a–33k** and **34a–34d**.

cantly increased the cell survival rate. However, when the cells experienced harm for 8 h, the protective action was not noticeable. Additionally, the complexes demonstrated a concentration-dependent anti-hypertensive impact on SHR rats.[198]

The cytotoxicity of two series of Co-based CORMs, **35a–35e**, **36a–36e** as well as 17α-ethinyl estradiol based complexes **37a–37c** (Fig. 9) were examined against HepG2, HeLa, and MDA-MB-231 cells.[199] These complexes have good solubility in organic solvents. The complexes showed IC_{50} values in the range 4.7–548.6 μM against the tested cell lines. Complex **35a** exhibited high selectivity to HepG2 with IC_{50} = 4.7 ± 0.76 μM. At a concentration of 50 μM, **35a** had a cytotoxic effect against HepG2, HeLa and MDA-MB231 cells with cell viability of 21.21%, 12.14% and 23.99%, respectively. However, the iCORM of **35a** showed minimum effect on the cells. It was suggested that the anticancer action could be the result of combined impacts of CO and CO depleted species. In HepG2 cells, complex **35a** increased the amounts of ROS in the mitochondria and decreased the dose-dependent mitochondrial membrane potential. According to a western blot investigation,

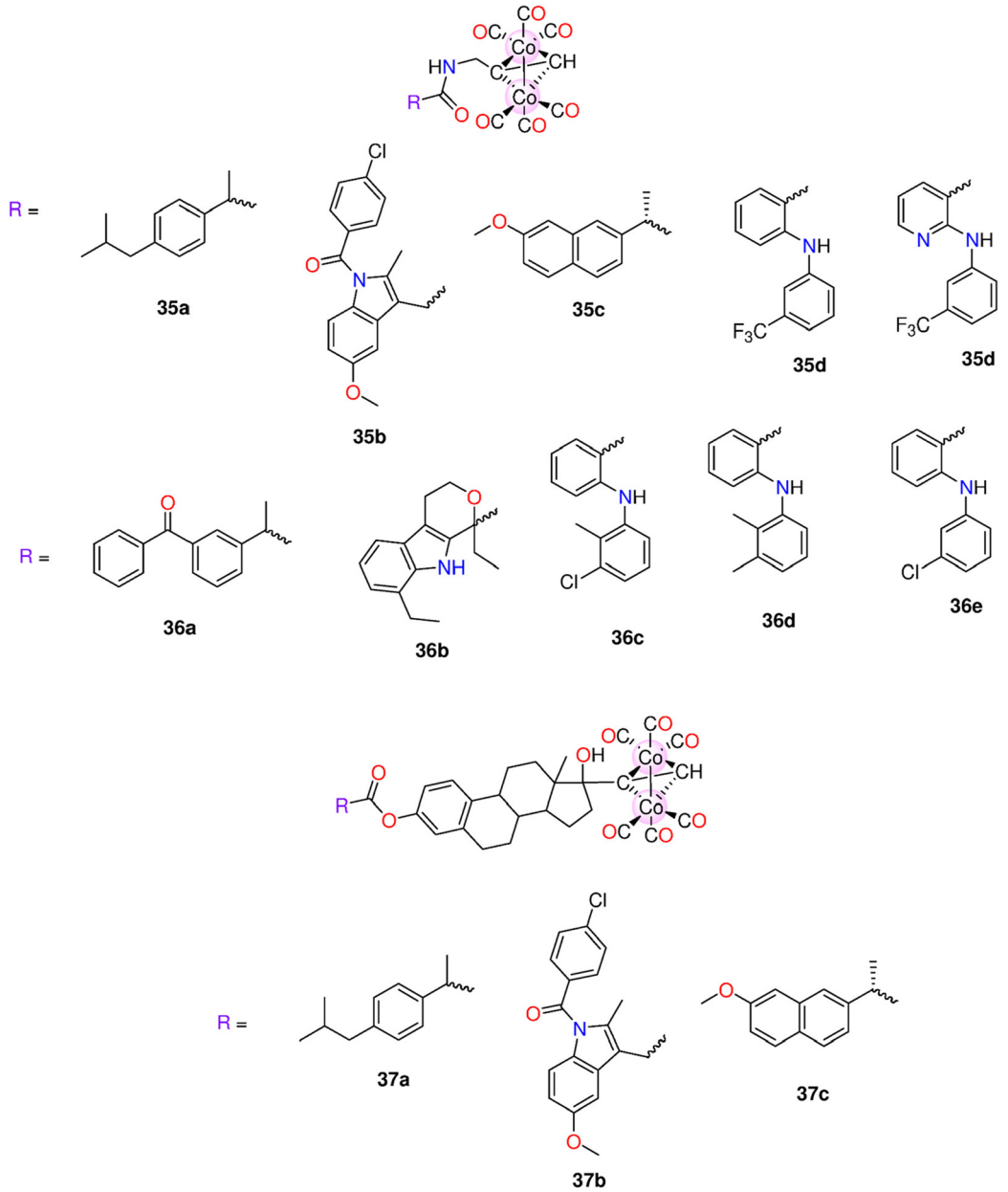

Fig. 9 Structures of the Co(0) CORMs **35a–35e**, **36a–36e** and **37a–37c**.

35a reduced COX-2 expression. Molecular docking calculations showed that **35a** can bind Arg120 in the protein active site through the formation of a hydrogen bond. The COX-2 and mitochondrial pathways may be targeted by **35a** to cause apoptosis in HepG2 cells.[199]

6.4 Iron(II) and iron(0) CORMs

Iron-based CORMs can release CO when triggered by light, redox state changes, and bond breakage caused by an enzyme at the ligand in enzyme-triggered CORMs. In 2005, Motterlini and co-workers presented the iron-containing complex CORM-F3, **38** (Fig. 10).[200] Complex **38** steadily released CO *via* the oxidation processes and has been proven to cause vasorelaxation and prevent inflammation *in vitro*. Next, three Fe-CORMs have been introduced such as CORM-F7, CORM-F8 and CORM-F11, **39–41**, respectively (Fig. 10). Motterlini's group investigated how the structure of CORMs can be altered to preserve CO dependent functions while reducing the cellular toxicity. The rate of CO release was greatly reduced by about 4.5-fold when the Br at the 4-position of the 2-pyrone in **38** (k_{CO} = 0.19 nmol min^{-1}) was replaced with a Cl in **40** (k_{CO} = 0.041 nmol min^{-1}). A further reduction was noticed when the substituent at positions 4- and 6- is a –CH_3 group in **41** (k_{CO} = 0.041 nmol min^{-1}) or a hydrogen in **39** (k_{CO} = 0.007 nmol min^{-1}). 100 μM of **38** induced vascular relaxation in detached aortic segments and suppressed endotoxin-stimulated a dose-

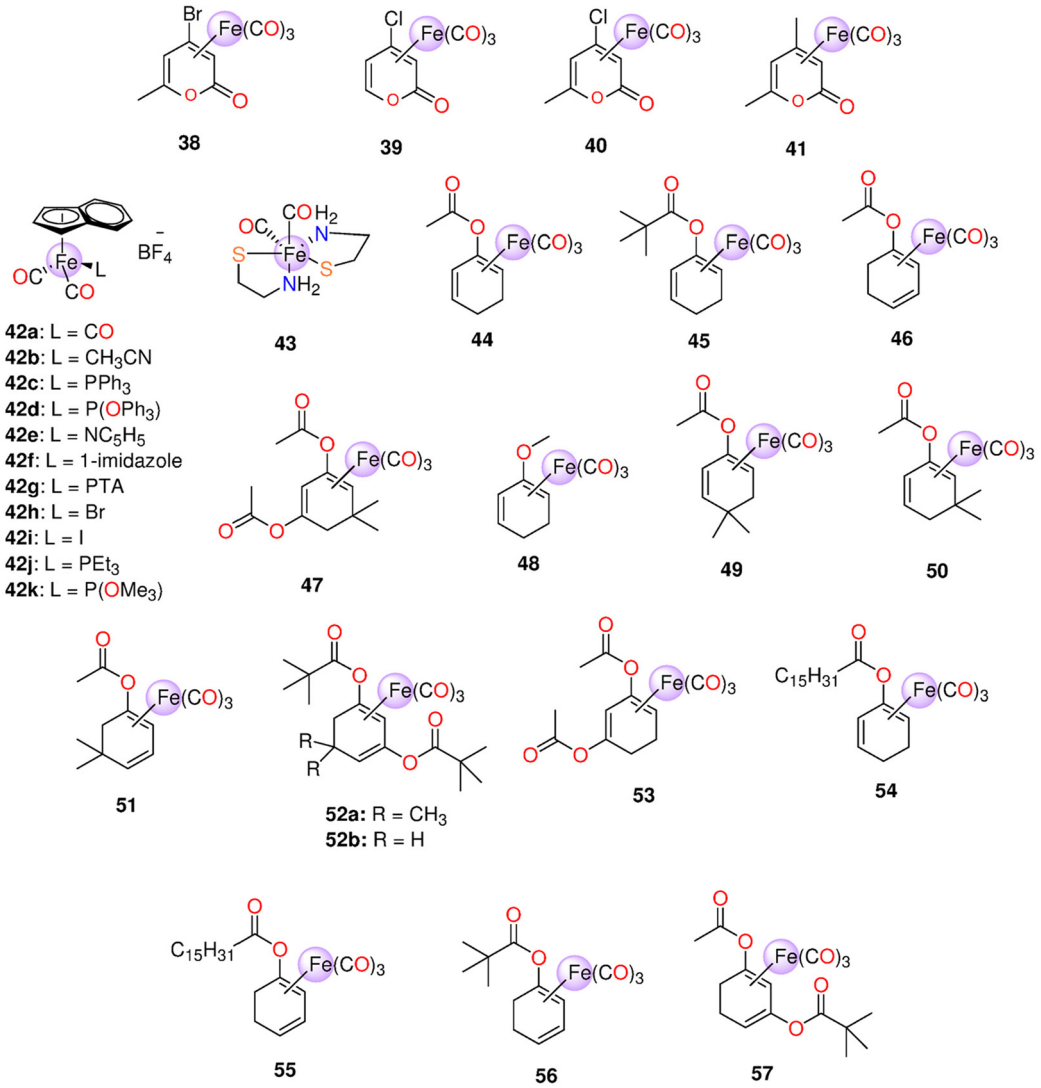

Fig. 10 Structures of the Fe(0) CORMs **38–57**.

dependent inflammation reaction in macrophages. Both **38** and **40**, with halogens and a $-CH_3$ group *meta* to each other, showed less toxicity against RAW246.7 macrophages.[201]

When indenyl ligand replaced cyclopentadienyl ligand, the rates of the substitution processes significantly increased.[202] This fact served as the basis for the synthesis of Fe-based CORMs **42a–42k** (Fig. 10) with indenyl ligands that may release CO more quickly than their equivalent cyclopentadienyl CORMs. Complex **42a** had the shortest $t_{1/2}$ value of one min, while **42j** exhibited the highest $t_{1/2}$ of >5000 min. Among this series of iron CORMs, **42b** exhibited no cytotoxicity even at 100 μM towards rodent RAW264.7 macrophages. **42a** was the only compound that released CO more quickly than the comparable cyclopentadienyl molecule. Also, indenyl CORMs are much more cytotoxic than the cyclopentadienyl ones.[203]

CORM-S1 (dicarbonyl-bis(cysteamine)iron(II)), **43** (Fig. 10), is a water-soluble Fe(II) photoCORM that can release CO *via* irradiation with visible light source higher than 400 nm.[204] The rate of CO release from **43** was proportional to the intensity of the irradiation source. Complex **43** is relatively stable under dark ambient conditions, however the irradiation with a 470 nm light for 15 min led to the release of two CO molecules. In the dark, **43** had no effect on ion currents that crossed voltage-activated potassium channels, and the cell membrane's structure remained unaffected. When exposed to light, a higher outward current was generated with a similar variation in the potential of the membrane, giving a measurement for CO released from **43**.[204]

Acyloxydiene–$Fe(CO)_3$ **44–46**, diacetoxydiene-$Fe(CO)_3$ **47**, and the methoxy-substituted **48**,[205] were prepared and are referred to as ET-CORMs. In cells, the complexes are cleaved by the intracellular esterases (*e.g.*: PLE, pig-liver esterase). An LCR (lipase of *Candida rugosa*) surpassed PLE for **44** and **45**. Complex **45** reacted far more slowly than **44**, **46**, and **47**. Under these conditions, the methoxy **48** did not show any reactivity, as anticipated. When PLE is present, CO was released from **46**

and **47**, and in the presence of LCR, from **44–46**. **47** does not release CO when esterases are not present. So, the hypothesised enzyme-triggered CO release was clearly shown to exist. Both **45** and **48** showed no toxicity against murine RAW267.4 macrophages up to 100 μM. On the other hand, **44**, **46** and **47** had IC_{20} values in the ranges 11–28 and 14–38 μM using MTT and crystal violet assays, respectively. The impact of ET-CORMs upon NO formation *via* inducible nitric oxide synthase was assessed. To limit the pseudo positive results due to cytotoxicity, only concentrations lower than the IC_{20} values were selected. In LPS-induced RAW267.4 cells, the diacetate **47** showed the highest inhibition of NO generation. With concentrations of 15 and 5 μM, **47** suppressed LPS-induced NO production by up to 68 ± 6% and 33 ± 6%, respectively. 5 μM of **46** led to 30 ± 7% suppression of NO production, while **44** (25 μM) reduced NO generation by only 16 ± 10%. For up to 50 μM, **45** and the esterase-insensitive **48** did not notably inhibit NO production.[48]

Next, the same research group identified the structure–activity relationships of the group of acyloxycyclohexadiene-Fe$(CO)_3$ ET-CORMs, **44–56**. PLE and LCR were used to induce the hydrolysis of the various compounds. When compared to the acetate-containing complexes, the rates of CO discharge from palmitate- and pivalate-based complexes were sluggish, correlating to slower hydrolysis rates. Complexes **46**, **55** and **56**, containing an ester moiety at the diene outer position, showed faster CO release rates than **44**, **45** and **54**, having the same ester group at the inner position. However, the diacetate complexes showed the fastest CO release rates. This could be brought on by a more rapid ester hydrolysis or by the initial enol complex's reduced stability. Additionally, it cannot be ruled out that the hydrolysis of the second ester function speeds up the CO release. Using murine macrophage cells (RAW264.7), the cytotoxicity and suppression of NO-production were evaluated. In particular, the ET-CORMs **47** and **51** showed promising characteristics. The NO-inhibition was shown to be highly influenced by the enone by-products of the monoester-containing complexes, and not the diester-containing ones.[49] The parent compound, whether cyclohexanedione or cyclohexenone, and the ester function location have a significant impact on the influence of ET-CORMs. ET-CORMs with an ester group bonded to the cyclohexenone ring through the outer (**46**) rather than the inner location (**44**) possess markedly higher toxicity towards human umbilical vein endothelial cells (HUVEC). This coincided with an increase in CO release from the formerly mentioned ET-CORM. Because the half maximal effective concentration (EC_{50}) values for **46** were much lower than those of $FeCl_2$ or $FeCl_3$ and were unaffected by iron chelation, the toxicity was not found to be mediated by iron. While the **44**-derived suppression of the expression of vascular cell adhesion molecule 1 (VCAM-1) in long-term HUVEC cultures decreased over time, the **57**-derived inhibition seemed to rise. Both **44** and **57** prevented NFκB without regard to nuclear factor of kappa light polypeptide gene enhancer in B-cells inhibitor α (IκBα) degeneration. Both **44** and **57** stimulated Nrf-2, which in turn caused HO-1 expression.[42]

Recently, the acetate-bearing complexes **44** and **46** along with the pivalate-bearing compound **52b** were examined *ex vivo* on small rat mesenteric arteries that had been pre-contracted with methoxamine. Both **44** and **46** caused significant dilation to the pre-contracted mesenteric arteries, while **52b** did not produce any effect. Alternatively, **46** did not cause vasodilation in the case of KCl-pre-treated mesenteric arteries. According to these findings, the primary K^+-channel by which **46** mediates vasodilation is Kv7.[206]

Motterlini and co-workers proposed four iron(II)–allyl CORMs, **58**, **59**, **60** and **61** (Fig. 11) that spontaneously release CO. Complexes **58–60** were soluble in DMSO, while **61** was soluble in water due to its ionic nature. In the concentration range of 10–40 μM, about one mole of CO/mole of each complex was released. Complexes **58–60** were found to be faster CO releasers than the water-soluble **61** ($t_{1/2}$ = 18 min). Compounds **58–60** caused more significant cytotoxic effects on vascular and inflammatory cells and isolated vessels when compared to **61**. Against macrophages, the IC_{50} values of **58–61** were 9.1, 11.9, 23.6 and 797 μM, respectively. Complex **58** and its iCORM caused substantial vasorelaxation in isolated aortic rings over time and reached maximum after 60 min. These findings imply that the CO-depleted molecule contributes to the observed effect. Treatment with **59** and **60** led to the same results, however their iCORMs had less vasorelaxation effect. Complexes **58–60** caused a total loss in the cell activity of murine smooth muscle cells. For **61**, the complex caused fast dose-dependent vasorelaxation that reached maximum after 10 min. In contrast to **58**, the iCORM of **61** showed minimum vasorelaxation implying that only the released CO is responsible for such effect. Complex **61** and not its iCORM greatly reduced LPS-induced NO production without any obvious toxicity up to 100 μM.[207]

In a concentration range of 1–1000 μM, the cytotoxicity of **44–48**, **52b** and **53–56** (Fig. 10) was tested on cultures of HUVEC and proximal tubular epithelial cells (PTEC). Complex **48** and three enones were used as controls. Only **46** and **53** showed cytotoxicity at low concentrations. Compound **46** was toxic only against HUVEC, while **53** exhibited cytotoxicity towards PTEC and HUVEC. The hydrolysis products of all complexes did not show any cell toxicity. Changing the substituent from acetate in **46** and **53** to pivalate in **52b** and **56** resulted in decreased toxicity. After 24 h of cold preservation, cell damage occurred in both cell lìnes. The cellular damage markedly diminished by treating the cells with 100 μM of **44**. Only ET-CORMs containing 2-cyclohexenone were able to reduce the damage caused by cold preservation. The cell protection was dramatically diminished when acetate in **44** was replaced with pivalate in **45**. The VCAM-1 expression was significantly suppressed by **44**, **52b** and **56** and to some extent by **45**. For 2-cyclohexenone CORMs, this inhibition could be mediated by 2-cyclohexenone since the ligand itself suppresses VCAM-1 expression.[208]

Protease-triggered Fe-based CORMs **62a–62d** (Fig. 11), containing a PGA (penicillin G amidase)-cleavable site, were prepared.[209] Headspace GC and the and the reduction of VCAM-1

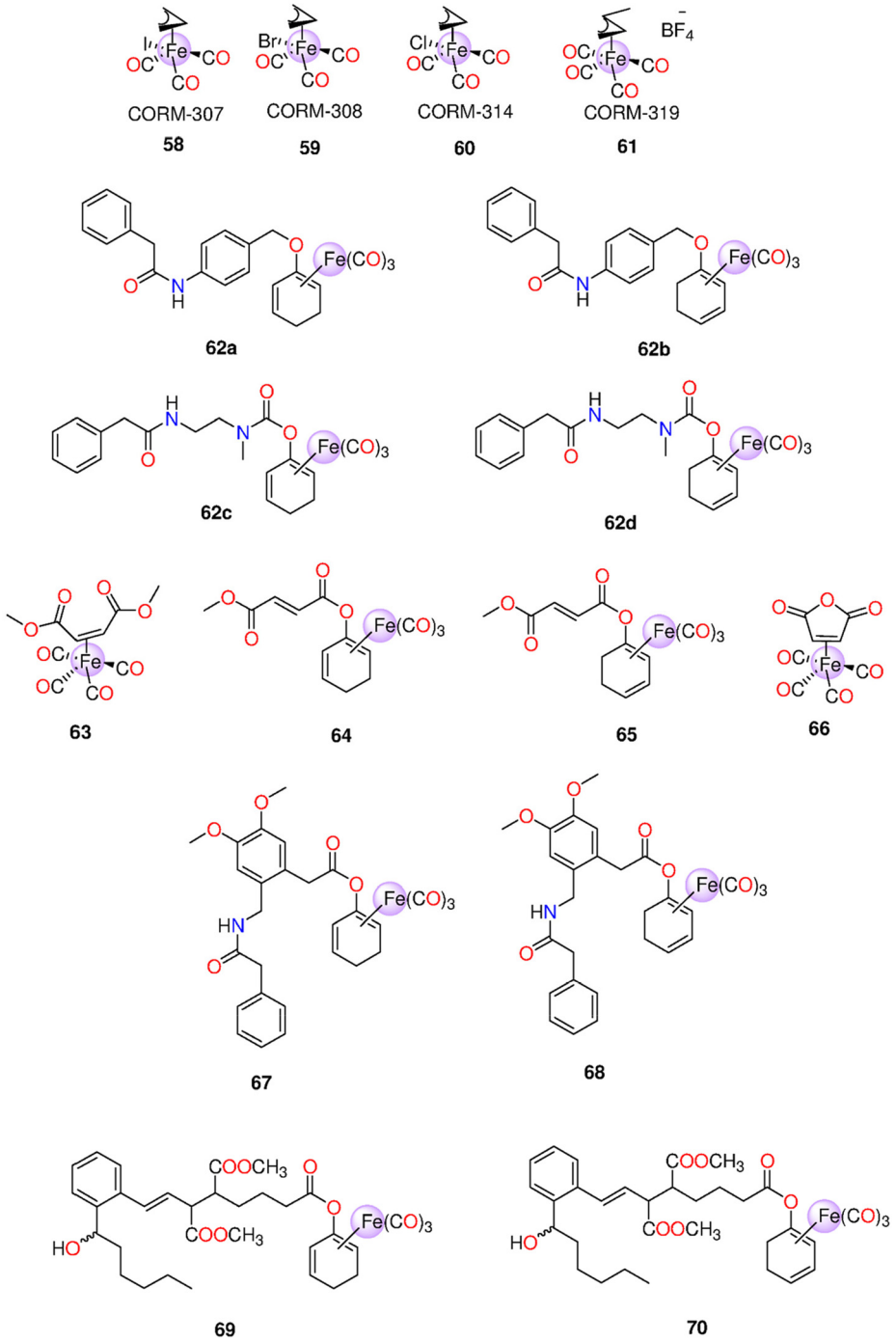

Fig. 11 Structures of the Fe(0) CORMs **58–70**.

expression in a cell-dependent experiment both supported the claim that **62a–62d** causes CO release. The phenylacetamide unit is first broken down by an enzyme, followed by linker self-immolation to create the sensitive dienol-$Fe(CO)_3$ intermediate and, finally, oxidation-triggered degeneration of the intermediate to liberate CO. Common biological effects of CO, such as the suppression of the inflammation reaction and the activation of HO-1 expression, were seen only when the CORM and PGA were administered together to human endothelial cells *in vitro*.

Autoimmune disorders are distinguished with the stimulation of T cells *via* dendritic cells. Small molecules like dimethyl fumarate or CO are used to treat these serious diseases. Bifunctional iron ET-CORMs **63–66** (Fig. 11), with simultaneous intracellular discharge of CO and methyl fumarate, were developed. The fumarate complexes **63–66** showed

enzyme-triggered CO release *in vitro* using PLE. The substantial suppression of LPS-stimulated pro-inflammatory signalling routes and blocking of (IL)-12 or (IL)-23 generation caused by **63–66** had been shown in bone marrow-derived dendritic cells. The findings also suggest that **63–66** can change dendritic cells into anti-inflammatory phenotypes.[210]

The effectiveness of iron(0) CORMs that can discharge CO either in response to an enzyme or spontaneously, both extracellularly and intracellularly, was compared. Different CORMs, CORM-2, CORM-3, ET-CORMs (**44** and **46**) (Fig. 10), and AT-CORMs (**62c**, **62d**, **67**, and **68**) (Fig. 11), were compared regarding the capacity to release CO, cytotoxicity, the capacity to promote HO-1 expression, and to suppress the production of VCAM-1 in TNF-α-activated HUVEC.[50] These impacts are correlated to the quantity of CO discharged by the complex and not to extra- or intracellular CO discharge. As expected, CORM-2 and CORM-3 primarily release CO_2 and tiny amount of CO.[211,212] However, following the enzymatic hydrolysis, no release of CO_2 from the ET- and AT-CORMs was observed. Using certain membrane-linked enzymatic action could allow tissue-targeted CO administration based on the previously mentioned finding that extra- and intracellular CO release generate equivalent anti-inflammatory characteristics.[50]

To create novel anti-inflammatory drugs, Schmalz and coworkers developed conjugates between lipoxin A_4 and an acyloxycyclohexadiene-Fe$(CO)_3$ compound, **69** and **70** (Fig. 11). Both **69** and **70** were toxic to cultured HUVEC in a dose-dependent manner, with **69** being somewhat more toxic. While both Fe-CORMs induced HO-1 sovraexpression in HUVEC, they were unable to decrease VCAM-1 expression induced by TNF-α in the tested cells. The HO-1 expression was greater in M2 polarized macrophages compared to M1 polarized ones. As anticipated, the enhanced HO-1 expression can be attributable to CO release.[213]

Mitochondria-targeting water-soluble ET-CORMs (Mito-CORMs) with *N*-methyl-pyridinium triflate motif bonded to the ester moiety (**71a–71g**) (Fig. 12) were reported.[214] When dissolved in PBS/DMSO (5 : 1) mixture, complexes having an acyloxy motif at 2-location of diene-Fe$(CO)_3$ unit exhibited hydrolysis sensitivity and released CO spontaneously with 1.8 equivalents for **71a** (after 2.5 days) and 2 equivalents for **71b** and **71c** after 2 days. However, this release was significantly suppressed in the presence of PLE (0.6 equivalents from **71b** and **71c** after 5 days). To determine if the high CO release from **71b** and **71c**, when PLE is absent, depends on ester moiety activation to hydrolysis, a *trans*-cyclopropane unit was introduced into **71g** to assure electronic and steric isolation of the two functions. Complex **71g** exhibited a reduced spontaneous CO release. However, in the presence of PLE, it released just 1.5 equivalents of CO, ruling out any possibility of intramolecular activation of the ester moiety. In contrast, the 1-substituted isomers demonstrated PLE-induced CO release. Three equivalents of CO were released from **71d** after 10 h incubation with and without PLE. In the presence of PLE, both **71e** and **71f** released much more CO (about 3 equivalents) than the spontaneous release without PLE (about one equivalent). Because of the required esterase-triggered CO release, both **71e** and **71f** were good candidates for biological evaluation. Mito-CORMs

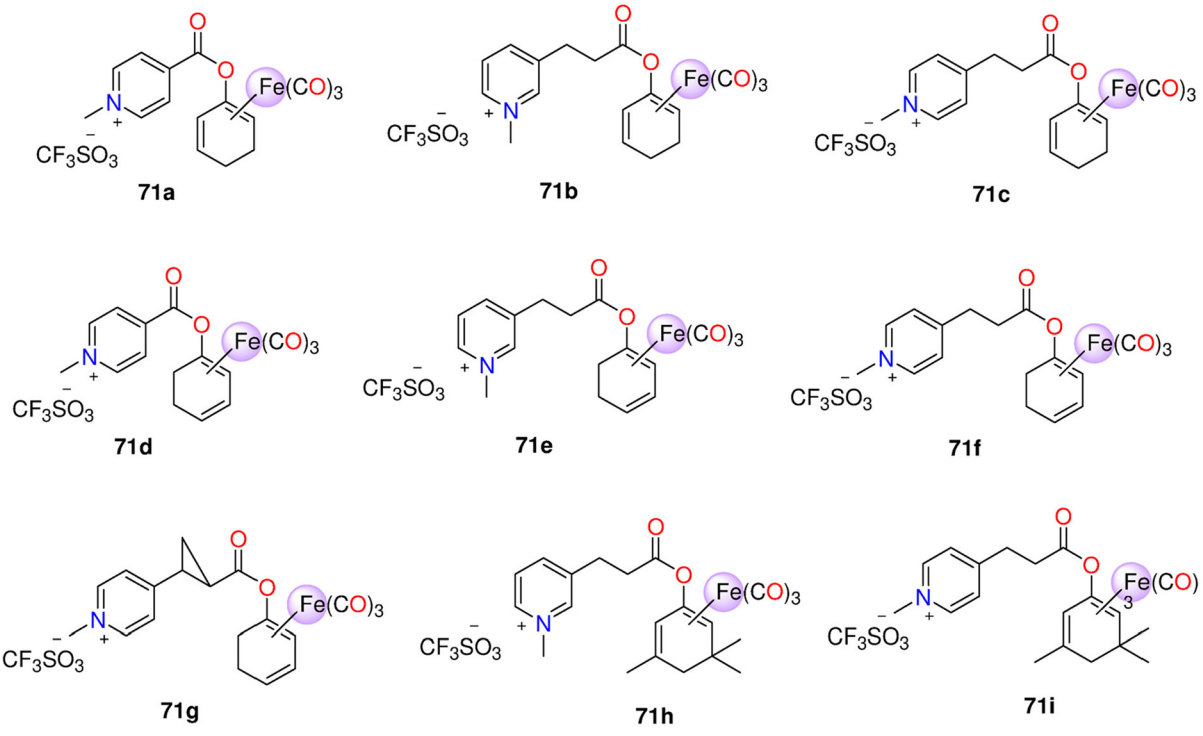

Fig. 12 Structures of the Fe(0) CORMs **71a**–**71i**.

71h and **71i**, which were derived from isophorone and not easily oxidized, were developed to rule out the possibility that the phenol produced from cyclohex-2-enone's oxidation contribute to the toxicity of **71e** and **71f**. Complexes **71e** and **71f** showed no toxicity against HUVEC up to 500 μM. However, their analogues **71h** and **71i**, which were supposed to be less toxic, showed pronounced toxicity at concentrations > 50 μM. Neither the hydrolysis by-product isophorone nor the methyl esters were toxic, indicating that the toxicity is probably caused by the released CO. The anti-inflammatory effect of **71h** and **71i** was shown to be stronger than **71e** and **71f**. This was noticeable for the suppression of the expression of VCAM-1, but there was not a significant variance in HO-1 inhibition among the two Mito-CORM classes. While both **71h** and **71i** suppressed mitochondrial respiration in both basal and stressful settings, glycolysis increased. Complexes **71e** and **71f** elevated both mitochondrial respiration and glycolysis.[214]

6.5 Ruthenium(II) CORMs

Although CORM-2 is widely used to spontaneously release CO when introduced to living tissues, various Ru(II)-based CORMs have been studied as photochemical CO-releasing agents since they do not release CO spontaneously. As a result of the fact that many Ru(II) carbonyls discharge CO after being lighted, such complexes possess the advantageous quality of regulating CO conveying. The CO release from next-generation Ru(II)-based CORMs is induced by a light source or ligand exchange. The solid Ru(II)-based complexes **72a–72i**, **73a–73d**, **74a** and **74b** (Fig. 13) are stable even when exposed to light and air. Complexes **72a–72d** are water-soluble, while the rest of the compounds exhibit poor solubility in water. The complexes show efficient CO release with $t_{1/2}$ values ranging from 1.1 to 15.8 min. Complexes with amino acids, **72a–72c**, are slightly faster CO releasers than the complexes containing amino-pyridine or Schiff-base ligands (**73a** and **74a**). The complexes show very weak antiproliferative activity against murine L929 fibroblasts (IC_{50} = 62.69–255.48 mg l^{-1}). Against mice, the complexes have lethal dose LD_{50} values of 800–1000 mg kg^{-1} (**72a** and **72h**), 1100–1500 mg kg^{-1} (**72g** and **74b**) and 150–200 mg kg^{-1} (**73a**). When tested on rats *in vivo*, the complexes have a little impact on liver function, but they do cause physiological harm to liver cells. Additionally, these complexes have a detrimental effect on both functional and physiological processes of the kidney. Metal buildup could be among the causes of adverse effects. The studied complexes do not accumulate in major tissues or organs, and they are unable to pass through the blood–brain barrier. The hepatic P450 enzymes oxidize Ru(II) in CORMs to Ru(III) throughout the metabolism process.[215]

For Ru(II) complexes **75a–75n** (Fig. 13), bearing monodentate ligand, it appeared that the ligand affects the stability of complexes in solution, CO release properties, anti-inflammatory activity and cytotoxicity. The phosphine PTA (1,3,5-triaza-7-phosphaadamantane) was unable to ensure the water solubility of the water-insoluble **75i**, despite being employed to enhance the water solubility the complexes. However, the diacetylated form of PTA gave a desirable level of solubility for **75j**. The isocyanide-based complexes **75l**, **75m**, and **75n** are slightly soluble in water where they easily degrade. The aqueous solutions of the complexes have shown instability when eluted using H_2O/MeOH gradient for 60 or 75 min. In the dark, instead of releasing CO to the headspace, the tricarbonyl complexes release CO_2 from aqueous solutions (PBS or water). However, the dicarbonyl (**75b** and **75c**) and the monocarbonyl **75d** do not release CO or CO_2 under the same conditions. Complex **75d** has a $t_{1/2}$ of about 50 min and is the most stable complex among the three DMSO-containing complexes. Binding studies of **75f**, **75g**, and **75h** with the model protein HEWL reveal that the $Ru(CO)_x$ fragments, *i.e.* the species missing of one or two COs and of the auxiliary ligands, that are exchanged by H_2O molecules, bind with the protein at various metal binding locations. In particular, elucidation of the adducts formed by these CORMs and HEWL demonstrates that $Ru(CO)_x$ motifs, formed by the CORMs degradation in solution or due to the presence of the protein, recognize His15, Asp18, Asp52, Asp101 and Asp119 residues with the His15 side chain as the primary binding site. Notably, the X-ray structure of the HEWL conjugated with **75g** identified the metallacarboxylate species $[His15\text{-}Ru^{II}(COOH)(CO)(H_2O)_3]$, which has been supposed to be an intermediate of the CO release reaction, resulting from the introduction of HO^- to the di-cation *cis*-$[Ru(CO)_2(H_2O)_3]^{2+}$. The attachment of the CORMs to the cell surface allowed the Ru framework to decompose or internalize into cells. CO could be easily delivered to the cells and its inner target areas in both circumstances. Up to 100 μM, none of the compounds examined were toxic to murine RAW264.7 macrophages. The CORMs reduced NO generation through LPS-activated RAW264.7 cells in a concentration-dependent fashion. The thioether derivative **75k** was the most effective at reducing NO generation.[216]

Bernardes and co-workers synthesized a tricarbonyl Ru(II) CORM with an *N*-acetyl cysteine ligand, **76** (Fig. 14). In general, CORM-3 generates ROS *via* a water–gas shift reaction, that dramatically increases its antibacterial activity.[103] However, **76** decreases ROS production during the release of CO and has no bactericidal activity. When compared to CORM-3, **76** shows higher stability due to its slower CO release in aqueous media and low toxicity against RAW264.7 cells even at 100 μM. Also, **76** exhibits anti-inflammatory properties through a synergistic effect upon the suppression of the NO production and TNF-α expression. As CORM-3, no CO release was detected from PBS solution of the water-soluble **76** in the dark at ambient conditions using GC-TCD. Both **76** and CORM-3 do not increase the amount of COHb in sheep blood when incubated at 37 °C.[217]

The antiproliferative properties of three $Ru(CO)_x$ complexes, **77–79** (Fig. 13), with benzimidazole derivatives, was also examined.[218] Complexes **77** and **78** show low solubility in H_2O and good solubility in different organic solvents. In PBS, both **77** and **78** show good stability for 72 h at ambient temperature. Both CORMs interact with HEWL and bovine pancreatic ribonuclease (RNase A) to form conjugates having one or two CO

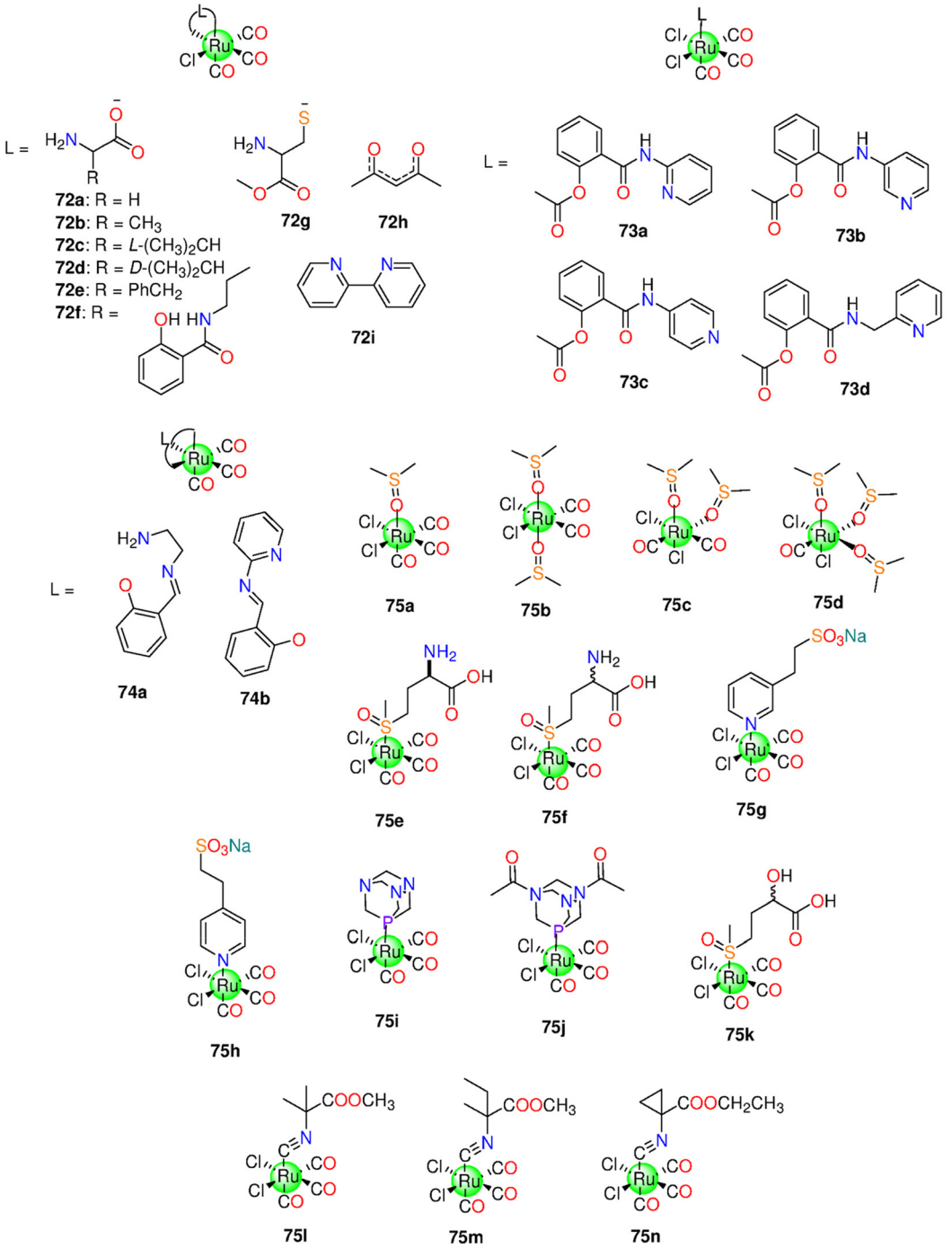

Fig. 13 Structures of the Ru(II) CORMs **72**–**75**.

ligands, thus losing CO ligands. Similar results[219] have been obtained using *fac*-[$Ru^{II}(CO)_3Cl_2(N^3$-imidazole)] and *fac*-[$Ru^{II}(CO)_3Cl_2(N^3$-methyl-imidazole)], that are moderately toxic to ovarian and colon cancer cells.[220] Both **77** and **78** show toxicity against the CH1/PA-1, A549 and SW480 (colon adenocarcinoma) cells with IC_{50} values that are nearly the same.[218] Complex **77** has no effect on the tumor, while CORM-3 enhance cell growth. With a dose of 2.5 mg, **78** significantly slows tumour growth of CT-26 (murine colorectal carcinoma) cells in Balb/c mice *in vivo*. Upon illumination at 350 nm, two amide-based $Ru(CO)_2$ bipyridyl complexes, one with an alkyne group (**80**) and the other with a fluorescent tag (BODIPY) (**81**) (Fig. 14), showed CO release properties. In particular, the complexes could release CO in a DMSO/H_2O (0.8% DMSO) mixture following illumination with 350 nm light. The first CO molecule is rapidly released, while the second one is released more

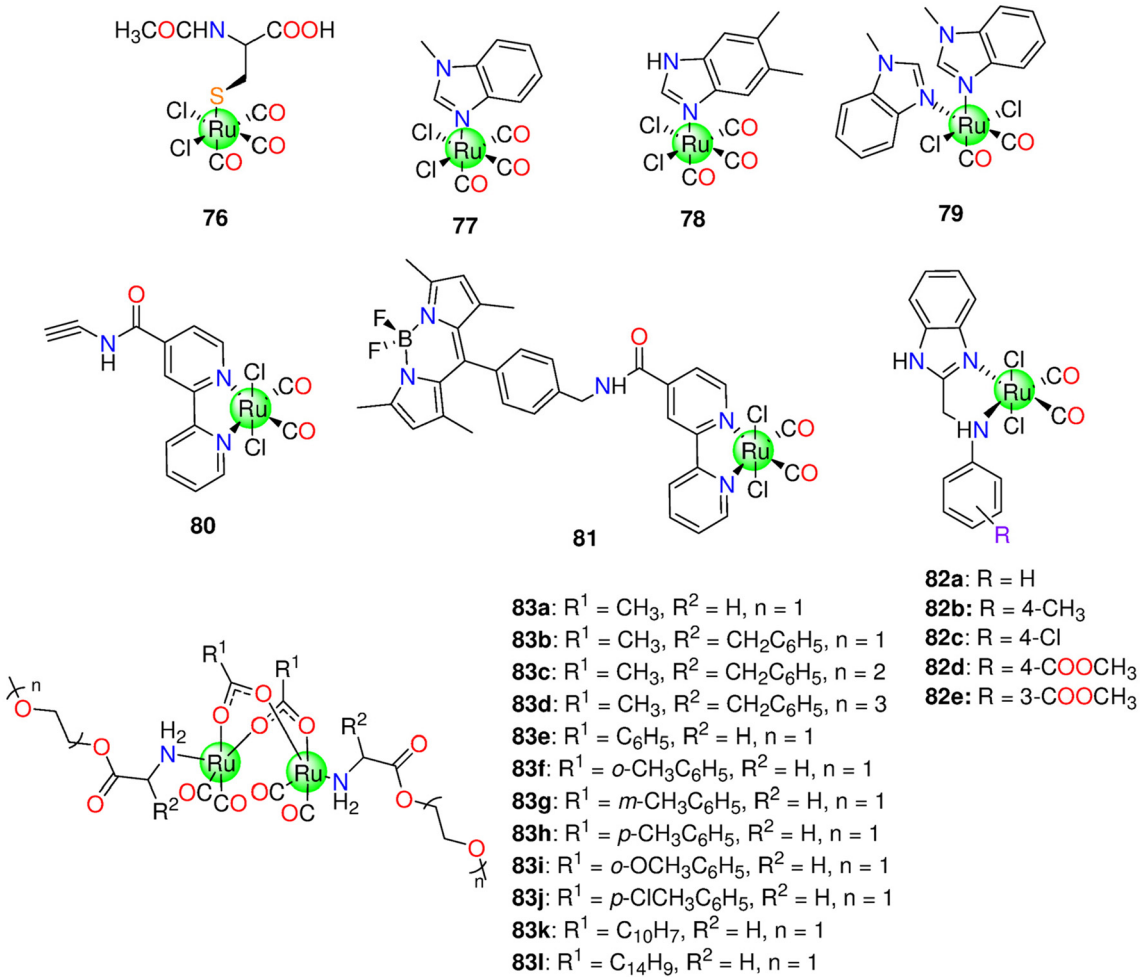

Fig. 14 Structures of the Ru(II) and Ru(I) CORMs **76–83**.

slowly. Both complexes show increased cytotoxicity against A431 (epidermoid carcinoma) cancer cells when illuminated at 350 nm. Complex **81** was promptly taken up by A431 and HEK-293 cell lines and distributed throughout the cytoplasm.[221]

Ru(II)-based complexes, with 1*H*-benzimidazol-2-ylmethyl-(*N*-phenyl) amine derivatives, (R = H (**82a**), 4-CH_3 (**82b**), 4-Cl (**82c**), 4-$COOCH_3$ (**82d**), and 3-$COOCH_3$ (**82e**)) were developed and photoactivated at 365 nm.[222] Except for **82d** (IC_{50} = 45.08 ± 3.5 μM), the studied complexes are non-toxic to MCF-7 in the dark. After being exposed to light, the complexes developed cytotoxicity based on the type of the substituent (**82a** > **82d** > **82b** > **82c** > **82e**). The cytotoxic action of the iCORM of **82a**, IC_{50} = 14.32 ± 1.2 μM, revealed that the gained toxicity might be related to the iCORM and emitted CO.[222]

To improve the hydrophilic properties and biological applicability of CO, Ru(I)-based sawhorse frame was attached to a water-soluble PEGylated sidearm yielding twelve Ru(I)-based complexes (**83a–83l**). PhotoCORMs **83a–83j** release therapeutic levels of CO under photolysis at 365 nm. By correlating the kinetics of CO release and hydrophilic properties of CORMs, it was revealed that the more hydrophilic the CORM, the faster it releases CO. CORMs **83a–83j** are stable in the dark and do not spontaneously deteriorate under physiological conditions. The $t_{1/2}$ values of **83a–83j** at 60 μM were in the range 166–2699 s. Although with a minimum toxicity against murine RAW264.7 macrophages, **83a** exhibits anticancer action against HT-29 cancer cells under illumination conditions. With a concentration of 50 μM, **83a** and **83h** show 12.5% and 6.65% loss in cells activity by illumination.[223]

6.6 Rhenium(I) and rhenium(II) CORMs

Two trigger methods are utilized to promote the CO release from rhenium carbonyls: changes in pH and exposure to light source. Zobi's group developed CORMs with the formula *cis–trans*-$[Re^{II}(CO)_2Br_2L_2]^n$ **84–90** (Fig. 15), and only complexes with monodentate ligands released CO.[39] The CO release rate depends on the pH, having $t_{1/2}$ values ranging from about 6 to 43 min, under the physiological conditions. Selected complexes protected new-born rat ventricular cardiomyocytes from ischemia-reperfusion stress *in vitro*. The needed time for complete saturation of Mb with the released CO steadily decreased

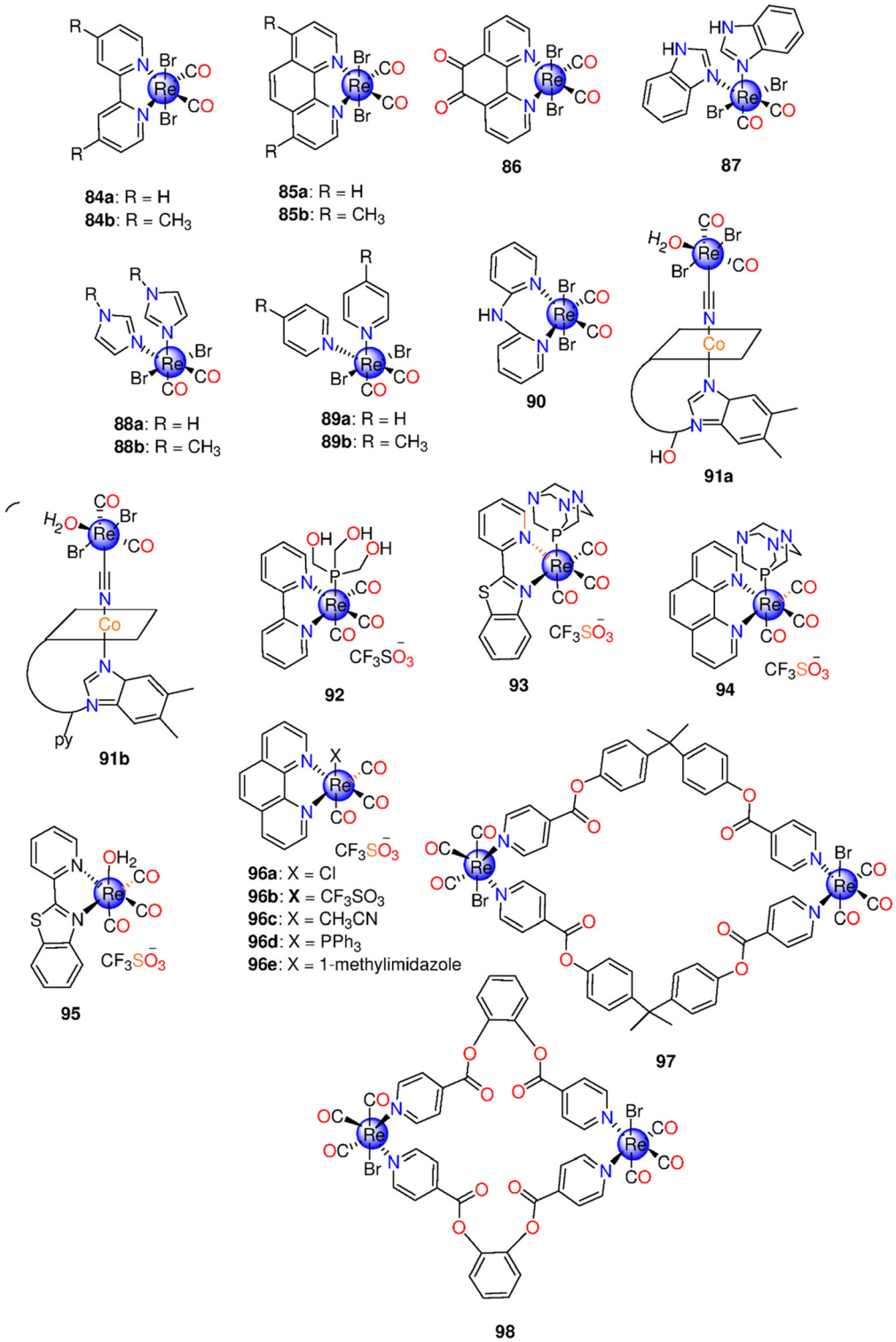

Fig. 15 Structures of the Re(I) and Re(II) CORMs **84**–**98**.

at lower pH levels. The findings seem to suggest that the protection of cardiomyocytes may not depend on the rate of CO released.

Later, the same group introduced two B_{12}-$Re^{II}(CO)_2$ conjugates, **91a** and **91b** (Fig. 15), capable of releasing CO in a PBS solution containing Mb, freshly reduced by $Na_2S_2O_4$. In general, the two conjugates are fully soluble in water, stable in the aqueous media and biocompatible. The rate of CO release from **91a** and **91b** was shown to be similar, with a $t_{1/2}$ of around 20 min, while the Re precursor salt,

$[Et_4N]_2[ReBr_4(CO)_2]$ had a $t_{1/2}$ of 6 min under the same conditions.[39] About one mol of CO per mol of **91a** and **91b** was released within 2 h.[224] The rate of CO discharge could be affected by ligand and pH changes on the basic Re-based moiety. The extracellular discharge of CO, as well as the antioxidant capabilities of both molecules, may contribute to the cytoprotective effects of **91a** and **91b**. Both complexes are non-toxic against cardiomyocytes, even after CO release, and exhibit cellular protective action from ischemia-reperfusion injury. The iCORM non-toxicity was ascribed to the metal oxidation in water under aerobic conditions and formation of the ReO_4^- anion, one of the least hazardous fragments among the rare inorganic compounds.[225]

The highly luminescent tricarbonyl bipyridine Re(I) complex, **92** (Fig. 15), functionalized with tris(hydroxymethyl) phosphine, is stable under aerated aqueous conditions, autoxidation-resistant and releases one CO when exposed to light source at 405 nm.[226] Also, the solvated photoproduct is luminescent, a property that enables tracing how **92** transforms into its solvated photoproduct inside cells. Complex **92** displays no activity against the human prostate cancer cell line PPC-1. Based on the luminescence results, it is clear that **92** accumulates throughout the cytoplasm, yet is unable to enter the nuclear membrane of the tested cells.[227]

Mascharak and co-workers proposed two photoactivatable luminescent tricarbonyl Re(I) complexes, bearing 1,3,5-triaza-7-phospha-adamantane, as well as *N*,*N*-bidentate ligand (2-(pyridyl)benzothiazole (**93**) and 1,10-phenanthroline (**94**)) (Fig. 15), which discharge CO moderately, *via* the exposure to low-energy UV light (360 nm). Complexes **93** and **94** are very stable in dark and easily soluble in aerobic/anaerobic aqueous conditions. When exposed to UV-A light, **93** and **94** only release one CO molecule. The luminescence properties of **93** and **94** at 550 nm fade gradually by illumination. The results showed that **93** is rapidly internalized by the MDA-MB-231 cancerous cells.[170]

The tricarbonyl Re(I) complex functionalized with 2-(pyridyl) benzothiazole **95** (Fig. 15) operates as theranostic two-tone luminescent photoCORM in cell targets. Under low-power UV light, the orange luminescence of **95** at 605 nm is completely replaced by a blue fluorescence at 400 nm as a result of complete CO loss and de-ligation of the benzothiazole ligand. According to Mb assay, the k_{CO} value of **95** is 0.31 min^{-1}. A dose-dependent loss in the survival of MDA-MB-231 cancer cells, caused by the CO-induced apoptosis, was observed when subjected to UV light.[228]

The dark-stable and promising theranostic Re(I)-based photoCORMs, $[ReX(CO)_3(Phen)]^{0/1+}$ (Phen = 1,10-phenanthroline, X = Cl^- (**96a**), $CF_3SO_3^-$ (**96b**), MeCN (**96c**), PPh_3 (**96d**), and methylimidazole (**96e**)), (Fig. 15) are able to emit CO when subjected to low-power UV light (5 mW cm^{-2}). In acetonitrile, the k_{CO} values of **96a**, **96d** and **96e** are 0.07 ± 0.02, 1.59 ± 0.02 and 0.07 ± 0.02 min^{-1}, respectively. The images obtained using fluorescent confocal microscopy revealed that the luminescent Re(I) compounds, cationic and neutral, with auxiliary ligands with varying lipophilic properties, show significant cellular penetration and are distributed largely throughout the cytoplasm in MDA-MB-231 cells. Complex **96d** (containing PPh_3) displays moderate nuclear accumulation along with cytosolic distribution.[229]

Two binuclear metallacyclophanes, (Fig. 15) (**97** and **98**) have been developed by reaction of $[Re(CO)_5Cl]$ with *N*-(2-hydroxybenzylidene)-benzimidazole. The complexes show good solubility in polar organic solvents and are stable at ambient temperature. The obtained IC_{50} values indicate that **97** is cytotoxic against HepG2 cells, IC_{50} = 14.2 ± 4.8 μM in comparison to cisplatin (IC_{50} = 15.89 ± 5.7 μM). Compound **98** inhibits HeLa malignant cells in a concentration-dependent fashion, having the lowest IC_{50} value of 12.4 ± 2.9 μM, while cisplatin has an IC_{50} = 17.56 ± 5.7 μM.[171] Cancer cells treated with **98** displayed apoptotic traits in the AO/EB staining, including altered nuclear fragmentation, cell shrinkage and development of apoptotic bodies. Although this has yet to be confirmed, the anticancer effect of **98** could be a result of apoptosis triggered by the CO release.[171]

7. General remarks, conclusions, and perspectives

It has been established that administering molecules that transport and discharge CO into living systems is a more effective option than using CO as a gas. A method of achieving a controlled, focused CO administration is based on the use of stable compounds that only lose CO upon provoking by an external or internal stimulus. These CO prodrugs are known as carbon monoxide releasing molecules (CORMs). CO, either as a gas or confined within a CORM, could be employed as a useful molecule to treat a broad spectrum of diseases and to preserve organs.[230] In this review, we have tried to briefly summarize most of the research done employing CORMs as chemotherapeutic agents focussing our attention on cytotoxic metal carbonyl complexes (MCCs). MCCs were classified according to how they are activated to release CO. Thus, examples of photoinduced CORMs (photoCORMs), solvent-triggered CORMs and enzymatically activated CORMs have been presented. A summary of the results obtained in the last 20 years on the first-generation CORMs is also reported. These molecules are highly reactive. Their chemical reactivities may interfere with the activity of biological macromolecules and/or intercept with CO signalling pathways producing unmanageable problems. These aspects have been critically summarized by Wang and coworkers in a recent review.[19]

To overcome these limitations many other CO-releasing molecules have been prepared. Recently, photoCORMs are attracting more attention than the other CORMs due to their widespread application and medicinal potential.[158] Mn(I)- and Ru(II)-based CORMs belong to this class, since they can release CO *via* illumination. In contrast to the visible-light induced Mn(I) carbonyls complexes, the majority of Ru(II)-based photoCORMs are inactive or lose CO when illuminated by UV light. Because of possible photochemical and biological advan-

tages, tri- and tetra-carbonyl Mn(I)-based complexes have attracted the spotlight.[231] Visible light-triggered CORMs, that discharge CO when illuminated by visible light ranging from 468 to 660 nm, could be designed by selecting highly conjugated ligand system. Also, included in the development of photoCORMs, is the utilization of materials such as scaffolds, crystals, matrices or up-conversion particles to either improve photoCORM water-solubility or enable encapsulation of potentially harmful metal-based photo-products.[232] Also, the used solvent seems to affect the stability of CORMs and the rate of CO release. Some Re-based CORMs are luminescent and can release CO through illumination. These MCCs can behave as a tracker to identify the site of CO discharge inside the cell.[227] Other Re CORMs are pH-dependent[39] and others can release CO by oxidation.[224] Iron-based CORMs can release CO in response to light, redox state changes, and enzymatic bond breaking at the ligand periphery in enzyme-triggered CORMs. The main mechanism for activating Co(0)-based CORMs is the ligand exchange reaction with the medium. CORMs could be therapeutically active through being anti-inflammatory agents, cytotoxic to cancer cells, preserving transplanted organs, antimicrobial, healing cardiovascular illnesses *etc*. Overall, these data reveal that the mechanism of MCCs activation is influenced by the type of metals as well as the composition of the auxiliary ligands. The features of the ancillary ligands in CORMs influence the metal core electronic density and the specific ability of a CORM to bind biological (macro)molecules that activate CO release. The properties of the ligands also affect the CORM resistance towards oxidation. In other words, the inner ligand sphere structure is crucial for tailoring a certain CORM stability to tolerate proteins in the plasma, react to a specific stimulus, or generate a particular CO release pattern.[36] The benefits that CORMs may provide represent a significant advantage over many typical organic medications, which might focus on just one problem. Instead of requiring a complex mixture of multiple medications, an individual CORM is able to treat a wide range of disorders. Another significant advantage of employing CORMs as medications is the variety of structures that can release CO.[230]

A key point in designing new CORMs is to take into account their toxicity, appropriate absorption, distribution, metabolism, and excretion (ADME) profile, tissue accumulation and their *in vivo* stability.[233] Unfortunately, little is known on the toxicity profiles of CORMs,[234] which could be toxic due to effects produced by both CO release and the formation of metal-containing fragments generated by the original prodrugs upon reaction with biomolecules, but the few studies carried out on tested complexes suggest severe damages of liver and kidney in both functional and morphological aspects.[215] Metal complexes can undergo oxidation or fragmentation prior to CO release. Changes in the metal oxidation state could interfere with electron transfer pathways in cellular components, thus producing harmful effects.[34] Furthermore, interaction with biomolecules can also occur prior to CO release. In this frame, further studies are needed to clarify which metal-containing fragments are formed by CORMs, which is their metabolic fate and their toxicity in the cellular environments. New approaches should be developed to understand the different contributions of CO and metal-containing fragments derived from CORMs to the biological properties of these potential drugs. In this respect, it should be also considered that metal-containing fragments generated by CORMs could have a different reactivity with biomolecules when compared to the original prodrugs and thus they could have different targets.

Finally, even after reviewing all the prior achievements in such a large prospective area as metal-based CORMs, several mysteries remain as intriguing questions for scientists. When it comes to physicochemical features of CORMs and their cytotoxic properties, before and after CO induction process, which factor is more important: the CORM itself or the iCORM? As a result, we recommend doing additional extensive studies to fully comprehend such miracles and maximise CORMs medically helpful effect on humanity. These studies should also evaluate the release kinetics, dose control, and safety profile of CORMs and i-CORMs.

Conflicts of interest

There are no conflicts to declare.

Acknowledgements

A. Mansour thanks United Arab Emirates University, Al-Ain, United Arab Emirates, for financial support. Merlino thanks MIUR PRIN 2022- Cod. 2022JMFC3X, “Protein Metalation by Anticancer Metal-based Drugs” for financial support.

References

1 S. H. Heinemann, T. Hoshi, M. Westerhausen and A. Schiller, *Chem. Commun.*, 2014, **50**, 3644–3660.
2 L. Wu and R. Wang, *Pharmacol. Rev.*, 2005, **57**, 585–630.
3 T. Sjöstrand, *Nature*, 1949, **164**, 580–581.
4 R. F. Coburn, W. J. Williams and R. E. Forster, *J. Clin. Invest.*, 1964, **43**, 1098–1103.
5 R. Tenhunen, H. S. Marver and R. Schmid, *Proc. Natl. Acad. Sci. U. S. A.*, 1968, **61**, 748–755.
6 M. D. Maines, *FASEB J.*, 1988, **2**, 2557–2568.
7 A. I. Archakov, I. I. Karuzina, N. A. Petushkova, A. V. Lisitsa and V. G. Zgoda, *Toxicol. in Vitro*, 2002, **16**, 1–10.
8 F. P. Guengerich, *Biochemistry*, 1978, **17**, 3633–3639.
9 R. Wang, *Can. J. Physiol. Pharmacol.*, 1998, **76**, 1–15.
10 A. Grilli, M. A. De Lutiis, A. Patruno, L. Speranza, F. Gizzi, A. A. Taccardi, P. Di Napoli, R. De Caterina, P. Conti and M. Felaco, *Ann. Clin. Lab. Sci.*, 2003, **33**, 208–215.
11 T. M. Brusko, C. H. Wasserfall, A. Agarwal, M. H. Kapturczak and M. A. Atkinson, *J. Immun.*, 2005, **174**, 5181–5186.

12 I. C. Alexandreanu and D. M. Lawson, *Exp. Biol. Med.*, 2003, **228**, 59–63.
13 S. W. Ryter, H. P. Kim, K. Nakahira, B. S. Zuckerbraun, D. Morse and A. M. K. Choi, *Antioxid. Redox Signal.*, 2007, **9**, 2157–2174.
14 S. J. Gibbons and G. Farrugia, *J. Physiol.*, 2004, **556**, 325–336.
15 M. Suematsu, N. Goda, T. Sano, S. Kashiwagi, T. Egawa, Y. Shinoda and Y. Ishimura, *J. Clin. Invest.*, 1995, **96**, 2431–2437.
16 X. Yang, M. De Caestecker, L. E. Otterbein and B. Wang, *Med. Res. Rev.*, 2020, **40**, 1147–1177.
17 A. Halilovic, K. A. Patil, L. Bellner, G. Marrazzo, K. Castellano, G. Cullaro, M. W. Dunn and M. L. Schwartzman, *J. Cell. Physiol.*, 2011, **226**, 1732–1740.
18 R. Motterlini and L. E. Otterbein, *Nat. Rev. Drug Discovery*, 2010, **9**, 728–743.
19 N. Bauer, Z. Yuan, X. Yang and B. Wang, *Biochem. Pharmacol.*, 2023, **214**, 115642.
20 S. S. Mendes, J. Marques, E. Mesterházy, J. Straetener, M. Arts, T. Pissarro, J. Reginold, A. Berscheid, J. Bornikoel, R. M. Kluj, C. Mayer, F. Oesterhelt, S. Friães, B. Royo, T. Schneider, H. Brötz-Oesterhelt, C. C. Romão and L. M. Saraiva, *ACS Bio. Med. Chem. Au*, 2022, **2**, 419–436.
21 L. S. Nobre, H. Jeremias, C. C. Romão and L. M. Saraiva, *Dalton Trans.*, 2016, **45**, 1455–1466.
22 S. N. Anderson, J. M. Richards, H. J. Esquer, A. D. Benninghoff, A. M. Arif and L. M. Berreau, *ChemistryOpen*, 2015, **4**, 590–594.
23 L. S. Lazarus, A. D. Benninghoff and L. M. Berreau, *Acc. Chem. Res.*, 2020, **53**, 2273–2285.
24 A. M. Mansour, R. M. Khaled, E. Khaled, S. K. Ahmed, O. S. Ismael, A. Zeinhom, H. Magdy, S. S. Ibrahim and M. Abdelfatah, *Biochem. Pharmacol.*, 2022, **199**, 114991.
25 M. A. Wright and J. A. Wright, *Dalton Trans.*, 2016, **45**, 6801–6811.
26 X. Ji, K. Damera, Y. Zheng, B. Yu, L. E. Otterbein and B. Wang, *J. Pharm. Sci.*, 2016, **105**, 406–416.
27 X. Ji and B. Wang, *Acc. Chem. Res.*, 2018, **51**, 1377–1385.
28 D. Wang, E. Viennois, K. Ji, K. Damera, A. Draganov, Y. Zheng, C. Dai, D. Merlin and B. Wang, *Chem. Commun.*, 2014, **50**, 15890–15893.
29 J. Cheng and J. Hu, *ChemMedChem*, 2021, **16**, 3628–3634.
30 J. S. Ward, R. Morgan, J. M. Lynam, I. J. S. Fairlamb and J. W. B. Moir, *MedChemComm*, 2017, **8**, 346–352.
31 M. Desmard, R. Foresti, D. Morin, M. Dagouassat, A. Berdeaux, E. Denamur, S. H. Crook, B. E. Mann, D. Scapens, P. Montravers, J. Boczkowski and R. Motterlini, *Antioxid. Redox Signal.*, 2012, **16**, 153–163.
32 A. F. Tavares, M. R. Parente, M. C. Justino, M. Oleastro, L. S. Nobre and L. M. Saraiva, *PLoS One*, 2013, **8**, e83157.
33 N. Rana, S. McLean, B. E. Mann and R. K. Poole, *Microbiology*, 2014, **160**, 2771–2779.
34 A. Ismailova, D. Kuter, D. S. Bohle and I. S. Butler, *Bioinorg. Chem. Appl.*, 2018, **2018**, 1–23.
35 A. C. Kautz, P. C. Kunz and C. Janiak, *Dalton Trans.*, 2016, **45**, 18045–18063.
36 C. C. Romão, W. A. Blättler, J. D. Seixas and G. J. L. Bernardes, *Chem. Soc. Rev.*, 2012, **41**, 3571.
37 R. Motterlini, J. E. Clark, R. Foresti, P. Sarathchandra, B. E. Mann and C. J. Green, *Circ. Res.*, 2002, **90**, e17–e24.
38 U. Schatzschneider, *Br. J. Pharmacol.*, 2015, **172**, 1638–1650.
39 F. Zobi, A. Degonda, M. C. Schaub and A. Yu. Bogdanova, *Inorg. Chem.*, 2010, **49**, 7313–7322.
40 B. J. Aucott, J. S. Ward, S. G. Andrew, J. Milani, A. C. Whitwood, J. M. Lynam, A. Parkin and I. J. S. Fairlamb, *Inorg. Chem.*, 2017, **56**, 5431–5440.
41 P. C. Kunz, H. Meyer, J. Barthel, S. Sollazzo, A. M. Schmidt and C. Janiak, *Chem. Commun.*, 2013, **49**, 4896.
42 E. Stamellou, D. Storz, S. Botov, E. Ntasis, J. Wedel, S. Sollazzo, B. K. Krämer, W. Van Son, M. Seelen, H. G. Schmalz, A. Schmidt, M. Hafner and B. A. Yard, *Redox Biol.*, 2014, **2**, 739–748.
43 J. E. Clark, P. Naughton, S. Shurey, C. J. Green, T. R. Johnson, B. E. Mann, R. Foresti and R. Motterlini, *Circ. Res.*, 2003, **9**, e2–e8.
44 A. J. Atkin, I. J. S. Fairlamb, J. S. Ward and J. M. Lynam, *Organometallic*, 2012, **31**, 5894–5902.
45 R. Motterlini, P. Sawle, S. Bains, J. Hammad, R. Alberto, R. Foresti and C. J. Green, *FASEB J.*, 2005, **19**, 1–24.
46 N. Bauer, X. Yang, Z. Yuan and B. Wang, *Chem. Sci.*, 2023, **14**, 3215–3228.
47 M. Klein, U. Neugebauer, M. Schmitt and J. Popp, *ChemPhysChem*, 2015, **17**(7), 985–993.
48 S. Romanski, B. Kraus, U. Schatzschneider, J. Neudörfl, S. Amslinger and H. Schmalz, *Angew. Chem., Int. Ed.*, 2011, **50**, 2392–2396.
49 S. Romanski, B. Kraus, M. Guttentag, W. Schlundt, H. Rücker, A. Adler, J.-M. Neudörfl, R. Alberto, S. Amslinger and H.-G. Schmalz, *Dalton Trans.*, 2012, **41**, 13862.
50 Y. Li, L. Hemmersbach, B. Krause, N. Sitnikov, A. Schlundt Née Göderz, D. O. Pastene Maldonado, H. Schmalz and B. Yard, *ChemBioChem*, 2022, **23**, e202100452.
51 J. D. Seixas, A. Mukhopadhyay, T. Santos-Silva, L. E. Otterbein, D. J. Gallo, S. S. Rodrigues, B. H. Guerreiro, A. M. L. Gonçalves, N. Penacho, A. R. Marques, A. C. Coelho, P. M. Reis, M. J. Romão and C. C. Romão, *Dalton Trans.*, 2013, **42**, 5985–5998.
52 Z. Yuan, X. Yang and B. Wang, *Chem. Sci.*, 2021, **12**, 13013–13020.
53 R. D. Rimmer, H. Richter and P. C. Ford, *Inorg. Chem.*, 2010, **49**, 1180–1185.
54 M. A. Gonzales and P. K. Mascharak, *J. Inorg. Biochem.*, 2014, **133**, 127–135.
55 D. Nguyen and C. Boyer, *ACS Biomater. Sci. Eng.*, 2015, **1**, 895–913.
56 C. Nagel, S. McLean, R. K. Poole, H. Braunschweig, T. Kramer and U. Schatzschneider, *Dalton Trans.*, 2014, **43**, 9986.

57 U. Sachs, G. Schaper, D. Winkler, D. Kratzert and P. Kurz, *Dalton Trans.*, 2016, **45**, 17464–17473.
58 H.-M. Berends and P. Kurz, *Inorg. Chim. Acta*, 2012, **380**, 141–147.
59 P. Rudolf, F. Kanal, J. Knorr, C. Nagel, J. Niesel, T. Brixner, U. Schatzschneider and P. Nuernberger, *J. Phys. Chem. Lett.*, 2013, **4**, 596–602.
60 B. J. Aucott, J. B. Eastwood, L. Anders Hammarback, I. P. Clark, I. V. Sazanovich, M. Towrie, I. J. S. Fairlamb and J. M. Lynam, *Dalton Trans.*, 2019, **48**, 16426–16436.
61 R. S. Herrick and T. L. Brown, *Inorg. Chem.*, 1984, **23**, 4550–4553.
62 S. Rattan, R. A. Haj and M. A. F. De Godoy, *Am. J. Physiol.: Gastrointest. Liver Physiol.*, 2004, **287**, G605–G611.
63 E. Fiumana, H. Parfenova, J. H. Jaggar and C. W. Leffler, *Am. J. Physiol.: Heart Circ. Physiol.*, 2003, **284**, H1073–H1079.
64 P. Koneru and C. W. Leffler, *A Am. J. Physiol.: Heart Circ. Physiol.*, 2004, **286**, H304–H309.
65 Q. Xi, D. Tcheranova, H. Parfenova, B. Horowitz, C. W. Leffler and J. H. Jaggar, *Am. J. Physiol.: Heart Circ. Physiol.*, 2004, **286**, H610–H618.
66 B. Arregui, B. López, M. G. Salom, F. Valero, C. Navarro and F. J. Fenoy, *Kidney Int.*, 2004, **65**, 564–574.
67 C. Bohlender, S. Gläser, M. Klein, J. Weisser, S. Thein, U. Neugebauer, J. Popp, R. Wyrwa and A. Schiller, *J. Mater. Chem. B*, 2014, **2**, 1454–1463.
68 V. Pathak, K. Roemhild, S. Schipper, N. Groß-Weege, T. Nolte, S. Ruetten, E. M. Buhl, A. El Shafei, M. Weiler, L. Martin, G. Marx, V. Schulz, F. Kiessling, T. Lammers and P. Koczera, *Small*, 2022, **18**, 2200924.
69 J. Zhu, J. Wang, G. Wang, J. Zhang, W. Tao, C. Liu, M. Liu, H. Zhang, R. Xie, F. Ye, Y. Liu, W. Fang, X. Chen and Y. Li, *J. Phys. Chem. Lett.*, 2021, **12**, 4658–4665.
70 J. P. Lomont, S. C. Nguyen and C. B. Harris, *Organometallics*, 2014, **33**, 6179–6185.
71 K. A. Machovec, D. S. Ushakumari, I. J. Welsby and V. G. Nielsen, *Thromb. Res.*, 2012, **129**, 793–796.
72 I. C. Winburn, K. Gunatunga, R. D. McKernan, R. J. Walker, I. A. Sammut and J. C. Harrison, *Basic Clin. Pharmacol. Toxicol.*, 2012, **111**, 31–41.
73 P. Sawle, R. Foresti, B. E. Mann, T. R. Johnson, C. J. Green and R. Motterlini, *Br. J. Pharmacol.*, 2005, **145**, 800–810.
74 K. Srisook, S.-S. Han, H.-S. Choi, M.-H. Li, H. Ueda, C. Kim and Y.-N. Cha, *Biochem. Pharmacol.*, 2006, **71**, 307–318.
75 G. Cepinskas, K. Katada, A. Bihari and R. F. Potter, *Am. J. Physiol.: Gastrointest. Liver Physiol.*, 2008, **294**, G184–G191.
76 K. Tsoyi, T. Y. Lee, Y. S. Lee, H. J. Kim, H. G. Seo, J. H. Lee and K. C. Chang, *Mol. Pharmacol.*, 2009, **76**, 173–182.
77 Q. Niu, F. Du, X. Yang, X. Yang and X. Wang, *Int. Immunopharmacol.*, 2022, **113**, 109441.
78 K.-B. Shiu, S.-J. Yu, Y. Wang and G.-H. Lee, *J. Organomet. Chem.*, 2002, **650**, 37–42.
79 B.-W. Sun, Q. Jin, Y. Sun, Z.-W. Sun, X. Chen, Z.-Y. Chen and G. Cepinskas, *World J. Gastroenterol.*, 2007, **13**, 6183.
80 J. Megías, J. Busserolles and M. J. Alcaraz, *Br. J. Pharmacol.*, 2007, **150**, 977–986.
81 H. Soni, P. Patel, A. C. Rath, M. Jain and A. A. Mehta, *Vasc. Pharmacol.*, 2010, **53**, 68–76.
82 A. F. N. Tavares, M. Teixeira, C. C. Romão, J. D. Seixas, L. S. Nobre and L. M. Saraiva, *J. Biol. Chem.*, 2011, **286**, 26708–26717.
83 C. S. Bang, R. Kruse, I. Demirel, A. Önnberg, B. Söderquist and K. Persson, *Microb. Pathog.*, 2014, **66**, 29–35.
84 C. Sahlberg Bang, I. Demirel, R. Kruse and K. Persson, *PLoS One*, 2017, **12**, e0178541.
85 L. S. Nobre, F. Al-Shahrour, J. Dopazo and L. M. Saraiva, *Microbiology*, 2009, **155**, 813–824.
86 T. S. Murray, C. Okegbe, Y. Gao, B. I. Kazmierczak, R. Motterlini, L. E. P. Dietrich and E. M. Bruscia, *PLoS One*, 2012, **7**, e35499.
87 N. A. M. Khir, A. S. M. Noh, I. Long, R. Zakaria and C. A. N. Ismail, *Mol. Cell. Biochem.*, 2023, **479**, 539–552.
88 M.-H. Li, Y.-N. Cha and Y.-J. Surh, *Biochem. Biophys. Res. Commun.*, 2006, **342**, 984–990.
89 A. Józkowicz, I. Huk, A. Nigisch, G. Weigel, W. Dietrich, R. Motterlini and J. Dulak, *Antioxid. Redox Signaling*, 2003, **5**, 155–162.
90 T. Vera, J. R. Henegar, H. A. Drummond, J. M. Rimoldi and D. E. Stec, *J. Am. Soc. Nephrol.*, 2005, **16**, 950–958.
91 M. Allanson and V. E. Reeve, *Cancer Immunol. Immunother.*, 2007, **56**, 1807–1815.
92 S. J. Stanford, M. J. Walters, A. A. Hislop, S. G. Haworth, T. W. Evans, B. E. Mann, R. Motterlini and J. A. Mitchell, *Eur. J. Pharmacol.*, 2003, **473**, 135–141.
93 L. Shao, C. Liu, S. Wang, J. Liu, L. Wang, L. Lv and Y. Zou, *Oncol. Lett.*, 2018, **16**, 3223–3230.
94 M. Juszczak, M. Kluska, D. Wysokiński and K. Woźniak, *Sci. Rep.*, 2020, **10**, 12200.
95 K. Fujita, Y. Tanaka, T. Sho, S. Ozeki, S. Abe, T. Hikage, T. Kuchimaru, S. Kizaka-Kondoh and T. Ueno, *J. Am. Chem. Soc.*, 2014, **136**, 16902–16908.
96 L. Zhang, L. Laug, W. Münchgesang, E. Pippel, U. Gösele, M. Brandsch and M. Knez, *Nano Lett.*, 2010, **10**, 219–223.
97 H. Tabe, K. Fujita, S. Abe, M. Tsujimoto, T. Kuchimaru, S. Kizaka-Kondoh, M. Takano, S. Kitagawa and T. Ueno, *Inorg. Chem.*, 2015, **54**, 215–220.
98 P. Kaczara, B. Sitek, K. Przyborowski, A. Kurpinska, K. Kus, M. Stojak and S. Chlopicki, *Arterioscler., Thromb., Vasc. Biol.*, 2020, **40**, 2376–2390.
99 M. Ryan, N. Jernigan, H. Drummond, G. Mclemorejr, J. Rimoldi, S. Poreddy, R. Gadepalli and D. Stec, *Pharmacol. Res.*, 2006, **54**, 24–29.
100 S. Basuroy, C. W. Leffler and H. Parfenova, *Am. J. Physiol.: Cell Physiol.*, 2013, **304**, C1105–C1115.
101 P. Fagone, K. Mangano, S. Mammana, E. Cavalli, R. Di Marco, M. L. Barcellona, L. Salvatorelli, G. Magro and F. Nicoletti, *Clin. Immunol.*, 2015, **157**, 198–204.

102 T. R. Johnson, B. E. Mann, I. P. Teasdale, H. Adams, R. Foresti, C. J. Green and R. Motterlini, *Dalton Trans.*, 2007, 1500.
103 T. Santos-Silva, A. Mukhopadhyay, J. D. Seixas, G. J. L. Bernardes, C. C. Romão and M. J. Romão, *J. Am. Chem. Soc.*, 2011, **133**, 1192–1195.
104 T. Santos-Silva, A. Mukhopadhyay, J. D. Seixas, G. J. L. Bernardes, C. C. Romao and M. J. Romao, *Curr. Med. Chem.*, 2011, **18**, 3361–3366.
105 M. Tinajero-Trejo, K. J. Denby, S. E. Sedelnikova, S. A. Hassoubah, B. E. Mann and R. K. Poole, *J. Biol. Chem.*, 2014, **289**, 29471–29482.
106 A. Bagul, S. A. Hosgood, M. Kaushik and M. L. Nicholson, *Transplantation*, 2008, **85**, 576–581.
107 G. Wang, T. Hamid, R. J. Keith, G. Zhou, C. R. Partridge, X. Xiang, J. R. Kingery, R. K. Lewis, Q. Li, D. G. Rokosh, R. Ford, F. G. Spinale, D. W. Riggs, S. Srivastava, A. Bhatnagar, R. Bolli and S. D. Prabhu, *Circulation*, 2010, **121**, 1912–1925.
108 M. D. Musameh, C. J. Green, B. E. Mann, B. J. Fuller and R. Motterlini, *J. Heart Lung Transplant.*, 2007, **26**, 1192–1198.
109 R. Foresti, J. Hammad, J. E. Clark, T. R. Johnson, B. E. Mann, A. Friebe, C. J. Green and R. Motterlini, *Br. J. Pharmacol.*, 2004, **142**, 453–460.
110 L. Lo Iacono, J. Boczkowski, R. Zini, I. Salouage, A. Berdeaux, R. Motterlini and D. Morin, *Free Radicals Biol. Med.*, 2011, **50**, 1556–1564.
111 M. G. Bani-Hani, D. Greenstein, B. E. Mann, C. J. Green and R. Motterlini, *Pharmacol. Rep.*, 2006, **58**(Suppl), 132–144.
112 M. L. Ferrandiz, N. Maicas, I. Garcia-Arnandis, M. C. Terencio, R. Motterlini, I. Devesa, L. A. B. Joosten, W. B. Van Den Berg and M. J. Alcaraz, *Ann. Rheum. Dis.*, 2007, **67**, 1211–1217.
113 A. Yabluchanskiy, P. Sawle, S. Homer-Vanniasinkam, C. J. Green, R. Foresti and R. Motterlini, *Crit. Care Med.*, 2012, **40**, 544–552.
114 M. Desmard, K. S. Davidge, O. Bouvet, D. Morin, D. Roux, R. Foresti, J. D. Ricard, E. Denamur, R. K. Poole, P. Montravers, R. Morterlini and J. Boczkowski, *FASEB J.*, 2009, **23**, 1023–1031.
115 S. M. Carvalho, J. Marques, C. C. Romão and L. M. Saraiva, *Antimicrob. Agents Chemother.*, 2019, **63**, e00643–e00619.
116 J. L. Wilson, H. E. Jesse, B. Hughes, V. Lund, K. Naylor, K. S. Davidge, G. M. Cook, B. E. Mann and R. K. Poole, *Antioxid. Redox Signaling*, 2013, **19**, 497–509.
117 T. Obara, H. Yamamoto, T. Aokage, T. Igawa, T. Nojima, T. Hirayama, M. Seya, M. Ishikawa-Aoyama, A. Nakao, R. Motterlini and H. Naito, *Transplantation*, 2022, **106**, 1365–1375.
118 J. Wang, D. Zhang, X. Fu, L. Yu, Z. Lu, Y. Gao, X. Liu, J. Man, S. Li, N. Li, X. Chen, M. Hong, Q. Yang and J. Wang, *J. Neuroinflamm.*, 2018, **15**, 188.
119 H. Yamamoto-Oka, S. Mizuguchi, M. Toda, Y. Minamiyama, S. Takemura, T. Shibata, G. Cepinskas and N. Nishiyama, *Inflammopharmacology*, 2018, **26**, 435–445.
120 K. Lu, W.-J. Wu, C. Zhang, Y.-L. Zhu, J.-Q. Zhong and J. Li, *Curr. Neurovasc. Res.*, 2020, **17**, 464–470.
121 C. Jin, B. Lin, G. Zheng, K. Tan, G. Liu, Z. Yao, J. Xie, W. Chen, L. Chen, T. Xu, C. Huang, Z. Wu and L. Yang, *Oxid. Med. Cell. Longevity*, 2022, **2022**, 1–21.
122 A. Stein, Y. Guo, W. Tan, W. Wu, X. Zhu, Q. Li, C. Luo, B. Dawn, T. Johnson and R. Motterlini, *J. Mol. Cell. Cardiol.*, 2005, **38**, 127–134.
123 Y. Guo, A. B. Stein, W.-J. Wu, W. Tan, X. Zhu, Q.-H. Li, B. Dawn, R. Motterlini and R. Bolli, *Am. J. Physiol.: Heart Circ. Physiol.*, 2004, **286**, H1649–H1653.
124 Y. Tayem, T. R. Johnson, B. E. Mann, C. J. Green and R. Motterlini, *Am. J. Physiol.: Renal Physiol.*, 2006, **290**, F789–F794.
125 L.-M. Zhang, D.-X. Zhang, W.-C. Zheng, J.-S. Hu, L. Fu, Y. Li, Y. Xin and X.-P. Wang, *Exp. Neurol.*, 2021, **341**, 113683.
126 Y. Dai, H. Chen, Y. Pan and H. Song, *BioMed Res. Int.*, 2022, **2022**, 1–10.
127 M. Seveso, M. Vadori, E. Bosio, F. Fante, F. Besenzon, L. Ravarotto, S. Bedendo, T. Johnson, B. Mann and R. Motterlini, *Am. J. Transplant.*, 2017, **17**, 557–564.
128 E. Masini, A. Vannacci, P. Failli, R. Mastroianni, L. Giannini, M. C. Vinci, C. Uliva, R. Motterlini and P. F. Mannaioni, *FASEB J.*, 2008, **22**, 3380–3388.
129 M. Vadori, M. Seveso, F. Besenzon, E. Bosio, E. Tognato, F. Fante, M. Boldrin, S. Gavasso, L. Ravarotto, B. E. Mann, P. Simioni, E. Ancona, R. Motterlini and E. Cozzi, *Xenotransplantation*, 2009, **16**, 99–114.
130 R. F. Lyon, H. M. Southam, C. R. Trevitt, C. Liao, S. F. El-Khamisy, R. K. Poole and M. P. Williamson, *Biochem. J.*, 2022, **479**, 1429–1439.
131 S. H. Crook, B. E. Mann, A. J. H. M. Meijer, H. Adams, P. Sawle, D. Scapens and R. Motterlini, *Dalton Trans.*, 2011, **40**, 4230.
132 S. McLean, B. E. Mann and R. K. Poole, *Anal. Biochem.*, 2012, **427**, 36–40.
133 S. V. C. Vummaleti, D. Branduardi, M. Masetti, M. De Vivo, R. Motterlini and A. Cavalli, *Chem. – Eur. J.*, 2012, **18**, 9267–9275.
134 R. Motterlini, A. Nikam, S. Manin, A. Ollivier, J. L. Wilson, S. Djouadi, L. Muchova, T. Martens, M. Rivard and R. Foresti, *Red. Biol.*, 2019, **20**, 334–348.
135 G. Yang, M. Fan, J. Zhu, C. Ling, L. Wu, X. Zhang, M. Zhang, J. Li, Q. Yao, Z. Gu and X. Cai, *Biomaterials*, 2020, **255**, 120155.
136 J. Chen, D. Chen, J. Chen, T. Shen, T. Jin, B. Zeng, L. Li, C. Yang, Z. Mu, H. Deng and X. Cai, *Acta Biomater.*, 2022, **146**, 49–65.
137 W. Ma, X. Chen, L. Fu, J. Zhu, M. Fan, J. Chen, C. Yang, G. Yang, L. Wu, G. Mao, X. Yang, X. Mou, Z. Gu and X. Cai, *ACS Appl. Mater. Interfaces*, 2020, **12**, 22479–22491.
138 J. Liu, R. S. Li, M. He, Z. Xu, L. Q. Xu, Y. Kang and P. Xue, *Biomaterials*, 2021, **277**, 121084.

139 L. K. Wareham, S. McLean, R. Begg, N. Rana, S. Ali, J. J. Kendall, G. Sanguinetti, B. E. Mann and R. K. Poole, *Antioxid. Redox Signaling*, 2018, **28**, 1286–1308.
140 S. Fayad-Kobeissi, J. Ratovonantenaina, H. Dabiré, J. L. Wilson, A. M. Rodriguez, A. Berdeaux, J.-L. Dubois-Randé, B. E. Mann, R. Motterlini and R. Foresti, *Biochem. Pharmacol.*, 2016, **102**, 64–77.
141 D. Zhang, Z. Lin, Y. Zheng, J. Song, J. Li, Y. Zeng and X. Liu, *ACS Nano*, 2020, **14**, 8985–8999.
142 M. Stojak, P. Kaczara, R. Motterlini and S. Chlopicki, *Pharmacol. Res.*, 2018, **136**, 160–171.
143 R. N. Bhattacharjee, M. Richard-Mohamed, Q. Sun, A. Haig, G. Aboalsamh, P. Barrett, R. Mayer, I. Alhasan, K. Pineda-Solis, L. Jiang, H. Alharbi, M. Saha, E. Patterson, A. Sener, G. Cepinskas, A. M. Jevnikar and P. P. W. Luke, *Transplantation*, 2018, **102**, 1066–1074.
144 D. Babu, G. Leclercq, R. Motterlini and R. A. Lefebvre, *Front. Pharmacol.*, 2017, **8**, 31.
145 S. F. Kobeissi, J. L. Wilson, B. Michel, J.-L. Dubois-Randé, R. Motterlini and R. Foresti, *Arc. Cardiovasc. Dis. Suppl.*, 2014, **6**, 17.
146 L. Wu, X. Cai, H. Zhu, J. Li, D. Shi, D. Su, D. Yue and Z. Gu, *Adv. Funct. Mater.*, 2018, **28**, 1804324.
147 F. Yang, W. Yu, Q. Yu, X. Liu, C. Liu, C. Lu, X. Liao, Y. Liu and N. Peng, *Small*, 2023, **19**, 2206124.
148 P. Kaczara, R. Motterlini, G. M. Rosen, B. Augustynek, P. Bednarczyk, A. Szewczyk, R. Foresti and S. Chlopicki, *Biochim. Biophys. Acta, Bioenerg.*, 2015, **1847**, 1297–1309.
149 L. Braud, M. Pini, L. Muchova, S. Manin, H. Kitagishi, D. Sawaki, G. Czibik, J. Ternacle, G. Derumeaux, R. Foresti and R. Motterlini, *JCI Insight*, 2018, **3**, e123485.
150 U. Hasegawa, A. J. Van Der Vlies, E. Simeoni, C. Wandrey and J. A. Hubbell, *J. Am. Chem. Soc.*, 2010, **132**, 18273–18280.
151 Y. Morimoto, W. Durante, D. G. Lancaster, J. Klattenhoff and F. K. Tittel, *Am. J. Physiol.: Heart Circ. Physiol.*, 2001, **280**, H483–H488.
152 G. S. Marks, H. J. Vreman, B. E. McLaughlin, J. F. Brien and K. Nakatsu, *Antioxid. Redox Signaling*, 2002, **4**, 271–277.
153 M. Klein, U. Neugebauer, A. Gheisari, A. Malassa, T. M. A. Jazzazi, F. Froehlich, M. Westerhausen, M. Schmitt and J. Popp, *J. Phys. Chem. A*, 2014, **118**, 5381–5390.
154 J. Esteban, J. V. Ros–Lis, R. Martínez-Máñez, M. D. Marcos, M. Moragues, J. Soto and F. Sancenón, *Angew. Chem.*, 2010, **122**, 5054–5057.
155 A. J. Atkin, J. M. Lynam, B. E. Moulton, P. Sawle, R. Motterlini, N. M. Boyle, M. T. Pryce and I. J. S. Fairlamb, *Dalton Trans.*, 2011, **40**, 5755.
156 B. W. Michel, A. R. Lippert and C. J. Chang, *J. Am. Chem. Soc.*, 2012, **134**, 15668–15671.
157 J. Wang, J. Karpus, B. S. Zhao, Z. Luo, P. R. Chen and C. He, *Angew. Chem., Int. Ed.*, 2012, **51**, 9652–9656.
158 K. Ling, F. Men, W.-C. Wang, Y.-Q. Zhou, H.-W. Zhang and D.-W. Ye, *J. Med. Chem.*, 2018, **61**, 2611–2635.
159 N. C. Burton and T. R. Guilarte, *Environ. Health Perspect.*, 2009, **117**, 325–332.
160 M. Liu, Z. J. Lim, Y. Y. Gwee, A. Levina and P. A. Lay, *Angew. Chem., Int. Ed.*, 2010, **49**, 1661–1664.
161 B. D. Chatterjee, A. Mitra and G. S. De, *Platinum Met. Rev.*, 2006, **50**, 2–12.
162 J. Niesel, A. Pinto, H. W. Peindy N'Dongo, K. Merz, I. Ott, R. Gust and U. Schatzschneider, *Chem. Commun.*, 2008, 1798.
163 U. Schatzschneider, *Inorg. Chim. Acta*, 2011, **374**, 19–23.
164 X. Xie, Y. Yan, N. Zhu and G. Liu, *Eur. J. Med. Chem.*, 2014, **76**, 67–78.
165 S. J. Carrington, I. Chakraborty and P. K. Mascharak, *Chem. Commun.*, 2013, **49**, 11254.
166 S. J. Carrington, I. Chakraborty, J. M. L. Bernard and P. K. Mascharak, *ACS Med. Chem. Lett.*, 2014, **5**, 1324–1328.
167 C. A. Kumar, R. Nagarajaprakash, W. Victoria, V. Veena, N. Sakthivel and B. Manimaran, *Inorg. Chem. Commun.*, 2016, **64**, 39–44.
168 E. Üstün, A. Özgür, K. A. Coşkun, S. Demir, İ. Özdemir and Y. Tutar, *J. Coord. Chem.*, 2016, **69**, 3384–3394.
169 E. Üstün, A. Özgür, K. A. Coşkun, S. Demir Düşünceli, İ. Özdemir and Y. Tutar, *Transition Met. Chem.*, 2017, **42**, 331–337.
170 I. Chakraborty, S. J. Carrington, G. Roseman and P. K. Mascharak, *Inorg. Chem.*, 2017, **56**, 1534–1545.
171 C. Ashok Kumar, D. Divya, R. Nagarajaprakash, V. Veena, P. Vidhyapriya, N. Sakthivel and B. Manimaran, *J. Organomet. Chem.*, 2017, **846**, 152–160.
172 P. Vidhyapriya, D. Divya, M. Bala and N. Sakthivel, *J. Photochem. Photobiol., B*, 2018, **188**, 28–41.
173 J. Jimenez, I. Chakraborty, A. Dominguez, J. Martinez-Gonzalez, W. M. C. Sameera and P. K. Mascharak, *Inorg. Chem.*, 2018, **57**, 1766–1773.
174 D. Musib, M. K. Raza, Kh. Martina and M. Roy, *Polyhedron*, 2019, **172**, 125–131.
175 H. G. Daniels, O. G. Fast, S. M. Shell and F. A. Beckford, *J. Photochem. Photobiol., A*, 2019, **374**, 84–94.
176 M. N. Pinto, I. Chakraborty, J. Jimenez, K. Murphy, J. Wenger and P. K. Mascharak, *Inorg. Chem.*, 2019, **58**, 14522–14531.
177 M. Hu, Y. Yan, B. Zhu, F. Chang, S. Yu and G. Alatan, *RSC Adv.*, 2019, **9**, 20505–20512.
178 A. M. Mansour and A. Friedrich, *Inorg. Chem. Front.*, 2017, **4**, 1517–1524.
179 U. Kumar, S. Roy, R. K. Jha, P. Vidhyapriya, N. Sakthivel and B. Manimaran, *ACS Omega*, 2019, **4**, 1923–1930.
180 U. Kumar, S. Jose, D. Divya, P. Vidhyapriya, N. Sakthivel and B. Manimaran, *New J. Chem.*, 2019, **43**, 7520–7531.
181 J. Jimenez, M. N. Pinto, J. Martinez-Gonzalez and P. K. Mascharak, *Inorg. Chim. Acta*, 2019, **485**, 112–117.
182 C. Zou, H. Zhang, Q. Li, H. Xiao, L. Yu, S. Ke, L. Zhou, W. Liu, W. Wang, H. Huang, N. Ma, Q. Liu, X. Wang, W. Zhao, H. Zhou and X. Gao, *Carcinogenesis*, 2011, **32**, 1840–1848.

183 J. Rossier, J. Delasoie, L. Haeni, D. Hauser, B. Rothen-Rutishauser and F. Zobi, *J. Inorg. Biochem.*, 2020, **209**, 111–122.
184 R. M. Khaled, A. Friedrich, M. A. Ragheb, N. T. Abdel-Ghani and A. M. Mansour, *Dalton Trans.*, 2020, **49**, 9294–9305.
185 D. Musib, M. K. Raza, M. Pal and M. Roy, *Appl. Organomet. Chem.*, 2021, **35**, e6110.
186 A. M. Mansour, K. Radacki, R. M. Khaled, M. H. Soliman and N. T. Abdel-Ghani, *J. Biol. Inorg. Chem.*, 2021, **26**, 135–147.
187 Y. Zhou, Y. Sun, K. Yi, Z. Wang, Y. Liu and C. He, *Inorg. Chem. Front.*, 2022, **9**, 5941–5949.
188 R. M. Khaled, D. A. Habashy, A. Y. Ahmed, O. S. Ismael, S. S. Ibrahim, M. Abdelfatah, K. Radacki and A. M. Mansour,, *Polyhedron*, 2022, **225**, 116048.
189 D. A. Habashy, R. M. Khaled, A. Y. Ahmed, K. Radacki, S. K. Ahmed, E. K. Tharwat, H. Magdy, A. Zeinhom and A. M. Mansour, *Dalton Trans.*, 2022, **51**, 14041–14048.
190 R. M. Khaled, K. Radacki, S. A. Al-Abraq, E. El-Hussieny, G. A. E. Mostafa, E. A. Ali, O. R. Shehab and A. M. Mansour, *Polyhedron*, 2023, **244**, 116574.
191 K. Fujita, Y. Tanaka, S. Abe and T. Ueno, *Angew. Chem., Int. Ed.*, 2016, **55**, 1056–1060.
192 W. Beck, W. Petri and J. Meder, *J. Organomet. Chem.*, 1980, **191**, 73–77.
193 M. Marín-García, N. Benseny-Cases, M. Camacho, Y. Perrie, J. Suades and R. Barnadas-Rodríguez, *Dalton Trans.*, 2018, **47**, 14293–14303.
194 D. Achatz, M. A. Lang, A. Völkl, W. P. Fehlhammer and W. Beck, *Z. Anorg. Allg. Chem.*, 2005, **631**, 2339–2346.
195 S. Reiländer, W. Schmehl, K. Popp, K. Nuss, P. Kronen, D. Verdino, C. Wiezorek, M. Gutmann, L. Hahn, C. Däubler, A. Meining, M. Raschig, F. Kaiser, B. Von Rechenberg, O. Scherf-Clavel and L. Meinel, *ACS Biomater. Sci. Eng.*, 2023, **9**, 2937–2948.
196 Y. Gong, T. Zhang, H. Liu, Y. Zheng, N. Li, Q. Zhao, Y. Chen and B. Liu, *Transition Met. Chem.*, 2015, **40**, 413–426.
197 Y. Gong, T. Zhang, M. Li, N. Xi, Y. Zheng, Q. Zhao, Y. Chen and B. Liu, *Free Radicals Biol. Med.*, 2016, **97**, 362–374.
198 J. Li, J. Zhang, Q. Zhang, Z. Bai, Q. Zhao, Z. Wang, Y. Chen and B. Liu, *J. Organomet. Chem.*, 2018, **874**, 49–62.
199 H.-P. Liu, Y. Liao, M.-Z. Ren, Z.-J. Quan and X.-C. Wang, *Bioorg. Chem.*, 2021, **107**, 104621.
200 R. Motterlini, B. E. Mann and R. Foresti, *Expert Opin. Invest. Drugs*, 2005, **14**, 1305–1318.
201 P. Sawle, J. Hammad, I. J. S. Fairlamb, B. Moulton, C. T. O'Brien, J. M. Lynam, A. K. Duhme-Klair, R. Foresti and R. Motterlini, *J. Pharmacol. Exp. Ther.*, 2006, **318**, 403–410.
202 D. J. Jones and R. J. Mawby, *Inorg. Chim. Acta*, 1972, **6**, 157–160.
203 L. Hewison, S. H. Crook, T. R. Johnson, B. E. Mann, H. Adams, S. E. Plant, P. Sawle and R. Motterlini, *Dalton Trans.*, 2010, **39**, 8967.
204 R. Kretschmer, G. Gessner, H. Görls, S. H. Heinemann and M. Westerhausen, *J. Inorg. Biochem.*, 2011, **105**, 6–9.
205 M.-C. P. Yeh and C.-C. Hwu, *J. Organomet. Chem.*, 1991, **419**, 341–355.
206 D. Zhang, B. M. Krause, H.-G. Schmalz, P. Wohlfart, B. A. Yard and R. Schubert, *Front. Pharmacol.*, 2021, **12**, 702392.
207 R. Motterlini, P. Sawle, J. Hammad, B. E. Mann, T. R. Johnson, C. J. Green and R. Foresti, *Pharmacol. Res.*, 2013, **68**, 108–117.
208 S. Romanski, E. Stamellou, J. T. Jaraba, D. Storz, B. K. Krämer, M. Hafner, S. Amslinger, H. G. Schmalz and B. A. Yard, *Free Radicals Biol. Med.*, 2013, **65**, 78–88.
209 N. S. Sitnikov, Y. Li, D. Zhang, B. Yard and H. Schmalz, *Angew. Chem., Int. Ed.*, 2015, **54**, 12314–12318.
210 B. Bauer, A. Göderz, H. Braumüller, J. M. Neudörfl, M. Röcken, T. Wieder and H. Schmalz, *ChemMedChem*, 2017, **12**, 1927–1930.
211 H. M. Southam, T. W. Smith, R. L. Lyon, C. Liao, C. R. Trevitt, L. A. Middlemiss, F. L. Cox, J. A. Chapman, S. F. El-Khamisy, M. Hippler, M. P. Williamson, P. J. F. Henderson and R. K. Poole, *Red. Biol.*, 2018, **18**, 114–123.
212 H. M. Southam, M. P. Williamson, J. A. Chapman, R. L. Lyon, C. R. Trevitt, P. J. F. Henderson and R. K. Poole, *Antioxidants*, 2021, **10**, 915.
213 L. Hemmersbach, R. Adam, C. Plevnali, X. Zhang, B. Yard and H. Schmalz, *Eur. J. Org. Chem.*, 2023, e202201424.
214 L. Hemmersbach, Y. Schreiner, X. Zhang, F. Dicke, L. Hünemeyer, J. Neudörfl, T. Fleming, B. Yard and H. Schmalz, *Chem. – Eur. J.*, 2022, **28**, e202201670.
215 P. Wang, H. Liu, Q. Zhao, Y. Chen, B. Liu, B. Zhang and Q. Zheng, *Eur. J. Med. Chem.*, 2014, **74**, 199–215.
216 J. D. Seixas, M. F. A. Santos, A. Mukhopadhyay, A. C. Coelho, P. M. Reis, L. F. Veiros, A. R. Marques, N. Penacho, A. M. L. Gonçalves, M. J. Romão, G. J. L. Bernardes, T. Santos-Silva and C. C. Romão, *Dalton Trans.*, 2015, **44**, 5058–5075.
217 J. D. Seixas, M. Chaves-Ferreira, D. Montes-Grajales, A. M. Gonçalves, A. R. Marques, L. M. Saraiva, J. Olivero-Verbel, C. C. Romão and G. J. L. Bernardes, *Chem. – Eur. J.*, 2015, **21**, 14708–14712.
218 G. Tamasi, A. Merlino, F. Scaletti, P. Heffeter, A. A. Legin, M. A. Jakupec, W. Berger, L. Messori, B. K. Keppler and R. Cini, *Dalton Trans.*, 2017, **46**, 3025–3040.
219 N. Pontillo, G. Ferraro, L. Messori, G. Tamasi and A. Merlino, *Dalton Trans.*, 2017, **46**, 9621–9629.
220 G. Tamasi, A. Carpini, D. Valensin, L. Messori, A. Pratesi, F. Scaletti, M. Jakupec, B. Keppler and R. Cini, *Polyhedron*, 2014, **81**, 227–237.
221 S. Geri, T. Krunclova, O. Janouskova, J. Panek, M. Hruby, D. Hernández-Valdés, B. Probst, R. A. Alberto, C. Mamat, M. Kubeil and H. Stephan, *Chem. – Eur. J.*, 2020, **26**, 10992–11006.
222 N. M. Ibrahim, R. M. Khaled, M. A. Ragheb, K. Radacki, A. M. Farag and A. M. Mansour, *Dalton Trans.*, 2021, **50**, 15389–15399.

223 X. Zhang, N. Guo, S. Yang, H. Khan and W. Zhang, *Materials*, 2022, **15**, 3597.
224 F. Zobi, O. Blacque, R. A. Jacobs, M. C. Schaub and A. Yu. Bogdanova, *Dalton Trans.*, 2012, **41**, 370–378.
225 T. J. Haley and F. D. Cartwright, *J. Pharm. Sci.*, 1968, **57**, 321–323.
226 K. Koike, N. Okoshi, H. Hori, K. Takeuchi, O. Ishitani, H. Tsubaki, I. P. Clark, M. W. George, F. P. A. Johnson and J. J. Turner, *J. Am. Chem. Soc.*, 2002, **124**, 11448–11455.
227 A. E. Pierri, A. Pallaoro, G. Wu and P. C. Ford, *J. Am. Chem. Soc.*, 2012, **134**, 18197–18200.
228 S. J. Carrington, I. Chakraborty, J. M. L. Bernard and P. K. Mascharak, *Inorg. Chem.*, 2016, **55**, 7852–7858.
229 I. Chakraborty, J. Jimenez, W. M. C. Sameera, M. Kato and P. K. Mascharak, *Inorg. Chem.*, 2017, **56**, 2863–2873.
230 J. S. Ward, in *Organomet. Chem*, ed. I. Fairlamb and J. Lynam, Royal Society of Chemistry, Cambridge, 2015, vol. 40, pp. 140–176.
231 A. M. Mansour, R. M. Khaled, K. Radacki, Z. Younes, M. Gamal, B. Guirguis, G. A. E. Mostafa, E. A. Ali and O. R. Shehab, *Dalton Trans.*, 2023, **52**, 10286–10293.
232 E. Kottelat and Z. Fabio, *Inorganics*, 2017, **5**, 24.
233 H.-I. Choi, A. Zeb, M.-S. Kim, I. Rana, N. Khan, O. S. Qureshi, C.-W. Lim, J.-S. Park, Z. Gao, H.-J. Maeng and J.-K. Kim, *J. Controlled Release*, 2022, **350**, 652–667.
234 M. I. Khan, M. I. Hossain, M. K. Hossain, M. H. K. Rubel, K. M. Hossain, A. M. U. B. Mahfuz and M. I. Anik, *ACS Appl. Bio Mater.*, 2022, **5**, 971–1012.